STOCHASTIC MODELING OF STOP-LOSS REINSURANCE AND EXPOSURE CURVES UNDER TIME DEPENDENT STRUCTURE

A THESIS SUBMITTED TO
THE GRADUATE SCHOOL OF APPLIED MATHEMATICS
OF
MIDDLE EAST TECHNICAL UNIVERSITY

BY

ÖZENÇ MURAT MERT

IN PARTIAL FULFILLMENT OF THE REQUIREMENTS
FOR
THE DEGREE OF DOCTOR OF PHILOSOPHY
IN
FINANCIAL MATHEMATICS

DECEMBER 2022

Approval of the thesis:

STOCHASTIC MODELING OF STOP-LOSS REINSURANCE AND EXPOSURE CURVES UNDER TIME DEPENDENT STRUCTURE

submitted by **ÖZENÇ MURAT MERT** in partial fulfillment of the requirements for the degree of **Doctor of Philosophy in Financial Mathematics Department, Middle East Technical University** by,

Prof. Dr. A. Sevtap Selçuk-Kestel _____
Dean, Graduate School of **Applied Mathematics**

Prof. Dr. A. Sevtap Selçuk-Kestel _____
Head of Department, **Financial Mathematics**

Prof. Dr. A. Sevtap Selçuk-Kestel _____
Supervisor, **Actuarial Sciences, METU**

Examining Committee Members:

Prof. Dr. Ceylan Yozgatlıgil
Department of Statistics, METU _____

Prof. Dr. A. Sevtap Selçuk-Kestel
Actuarial Sciences, METU _____

Assoc. Prof. Dr. Könül Bayramoğlu Kavlak
Department of Industrial Engineering, BOUN _____

Assoc. Prof. Dr. Ceren Vardar Acar
Department of Statistics, METU _____

Assist. Prof. Dr. Sinem Kozpınar
Department of Insurance, Başkent University _____

Date: _____

I hereby declare that all information in this document has been obtained and presented in accordance with academic rules and ethical conduct. I also declare that, as required by these rules and conduct, I have fully cited and referenced all material and results that are not original to this work.

Name, Last Name: ÖZENÇ MURAT MERT

Signature :

ABSTRACT

STOCHASTIC MODELING OF STOP-LOSS REINSURANCE AND EXPOSURE CURVES UNDER TIME DEPENDENT STRUCTURE

Mert, Özenç Murat
Ph.D., Department of Financial Mathematics
Supervisor : Prof. Dr. A. Sevtap Selçuk-Kestel

December 2022, 109 pages

Insurance markets play an essential role in the economy of the world and its structure requires reinsurance policies due to the growth in populations, extreme (catastrophic) events, political and economical perspectives. In this thesis, stop-loss contracts, one of the reinsurance policy types, are covered for two different contract types: (i) contracts with retention and (ii) contracts with both retention and cap (maximum). This thesis covers two different methodologies, distributional and stochastic behaviors of the claim amounts for the analysis of loss modeling, the costs of insurer and reinsurer, and exposure curves to obtain a fair premium share. Unlike most studies on reinsurance policies, the thesis makes emphasizes the time-dependent and time-influenced structure of claims and gives comprehensive derivations to model claims amounts and to examine the costs of parties and the exposure curves. In the distributional approach, heavy-tailed distributions, specifically, Pareto, Gamma, and Inverse Gamma, are used and the costs of parties and the exposure curves are derived analytically under the selected distributions. Using Monte Carlo simulations and considering the joint analysis of parties' loss ratios, the optimal retention and maximum levels are found and compared with the values minimizing the risks of parties under VaR and CVaR risk measures. In the stochastic modeling approach, in order to express both random and time-dependent mechanisms of the claim amounts, Geometric Brownian Motion with time-varying parameters is used and the costs of parties and the exposure curves

are derived analytically since the time elapses during the contract period brings dissimilarities on the claim behavior so does on the cost, premium share. Furthermore, Pareto-Beta stochastic jump diffusion (PBJD) model and its theory are implemented for capturing possible extreme losses. The analytical derivations for the costs and the exposure curves under PBJD are also collected. The emphasis on the applications of real-life data, specifically Turkey's compulsory traffic insurance claims, is made for the stochastic approaches. The results for the expected costs and the exposure curves are presented. In order to obtain the forecasts values of the loss amounts, the expected costs, and the exposure curves, the time-varying parameters are taken as time series and ARIMA family models and cubic spline extrapolation are applied to these series in order to keep the structure of stochastic models.

Keywords: Stop-Loss Reinsurance, Exposure Curves, GBM, PBJD, The Costs of Insurer and Reinsurer, Premium share, ARIMA, Cubic Spline Extrapolation, Forecasting

ÖZ

ZAMANA BAĞLI HASAR FAZLASI REÜSÜRANS VE RİZİKO EĞRİLERİNİN STOKASTİK MODELLEMESİ

Mert, Özenç Murat
Doktora, Finansal Matematik Bölümü
Tez Yöneticisi : Prof. Dr. A. Sevtap Selçuk-Kestel

Aralık 2022, 109 sayfa

Dünya ekonomisinde önemli bir rol oynayan sigorta piyasaları, nüfus artışı, katastrofik olaylar, politik ve ekonomik perspektifler nedeniyle reasürans politikalarını gerektirmektedir. Bu tezde, reasürans poliçe türlerinden biri olan zarar-durdur sözleşmeleri, (i) rehinli sözleşmeler ve (ii) hem reasüranslı hem de üst limitli (maksimum) sözleşmeler olmak üzere iki farklı sözleşme türü için ele alınmıştır. Bu tez, hasar modellemesinin analizi için hasar tutarlarının dağıtımsal ve stokastik davranışları, sigortacı ve reasürör maliyetleri, adil prim payı elde etmek için riziko eğrileri olmak üzere iki farklı metodolojiyi kapsamaktadır. Reasürans politikaları üzerine yapılan çoğu çalışmanın aksine, tez, hasarların zamana bağlı yapısını vurgular ve hasar tutarlarını modellemek ve tarafların maliyetlerini ve riziko eğrilerini incelemek için kapsamlı çıkarımlar verir. Dağılım yaklaşımında, özellikle Pareto, Gamma ve Ters Gamma olmak üzere kalın kuyruklu dağılımlar kullanılır ve seçilen dağılımlar altında tarafların maliyetleri ve riziko eğrileri analitik olarak türetilir. Monte Carlo simülasyonları kullanılarak ve tarafların kayıp oranlarının ortak analizi göz önünde bulundurularak, VaR ve CVaR risk ölçütleri kapsamında optimal elde tutma ve maksimum seviyeler bulunur ve tarafların risklerini minimize eden değerler ile karşılaştırılır. Stokastik modelleme yaklaşımında, talep tutarlarının hem rastgele hem de zamana bağlı mekanizmasını ifade etmek için zamanla değişen parametrelerle Geometrik Brown Hareketi kullanılmış ve sözleşme sırasında geçen süre nedeniyle tarafların maliyetleri ve riziko

eğrileri analitik olarak türetilmiştir. Zaman, hasar davranışında olduğu gibi maliyet, prim payı üzerinde de farklılıklar getirir. Ayrıca, olası aşırı kayıpları yakalamak için Pareto-Beta stokastik sıçrama difüzyon (PBJD) modeli ve arkasındaki teori uygulanmaktadır. Bu tez, maliyet türevlerini ve PBJD kapsamında riziko eğrilerini birleştirir. Stokastik yaklaşımlar için gerçek hayat verileri kullanılıp, özellikle Türkiye'nin zorunlu trafik sigortası hasar veri uygulamalarına vurgu yapılmıştır. Beklenen maliyetler için sonuçlar, riziko eğrileri sunulmaktadır. Kayıp miktarları, beklenen maliyetler ve riziko eğrilerinin tahmin değerlerini elde etmek için zamanla değişen parametreler zaman serisi olarak alınmış ve stokastik yapıyı korumak için ARIMA ailesi modelleri ve bu serilere kübik spline ekstrapolasyonu uygulanmıştır.

Anahtar Kelimeler: Zarar-Durdur Reasürans, Riziko Eğrileri, Sigortacı ve Reasürör Maliyetleri, Prim Payı, ARIMA, Kubik Spline Ekstrapolasyonu, Tahmin

To My Dear Mother and Father

ACKNOWLEDGMENTS

This thesis is a result of four years of research. It would not have emerged without the support and input of my supervisor, professors in the Institute of Applied Mathematics (IAM), dear friends, and my family.

I would like to express my very great appreciation to my thesis supervisor Prof. Dr. A. Sevtap Selcuk-Kestel for her patient guidance, enthusiastic encouragement and valuable advices during the development and preparation of this thesis. Her willingness to give her time and to share her experiences has brightened my path. Her patient, sincere and supportive efforts in recognizing academic innovations, writing academic articles, listening to and developing my ideas helped me gain experiences for the rest of my life. Beside these, the fact that she listened to and understood the problems I faced in my social life outside of academia, and helped me to solve them, provided me within my PhD. period that I will remember gratefully in every period of my life.

I also want to thank my Ph.D. thesis monitoring committee members, Prof.Dr. Ceylan Yozgatlıgil and Assoc Prof. Dr. Könül Bayramoğlu Kavlak for their valuable comments and suggestions to make my research more qualified and for their positive and constructive feedback.

I also want to thank my family for their patience, support during not only in my Ph.D. period but also in my entire education. Without their sacrifices, I would not complete this thesis.

TABLE OF CONTENTS

LIST OF TABLES

LIST OF FIGURES

LIST OF ALGORITHMS

ALGORITHMS

LIST OF ABBREVIATIONS

d	Retention Level
k	Retention Level under Chapter 5
m	Cap or Maximum level
Case I	Conntracts with Retention
Case II	Contracts with Retention and Maximum (Cap)
$\mathbb{P}(.)$	Probability Measure
$\mathbb{E}[.]$	Expectation Operator
$\mathbb{V}[.]$	Variance Operator
$\rho(.\ ,\ .)$	Correlation Coefficient
$Cov(,\ .\ ,)$	Covariance Operator
Pareto(a, b)	Pareto Distribution with Shape Parameter a and Scale Parameter b
Gamma(a, b)	Gamma Distribution with Shape Parameter a and Scale Parameter b
IG(a, b)	Inverse Gamma Distribution with Shape Parameter a and Scale Parameter b
S	Total Claim Costs
I	Costs of Insurer
R	Costs of Reinsurer
$G(.)$	Exposure Curve under Distributional Approach
$PI_r(.)$	Loss Ratio of Insurer
$PR_r(.)$	Loss Ratio of Reinsurer
VaR	Value at Risk
CVaR	Conditional Value at Risk
SDE	Stochastic Differential Equation
GBM	Geometric Brownian Motion
$X^G(t)$	Aggragate Claim at Time t under GBM
MLE	Maximum Likelihood Estimator
$N(,\ .\ ,)$	Normal Distribution

$G_I(.)$	Exposure Curve for Insurer
$G_R(.)$	Exposure Curve for Reinsurer
$(\Omega, \mathcal{F}, \mathbb{P})$	Probability Space Equipped with Filtration $\mathcal{F}$
PBJD	Pareto-Beta Jump Diffusion
$X^J(t)$	Aggragate Claim at Time t under PBJD
MME	Moment Matching Estimator

CHAPTER 1

INTRODUCTION

A reinsurance contract shows different characteristics depending on the type of agreement. Among all other types of reinsurance forms, stop-loss is the most common type of agreement at which the partition rule of the risk is determined by a prescribed retention level. Additional to this constraint, depending on the type of the risk, the reinsurer may decide to set an upper bound (cap or maximum) on the severity of the risk (claim amount, cost). The partition of the risk with respect to the levels of these factors (d and m) between two parties creates a natural correlation that contributes to the set the optimal value maximizing the interest of insurer and reinsurer. The stop-loss reinsurance has an interesting property such that its optimal value is depicted when the variance of the cost, especially for the insurer, is minimized. Besides the dependence between insurer's and reinsurer's behavior on their expected claims, the time influence on this balance is influential, due to extreme events such as natural disasters and economic recessions. For this reason, this thesis analyzes the equilibrium between parties under three approaches:

(i) No time influence on the claims but there is statistical behavior, which leads us to study the dependence with respect to parametric evaluations;

(ii) Time influence leading to the stochastic behavior on the aggregate claims;

(iii) Time influence with extreme event impact incorporated with stochastic behavior on the aggregate claims.

Most of the optimal reinsurance studies in literature minimize the variance of cost for the insurer but rarely consider the reinsurer's aspect (see [10, 20, 24, 21, 17]). The

insurer's optimal strategy under the standard deviation premium principle with several constraints, [20], optimal reinsurance arrangements under various mean-variance premium principles, [7, 29], the relation between the adjustment coefficient and maximum expected utility of wealth with respect to the retained risk, [24, 21], the optimal retentions by minimizing the value-at-risk (VaR) and the conditional tail expectation (CTE) of the insurer's total risk, and some other risk measures, [13, 4, 45, 23, 16, 34], can be counted among many remarkable studies in reinsurance optimization. Some other literature such as Markowitz type efficient frontier solution to determine the optimal retention and limiting levels under a joint survival probability, [18, 19], designing an optimal reinsurance contract maximizing the joint survival and profitable probabilities, [11], two state-of-the-art evolutionary and swarm intelligence approaches, [39], and optimal reinsurance contracts minimizing the convex combination of the VaR for both parties, [12], concentrate on the joint behavior of the insurer and reinsurer in optimizing the retention offer different approaches. Additionally, the optimal values of the contract by minimizing the total risks of the insurer VaR, CVaR, and CTE can be found in [13, 39, 49, 15]. The other risk measures such as ES (expected shortfall) and RCVaR (robust conditional value-at-risk, [25]) can also be considered in this framework. However, we stick with the coherent measures to be consistent with insurance literature.

On the other hand, for the partition of risk premium between insurer and reinsurer, exposure curves are commonly used in practice. Based on the level of retention, the premium share is mostly considered in non-proportional reinsurance contracts. The "rating by a layer of insurance" method evaluates the proportion of losses with respect to the size of loss from aggregate loss distributions [40]. In [30], the liability insurance in which the claim sizes can not be assumed to be scaled by sums insured is introduced. They analyze Riebesell's system introduced in 1936 from the perspective of the collective risk model theory. The well-known exposure curves, which are a form of analytic function with two parameters by using Maxwell-Boltzman, Bose-Einstein, Fermi-Dirac (MBBEFD) distribution class for a single risk in [6] and extended in [2] for two dependent risks, is derived as a sole function of the retention. The dependence between the costs of insurer and reinsurer measured by the correlation coefficient as a function of retention and maximum levels under Normal,

Gamma, and translated Gamma loss distribution assumptions are introduced by [14], at which the optimal stop-loss contract attains the maximum correlation. However, the literature lacks the studies about the exposure curves for stop-loss contracts under optimal constraints and dependence framework.

Due to the other varieties in the loss distributions and the direct influence of the dependence created with respect to the upper and lower bounds (retention and cap) in reinsurance agreements, we aim to examine the influence of the correlation coefficient on the valuation of premiums for insurer and reinsurer, and then, evaluate the optimal stop-loss contract in the frame of Pareto, Gamma, and Inverse Gamma as aggregate claim distributions under two cases. **Case I** refers to the contracts only with retention(d); **Case II** quotes the ones with both retention and maximum (m) as defining constraints. The optimal value for d and m are determined in such a way that the maximum level of these bounds optimizes (minimizes) the cost of both insurer and reinsurer under the selected loss distributions. To do so, we derive the expressions for the mean and the variance of the aggregate claims for insurer and reinsurer and the correlation coefficient (ρ) between the costs of both parties. Keeping up the value of the correlation between their respective costs, we determine the optimum premium and its partition between the insurer and the reinsurer. Under this framework, the exposure curves as functions of retention and maximum levels for each distribution are analytically derived. Monte Carlo simulations are employed to illustrate the impact of parameters on determining the premium share. We employ a dynamic optimization scheme to determine the retention and maximum levels, which yields an equilibrium maximizing risk premiums for both parties. The convergence to optimal bounds in two cases is determined according to the values achieving the maximum correlation minimizing the expected cost. Under the proposed framework, we investigate the effectiveness of the optimized d and m levels compared to the risk measures VaR and CVaR. Our results show that the optimal values for both cases also maximize the correlation between the costs. We expect the findings are utilized to determine the optimum level, its related retention value with respect to their cost distribution under derived exposure curves.

Additionally, stop-loss takes into account the balance between insurer and reinsurer under certain conditions, which requires a good understanding of historical loss data.

Loss modeling is one of the most celebrated mathematical approaches in actuarial sciences. It offers valuable theoretical and practical guidance for expected claims and risk management. Methods such as the chain ladder and interactive modeling to estimate the claims ([38]), the framework of double generalized linear models to model the dispersion of the costs as well as the mean of the claim costs ([44]), and actuarial loss functions based on a symmetrized version of the semiparametric transformation approach to kernel smoothing to estimate both the initial mode and the heavy tail that is suitable for actuarial loss distributions ([8]) can be given as striking examples from literature. However, no specific study in the literature determines the exposure curves for time-dependent stop-loss contracts. The expansion of the premium income or loss over the contract's time frame is important to capture the time influence on the random loss.

In this part, we consider the daily aggregate loss per day to follow the claims in a time-dependent mechanism that can be utilized as a stochastic model under a discrete-time framework. Moreover, we assume that the claims follow a stochastic behavior, specifically the geometric Brownian motion with time-varying parameters. We employ a continuous-time model and an increasing σ- algebra filtration to achieve the discrete-time formalism. In the stop-loss scheme, we consider Case I, Case II. Under this framework, the time-dependent costs of the insurer and the reinsurer under both cases are analytically investigated. Here, each party's costs refer to the amount of payment done by the insurer and the reinsurer, which results from a random loss (claims). Furthermore, the partition of the premium is proposed under the time-dependent setup for both insurer and reinsurer. To illustrate the findings, an application to the real data on Turkey's compulsory traffic insurance claims for the year 2006 is employed. The claim distribution within the policy year supports the influence of time on the claims as well. In the literature, the parameter estimation in stochastic models is crucial to develop a better understanding of real-world problems in insurance, finance, and physics ([48]). In this thesis, the time-varying parameters required in modeling are found using dynamic maximum likelihood parameter estimation (DMLE). Based on those estimates, the simulated claims are used to depict the cost of parties, exposure curves under **Case I** and **Case II**. Having attained proper performance in simulations, we forecast the claims, the costs, and the exposure curves using two

approaches: (i) the cubic spline extrapolation as its implementation is straightforward due to equally-distanced discrete time intervals, (ii) dynamic AutoRegressive Integrated Moving Average (ARIMA) as parameters vary with respect to time. The performance of simulations is tested using MAPE and RMSE. Our findings illustrate that time influence on the claims should be taken into account as well. The proposed approach and analytical results can be a useful tool and guide to determine the fair premium share.

Subsequently, in line with a fully stochastic approach, we investigate how extreme losses influence costs and premium share under the constraints using the stochastic jump-diffusion process for the claims. In this frame, the Pareto-Beta jump-diffusion (PBJD) process is chosen as it allows up-and-down jumps generated by two independent Poisson processes at which jump magnitudes are drawn from Pareto and Beta distributions. Choosing PBJD to capture the extremes in claim amounts stems from the number and magnitude of the up-jumps that are more frequent than the down jumps. With this motivation, we derive the probability density of the log return process of PBJD for each time increment within time-varying perspectives as a novel contribution. The probability density is constructed by the weighted mixture of Normal, Pareto, and Beta distributions for each time increment to derive the expected costs of the insurer and the reinsurer for two types of contracts: (i) **Case I** and **Case II**. Furthermore, we derive the exposure curves under the prescribed assumptions. The numerical approximations are utilized to evaluate challenging integrations, and applications are performed using the same data set daily containing compulsory traffic insurance claims (MTPL) from the Turkish insurance market. Based on the proposed model, the MTPL claims are forecasted with respect to the calibrated time-varying parameters whose values are estimated by dynamic ARIMA with trend search. The performance of the forecast is determined by RMSE and MAPE. The time-varying parameter estimations made in two stages: dynamic moment matching estimation for the jump part and dynamic maximum-likelihood estimation for the continuous part. Even though the literature offers many studies on jump-diffusion processes within the perspectives of finance and economy (see [37], [1], [36]), the actuarial implementations of those are scarce (see [3], [41], [22]). Therefore, we aim to contribute to the reinsurance loss modeling literature by implementing a jump-diffusion approach to

involve the impact of extreme losses having jumps in its claim history. The outcome of our approach enables researchers the analytical derivations of the expected loss and premium shares via exposure curves. The verifications through Monte Carlo simulations based on real-life data-driven calibrated parameters are found to be promising aid for practitioners.

1.1 The organization of the thesis

Chapter 2 gives the basic definitions and types of reinsurance policies, the exposure curves usage by considering the relations of the risk on the insurer and reinsurer with the premium share, and the mathematical background of stochastic differetional equations and stochastic jump diffusions in order to constitute definitions and theorems that are used in this thesis.

In Chapter 3, the derived expressions for the expected value, variance, and correlation coefficient for the two cases are presented in Section 3.1. Moreover, the derivations of these statistics under Pareto, Gamma, and Inverse Gamma assumptions are introduced. Section 3.2 presents the premium share between the insurer and reinsurer by implementing the proposed exposure curves under three distributional assumptions. Section 3.3 sets up an optimization problem and corresponding algorithms to obtain the solutions. Section 3.4 is devoted to numerical illustrations at which the simulations based on the framework for the insurer and the reinsurer are presented as well as their behavior with respect to VaR and CVaR risk measures. Section 3.5 gives concluding remarks.

Chapter 4 is structured as follows: Sections 4.1 and 4.2 present analytical derivations of the time-varying cost and exposure curves under geometric Brownian motion assumption. Section 4.3 examines parameter estimation by dynamic maximum likelihood estimator. The simulations of loss, the costs, and exposure curves based on real data are found in Section 4.4. Section 4.5 is devoted to forecasting and its performance with respect to real observations. Section 4.6 concludes the chapter.

Chapter 5 investigates the influence of extreme losses on a stop-loss agreement between insurer and reinsurer in the frame of stochastic loss amount process with jump

influence. We assume that the extreme losses can be captured by PBJD and investigate the plausibility of the models on real-life data set. The analytical derivations to find expected costs and premium shares via exposure curves are novel. The verifications using Monte Carlo simulations based on data-driven calibrated parameters are more than promising as an aid for practitioners. In numerical analysis, the use of MTPL data is original, and estimating time-varying parameters in two stages which are dynamic moment matching estimation for the jump part $(\hat{\lambda}_u, \hat{\lambda}_d, \hat{\nu}_u(i), \hat{\nu}_d(i))$ and dynamic maximum-likelihood estimation for the continuous part $(\hat{\mu}(i), \hat{\sigma}(i))$, is shown to be effective for the estimation of daily aggregate losses. Forecasting is achieved by implementing both dynamic structures of parameters in time and time dependence offers researchers and practitioners to make predictions of daily aggregate claims for a policy year.

CHAPTER 2

PRELAMINARIES

2.1 Reinsurance

An insurance company can take on an obligation of a reinsurance contract in order to protect itself from the greater risks or to reduce its own expected higher risks. By the reinsurance contract, the insurer transfers its part of risks to the reinsurer in return of giving a part of the premiums earned from the policy holders.

The reinsurance contracts can be classified into two groups as the proportional and the non-proportional reinsurance. In proportional reinsurance, the insurer and the reinsurer share liabilities in a predetermined proportion as described within the underlying aggrement. The spliting up of premiums and claims is shared between the insurer and the reinsurer according to the proportion. There are two types of proportional reinsurance contracts as quota-share and surplus. In quota-share treaty, the insurer and reinsurer share premiums and losses according to a fixed percentage. Quota share reinsurance allows an insurer to retain some risk and premium while sharing the rest with an insurer up to a predetermined maximum coverage. Surplus reinsurance treaty is defined as in which the insurer retains a fixed amount of policy liability and the reinsurer takes responsibility for what remains. In non-proportional contracts, the reinsurer only has a concrete liability to the insurer if individual claims or aggregated claims amounts exceed the amount specified in the contract. The reinsurer is obliged to compansate the insurer's loss exceeding this amount. There are two types of non-proportional reinsurance contracts as stop-loss and excess-loss. In stop-loss reinsurance, losses over a specific amount are covered solely by the reinsurer and not

by insurer company. Aggregate stop-loss reinsurance caps the aggregate amount of losses that a insurance company is responsible for, called the retention level or the deductible, and would only apply when the value of claims occurrences reaches the retention level. In excess of loss, the reinsurer indemnifies the insurer company for losses that exceed a specified limit. Depending on the treaty, it can apply to either the all loss events during the policy period or can apply to losses in aggregate. Treaties may also use bands of losses that are reduced with each claim.

In this thesis, we focus on stop-loss reinsurance, which can written as two different kinds of contracts. These are contract with retention and contract with both retention and maximum. In the literature, the investigation of stop-loss contracts depend highly on loss modeling. In general, the studies of loss modeling assume that the claim amounts are determined by a distribution. The nature of actuarial losses and the studies show that the selection of a heavy tailed distribution for the loss modeling is beneficial in terms of more accurate risk analysis.

2.2 Exposure Curves

Non-proportional reinsurance treaties should be rated based not only on losses in the past experience, but also on actual exposure. The rating of exposure is conditional to risk profiles for the risk collaterals. A risk band summarizes all risks of similar size (SI, MPTL, or EML) that belong to the same risk category. For the purposes of rating, all risks in a given band are assumed to be homogeneous. They can thus be modeled using a single loss distribution function.

The exposure rating problem is determining how to divide the total premiums of one band between the ceding company and the reinsurer. The issue is resolved in two steps. First, the overall risk premiums (per band) are calculated by applying a suitable loss ratio to the gross premiums. These risk premiums are then subdivided into risk premiums for retention and risk premiums for cession in a subsequent step. Because of the nature of non-proportional reinsurance, this is possible with the assistance of the loss distribution function. In practice, however, the accurate loss distribution function for an individual band of a risk profile is rarely known. This information

gap is bridged by using distribution functions derived from large portfolios of similar risks. These distribution functions can be found in the form of so-called exposure curves. These curves allow the reinsurer to directly extract the risk premium ratio as a function of the deductible.

Underwriters frequently have a limited number of discrete exposure curves at their disposal. These curves are available in graphical and tabular formats, and they are also used in computerized underwriting tools. For each risk band, one of the curves must be chosen, but it is not always clear which curve should be used. In such cases, the underwriter may wish to employ a virtual curve that lies between two discrete curves.

This can be accomplished by substituting analytical exposure curves for the discrete curves. Then, for each set of parameters, another curve is defined. When a continuous set of parameters is available, the exposure curves can be smoothly varied across the entire range of available curves. However, the curves must meet certain conditions, which limit the parameter range. Furthermore, if a curve family with many (more than two) parameters is used, practical issues may arise. Finding a set of parameters that can be associated with the information available for a class of risks may then become extremely difficult. This issue can be solved by restricting a curve family to a one- or two-parameter subclass and introducing new parameters.

2.3 Backround in Stochastic Modeling

In this part, we present some definitions and theorems that are used in this thesis, which are required for the construction of stochastic loss modeling. For this reason, we begin with the construction of Brownian motion. Then, we continue with the backround, basics, and properties of stochastic processes, which are geometric Brownian motion (GBM) and Pareto-Beta jump diffusion process (PBJD).

2.3.1 Brownian motion and its properties

Construction of a symmetric random walk is necessary to create a Brownian motion. For this, a fair coin is tossed repeatedly where the probabilities of H, "head", and T, "tail", on each toss are $\frac{1}{2}$. Let ω be the infinite sequence of tosses, and ω_n is the outcome of nth toss. Define

$$C_j = \begin{cases} 1 \text{ if } \omega_j = H, \\ -1 \text{ if } \omega_j = T, \end{cases} \tag{2.1}$$

and, $M_0 = 0$, such that

$$M_k = \sum_{j=1}^{k} C_j, \quad k = 1, 2, \ldots \tag{2.2}$$

Here, M_k is the process called as a symmetric random walk. Additionaly, the aim is to quicken the time and scale down the step size in a symmetric random walk in order to obtain a scaled symmetric random walk; therefore, to obtain the approximation of a Brownian motion.

$$W^n(t) = \frac{1}{\sqrt{n}} M_{nt}, \tag{2.3}$$

where n is a fixed positive integer. Here, $W^n(t)$ is called as a scaled symmetric random walk.

Brownian motion is obtained by the limit of $W^n(t)$, defined in Equation (2.3), as $n \to \infty$.

Definition 2.1. *[43] Let $(\Omega, \mathcal{F}, \mathbb{P})$ be a probability space. Assume that $W(t)$, $t \geq 0$, is a continuous function with $W(0) = 0$ and depends on ω for each $\omega \in \Omega$. Then $W(t)$ is a Brownian motion if the increments*

$$W(t_1) = W(t_1) - W(t_0), W(t_2) - W(t_1), \ldots, W(t_k) - W(t_{k-1}) \tag{2.4}$$

are indepedent to each other for all $0 = t_0 < t_1 < \cdots < t_k$. Moreover, each increment has a normal distribution with mean 0 and variance $t_i - t_{i-1}$ for $i = 0, 1, \ldots, k$, i.e.,

$$\begin{aligned} \mathbb{E}[W(t_i) - W(t_{i-1})] &= 0, \\ \mathbb{V}[W(t_i) - W(t_{i-1})] &= t_i - t_{i-1}. \end{aligned} \tag{2.5}$$

Moreover, the time elapsing bring the change in the information available at each time. For the representation of this, filtration usage and its relation with a Brownian motion are essential for the further analysis in the thesis.

Definition 2.2. *[43] Let $W(t)$ be a Brownian motion and defined in a probability space $(\Omega, \mathcal{F}, \mathbb{P})$. Let $\mathcal{F}(t),\ t \geq 0$, be a filtration for the Brownian motion. $\mathcal{F}(t)$ is a collection of σ-algebras and satisfies*

(i) $\mathcal{F}(s) \subseteq \mathcal{F}(t)$ for $0 \leq s < t$.

(ii) $W(t)$ is $\mathcal{F}(t)$-measurable.

(iii) The increment $W(u) - W(t)$ is independent of $\mathcal{F}(t)$ for $0 \leq t < u$.

The properties of Definition (2.2) need to be evaluated for a better understanding. Property (i) stands for representing accumulation of information, i.e., $\mathcal{F}(t)$ has at least as much information available as than $\mathcal{F}(s)$. Property (ii) indicates the adaptivity of a Brownian motion, i.e., the information available at time t is sufficient to evaluate $W(t)$. Property (iii) says that after time t, any increment of the Brownian motion is independent of the information at time t, i.e., the information available at earlier time can not be used for prediciting future behavior of Brownian motion.

The derivations and analysis in the thesis are used under expected operator, $\mathbb{E}[.]$, with respect to the information available in earlier time, $\mathcal{F}(.)$, to construct the sliding pattern and to obtain closed form solutions. For this, we need the following Theorem [2.1], which shows the martingale represention of a Brownian motion.

Theorem 2.1. *[28] For $0 \leq s < t$,*

$$\mathbb{E}[W(t)|\mathcal{F}(s)] = W(s). \tag{2.6}$$

The quadratic variation of a Brownian motion needs to be taken into acccount for the solution of models in the thesis and the usage of Ito's calculus. Moreover, a fixed time interval is required to build the continous models in the thesis in terms of their discretization. For this reason, let Q_v be the partition of time interval $[0, T]$, which is set as

$$0 = t_0 < t_1 < \cdots < t_n = T.$$

The step size of partition points is not required to be equally distanced, although we use equally spaced step size in the thesis. Let $||\Pi|| = \underset{j=0,t_1,\ldots,n-1}{max} t_{j+1} - t_j$.

Theorem 2.2. *[5] Let W be a Brownian motion. The quadratic variation of W up to time T is*

$$[W,W](T) = \lim_{||\Pi||\to 0} \sum_{j=0}^{n-1} [W(j+1) - W(j)]^2 = T, \ \forall T \geq 0, \tag{2.7}$$

almost surely.

2.3.2 Ito Processes and Ito's Lemma

The stochastic model and finding its solutions require the descriptions of Ito processes and Ito's formula.

Definition 2.3. *[43] A stochastic process $X(t)$ defined on $(\Omega, \mathcal{F}, \mathbb{P})$ is called one-dimensional Ito process if it has a form*

$$X(t) = X(0) + \int_0^t \mu(X(s), s)ds + \int_0^t \sigma(X(s), s)dW(s), \ 0 \leq t \leq T. \tag{2.8}$$

Here, $\mu(X(t), t)$ and $\sigma(X(t), t)$ are square integrable and adapted drift and volatility processes with respect to the filtration $\{\mathcal{F}\}_t$.

The differential form of Equation (2.8) is written as

$$dX(t) = \mu(X(t), t)dt + \sigma(X(t), t)dW(t), \ 0 \leq t \leq T.$$

Theorem 2.3. ***(Ito's Lemma)***
[28] Let $f(x,t)$ be a function, which has continuous partial derivatives $\frac{\partial f}{\partial x}$, $\frac{\partial^2 f}{\partial x^2}$ and $\frac{\partial f}{\partial t}$. Let $X(t)$ be an Ito process, which has an SDE form

$$dX(t) = \mu(X(t), t)dt + \sigma(X(t), t)dW(t), \ 0 \leq t \leq T.$$

Let $Y(t) = f(X(t), t), \ 0 \leq t \leq T$. Then $Y(t)$ is also an Ito process with SDE

$$\begin{aligned} dY(t) = &\left(\frac{\partial f}{\partial t}(X(t), t) + \mu(X(t), t)\frac{\partial f}{\partial x}(X(t), t) + \frac{\sigma^2(X(t), t)}{2}\frac{\partial^2 f}{\partial x^2}(X(t), t) \right) dt \\ &+ \sigma(X(t), t)\frac{\partial f}{\partial x}(X(t), t)dW(t). \end{aligned} \tag{2.9}$$

2.3.3 Geometric Brownian Motion

The construction of GBM is build on a Brownian motion with drift and scaling, which is stated in the following:

Definition 2.4. *[43] A stochastic process $Y(t)$ is said to be a Brownian motion with drift and scaling if $Y(t)$ is the solution of the stochastic differention equation (SDE)*

$$dY(t) = \mu dt + \sigma dW(t), \tag{2.10}$$

where μ and $\sigma > 0$ are constants.

Definition 2.5. *[42] A stochastic process $X(t)$ is said to be a geometric Brownian motion (GBM) if $X(t)$ is the solution of the stochastic differention equation (SDE)*

$$dX(t) = \mu X(t)dt + \sigma X(t)dW(t), \tag{2.11}$$

where μ and $\sigma > 0$ are constants.

The solution of SDE in Equation (2.11) is found using Ito's lemma on $f(x) = \ln(x)$ with $X(0) > 0$ as

$$X(t) = X(0)e^{(\mu - \frac{\sigma^2}{2})t + \sigma W(t)}. \tag{2.12}$$

Since we can easily change the starting point $X(0)$, we take it as 1 for simplicity. The basic properties of GBM are collected as

i) *Distributions*: For $t \in (0, \infty)$, $X(t)$ has the lognormal distribution with mean $(\mu - \sigma^2/2)t$ and standard deviation $\sigma\sqrt{t}$. The probability density function f_t and the cumulative distribution function F_t are

$$f_t(x) = \frac{1}{\sigma x\sqrt{2\pi t}} \exp\left(-\frac{[\ln(x) - (\mu - \sigma^2/2)t]^2}{2\sigma^2 t}\right),$$
$$F_t(x) = \Phi\left[\frac{\ln(x) - (\mu - \sigma^2/2)t}{\sigma\sqrt{t}}\right],$$

respectively, for $x \in (0, \infty)$, where Φ is the standard normal distribution function. Furthermore, the quantile function F_t^{-1} is

$$F_t^{-1} = \exp((\mu - \sigma^2/2)t + \sigma\sqrt{t})\Phi^{-1}(p),\ p \in (0, 1),$$

where Φ^{-1} is the quantile function of standard normal.

ii) *Moments*: For $n \in \mathbb{N}$ and $t \in [0, \infty)$, the nth moment of $X(t)$ is

$$\mathbb{E}[X_t^n] = \exp\left(n\mu t + \frac{\sigma^2}{2}t(n^2 - n)\right).$$

The mean and variance of $X(t)$ follow from n^{th} moment as

$$\mathbb{E}[X(t)] = e^{\mu t},$$
$$\mathbb{V}[X(t)] = e^{2\mu t}(e^{\sigma^2 t} - 1),$$

respectively.

2.3.4 Poisson and Compound Poisson Processes

Assume that $\mathcal{E}$ is a random variable with the probability density function $f_{\mathcal{E}}(t)$ and the cumulative distribution function $F_{\mathcal{E}}(t)$

$$f_{\mathcal{E}}(t) = \begin{cases} \lambda e^{-\lambda t}, & t \geq 0 \\ 0, & t < 0, \end{cases}, \tag{2.13}$$
$$F_{\mathcal{E}}(t) = 1 - e^{-\lambda t},\ t \geq 0,$$

where $\lambda > 0$ is a constant. $\mathcal{E}$ is said to be an exponential random variable with mean $\frac{1}{\lambda}$. Furthermore, one of the important property of the exponential distribution is memoryless, which can be hightlighted as

$$\begin{aligned} \mathbb{P}(\mathcal{E} > t + s | \mathcal{E} > s) &= \frac{\mathbb{P}(\mathcal{E} > t + s)}{\mathbb{P}(\mathcal{E} > s)} \\ &= \frac{e^{-\lambda(t+s)}}{e^{-\lambda s}} = e^{-\lambda t} = \mathbb{P}(\mathcal{E} > t). \end{aligned} \tag{2.14}$$

Consider a sequence $\mathcal{E}_1, \mathcal{E}_2, \ldots$ of independent exponential random variables with each having the same mean $\frac{1}{\lambda}$. We set up an event, called a jump, which occurs at the time of $\mathcal{E}_1, \mathcal{E}_2, \ldots$. Here, each of $\mathcal{E}_j,\ j = 1, 2, \ldots$, is called the interarrival times and the arrival times are defined as

$$A_n = \sum_{j=1}^{n} \mathcal{E}_j. \tag{2.15}$$

Moreover, A_n is nth jump time and has the gamma density

$$f_{A_n}(t) = \frac{t^{n-1}}{(n-1)!}\lambda^n e^{-\lambda t},\ t \geq 0. \tag{2.16}$$

The Poisson process $N(t)$ enumerates the number of jumps up to time t, which is displayed as

$$N(t) = \begin{cases} 0, \ 0 \leq t < A_1, \\ 1, \ A_1 \leq t < A_2, \\ \vdots \\ n, \ A_n \leq t < A_{n+1} \\ \vdots \end{cases} . \tag{2.17}$$

Since $\frac{1}{\lambda}$ is the expected time between jumps, the arriving times of jumps is an average rate of λ for a time unit. Thus, the Poisson process $N(t)$ has intensity λ.

Furthermore, $N(t)$ with intensity λ has the distribution

$$\mathbb{P}(N(t) = n) = \frac{(\lambda t)^n}{n!} e^{-\lambda t}, \ n = 0, 1, 2, \ldots. \tag{2.18}$$

One of the important property of Poisson Process is that it has stationary and independent increments, which is a consequence of the memorylessness of exponential random variables. The following Theorem 2.4 also indicates this.

Theorem 2.4. *[27] Let $N(t)$ be a Poisson process with λ intensity and $0 = t_0 < t_1 < \cdots < t_j < \cdots < t_n$. The increments*

$$N(t_1) - N(t_0), N(t_2) - N(t_1), \ldots, N(t_j) - N(t_{j-1}), \ldots, N(t_n) - N(t_{n-1})$$

are stationary and independent. Moreover,

$$\mathbb{P}(N(t_j) - N(t_{j-1}) = J) = \frac{\lambda^J (t_{j+1} - t_j)^J}{J!} e^{-\lambda(t_{j+1} - t_j)}, \ J = 0, 1, \ldots. \tag{2.19}$$

Consider a sequence of independent and identically distributed random variables $R_1, R_2, \ldots$ in which each has mean β. Additionally, each $R_i, \ i = 1, 2, \ldots$, is also independent of Poisson process $N(t)$. The compound Poisson process is defined as

$$Q(t) = \sum_{i=1}^{N(t)} R_i, \ t \geq 0. \tag{2.20}$$

The jump times of $Q(t)$ and $N(t)$ are the same; however, the difference betwwen them is their jumps sizes. $N(t)$ has the jump size 1, whereas $Q(t)$ has the jumps of random sizes denoted by random variables R_i.

As in the Poisson process $N(t)$, the increments of the compound Poisson process $Q(t)$ are stationary and independent.

Theorem 2.5. *[43] Let $Q(t)$ be a compound Poisson process and $0 = t_0 < t_1 < \cdots < t_j < \cdots < t_n$. The increments*

$$Q(t_1) - Q(t_0), Q(t_2) - Q(t_1), \ldots, Q(t_j) - Q(t_{j-1}), \ldots, Q(t_n) - Q(t_{n-1})$$

are stationary and independent. Moreover, the distributions of $Q(t_j) - Q(t_{j-1})$ and $Q(t_j - t_{j-1})$ are the same.

Let the moment generating function of R_i be

$$M_R(z) = \mathbb{E}[e^{zR_i}].$$

Then, the moment generating function of $Q(t)$ is

$$M_{Q(t)}(z) = \mathbb{E}[e^{zQ(t)}] = e^{\lambda t(M_R(z)-1)}. \tag{2.21}$$

If R_i's are not random but a constant value r, then $Q(t) = rN(t)$. This yields the moment generating function of $rN(t)$ as

$$M_{rN(t)}(z) = e^{\lambda t(e^{zr}-1)}.$$

By taking $r = 1$, we have the moment genrating function of $N(t)$ as

$$M_{N(t)}(z) = e^{\lambda t(e^{z}-1)}. \tag{2.22}$$

2.3.4.1 Jump Processes

Let $(\Omega, \mathcal{F}, \mathbb{P})$ be a probability space with filtration $\mathcal{F}(t),\ t \geq 0$.

Define a stochastic process $K(t)$ such that K is allowed to have jumps, i.e.,

$$K(t) = K(0) + I(t) + R(t) + J(t), \tag{2.23}$$

where $X(0)$ is the initial value,

$$I(t) = \int_0^t \Gamma(s) dW(s)$$

is an Ito integral of an adapted process $\Gamma(t)$ with respect to the filtration and $W(t)$ is a Brownian motion,

$$R(t) = \int_0^t \Theta(s)ds$$

is a Riemann integral and $\Theta(t)$ is also adapted, and $J(t)$ is an adapted pure jumps process with $J(0) = 0$. Moreover, $J(t)$ is right-continuous, i.e., $J(t)$ is the value after the jump and we denote $J(t-)$ is the value right before the jump.

The continuous part of $X(t)$ is denoted by

$$K^c(t) = K(0) + I(t) + R(t).$$

Moreover, the left continuous part of $X(t)$ is

$$K(t-) = K(0) + I(t) + R(t) + J(t-).$$

Thus, the jump size of X at time t is

$$\Delta K(t) = K(t) - K(t-).$$

Let $\Psi(t)$ be an adapted process and $X(t)$ of the form given in Equation (2.23). The stochastic integral of Ψ with respect to X is

$$\int_0^t \Psi(s)dK(s) = \int_0^t \Psi(s)\Gamma(s)dW(s) + \int_0^t \Psi(s)\Theta(s)ds + \sum_{0<s\leq t} \Psi(s)\Delta J(s). \tag{2.24}$$

In differentiation form,

$$\Psi(t)dK(t) = \Psi(t)\Gamma(t)dW(t) + \Psi(t)\Theta(t)dt + \Psi(t)dJ(t). \tag{2.25}$$

Now, our aim is to compute quadratic and cross variations of jump process K on a time interval $[0, T]$. Consider the partition on $[0, T]$ of the form

$$0 = t_0 < t_1 < \cdots < t_n = T.$$

Let $||\Pi|| = \underset{j=0,t_1,\ldots,n-1}{max} t_{j+1} - t_j$ be the longest subinterval. Define

$$Q_v(K) = \sum_{j=0}^{n-1} (K(t_{j+1}) - K(t_j))^2.$$

The quadratic variation of K on $[0, T]$ is

$$[K, K](T) = \lim_{||\Pi||\to 0} Q_v(K). \tag{2.26}$$

Let $K_1(t)$ and $K_2(t)$ be jump processes. Define

$$C_v(K_1, K_2) = \sum_{j=0}^{n-1} (K_1(t_{j+1}) - K_1(t_j))(K_2(t_{j+1}) - K_2(t_j)).$$

The cross variation of K_1 and K_2 on $[0, T]$ is

$$[K_1, K_2](T) = \lim_{||\Pi||\to 0} C_v(K_1, K_2). \tag{2.27}$$

According to these notations, we give the quadratic and cross variations of jump processes in the following Theorem 2.6.

Theorem 2.6. *[46] Let $K_1(t) = K_1(0) + I_1(t) + R_1(t) + J_1(t)$ and $K_2(t) = K_2(0) + I_2(t) + R_2(t) + J_2(t)$ be jump processes, where*

$$I_i(t) = \int_0^t \Gamma_i(s)dW(s),\ R_i(t) = \int_0^t \Theta_i(s)ds,\ i = 1, 2,$$

$J_1(t)$ and $J_2(t)$ are pure jump processes. Then

$$[K_1, K_1][T] = \int_0^T \Gamma_1^2(s)ds + \sum_{0<s\leq t} (\Delta J_1(s))^2, \tag{2.28}$$

$$[K_1, K_2][T] = \int_0^T \Gamma_1(s)\Gamma_2(s)ds + \sum_{0<s\leq t} \Delta J_1(s)\Delta J_2(s). \tag{2.29}$$

For the solution of a stochastic jump processes, it is required to use Ito-Doeblin formula, which is indicated in the following Theorem 2.7

Theorem 2.7. ***(Ito-Doeblin formula)***
[46] Let $K(t)$ be a jump process and a function $f(.)$ have the continuous first order, $f'(.)$, and second order, $f''(.)$ derivatives. Then

$$\begin{aligned} f(K(t)) =& f(X(0)) + \int_0^t f'(K(s))dK^c(s) + \frac{1}{2}\int_0^t f''(K(s))d[K^c, K^c](s) \\ &+ \sum_{0<s\leq t} [f(K(s)) - f(K(s-))], \end{aligned} \tag{2.30}$$

where $K^c(t)$ is the continuous part of the jump process $K(t)$.

For the determination of solution, it is useful to understand stochastic exponential terminology presented in Theorem 2.8 below.

Theorem 2.8. ***(Doleans-Dade Exponential)***
[33] Let $K(t)$ be a jump process. The stochastic expnential of (Doleans-Dade exponential) the process K is also a process defined to be

$$\varepsilon^K(t) = exp\left(K^c(t) - \frac{1}{2}[K^c, K^c](t)\right) \prod_{0<s\leq t} (1 + \Delta K(s)). \tag{2.31}$$

CHAPTER 3

OPTIMAL PREMIUM ALLOCATION

This chapter presents the analytical derivations of stop-loss reinsurance cost, variance and covariance under dependence structure. It also gives the derivations for exposure curves under the assumption that losses are distributed Pareto, Gamma, and Inverse Gamma.

3.1 Implemenation of distributional approach

Our aim is to investigate the effects of correlation coefficient on the estimation of premium valuation for the insurer and the reinsurer. Furthermore, because of the other variations in loss distributions and the direct impact of the dependence formed in reinsurance agreements with respect to the upper and lower bounds (retention and cap), we analyze the optimal stop-loss contract if the aggregate claims are distributed by Pareto, Gamma, and Inverse Gamma.

3.1.1 The costs of insurer and reinsurer

The stop-loss contract is started or rejected based on the positions including the retention or both retention and cap levels when the claim occurs. With respect to these parameters' values, expected costs and premiums vary for both parties, creating a natural dependency between claims to be paid. Figs. 3.1a and 3.1b indicate that the risk margin follows an inverse pattern between the insurer and the reinsurer for each case.

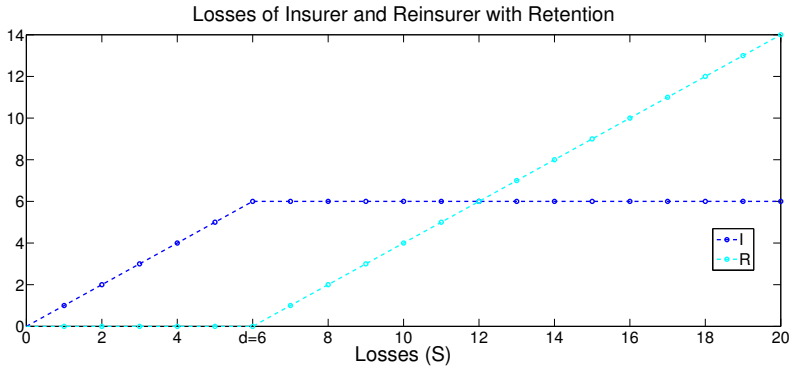

(a) Case I

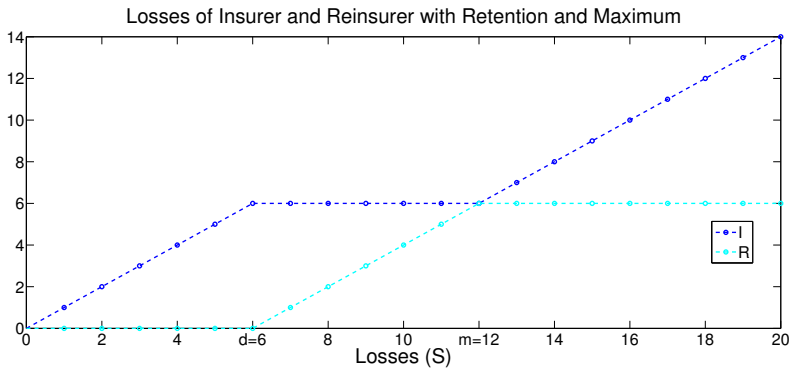

(b) Case II

Figure 3.1: The risk share between parties

Suppose that the total claim costs in one period is denoted by the random variable S and shared among the insurer and the reinsurer. Moreover, the costs of insurer and reinsurer are denoted by I and R, respectively. We can represent the costs' partitions on S as

$$S = I + R. \tag{3.1}$$

If we use a well-known distribution for S, we are able to obtain the probability distributions for insurer and reinsurer. This directs us to derive the expressions of the expected costs and the variance for each contract types (Case I and Case II) analytically if they exist. Although these derivations are unambiguous in actuarial literature, the custom-made analytics with respect to certain distributions are distinctively presented in this chapter.

In [14], the aggregate loss distribution function, the distributions functions for the

costs of insurer and reinsurer, denoted by $F_S(s)$, $F_I(s)$, and $F_R(s)$ respectively, the expected value, the variance, the correlation coefficient, dentoed by $\mathbb{E}[.]$, $\mathbb{V}[.]$, and $\rho(.,.)$ are provided. The costs of insurer and reinsurer under the contracts with retention (Case I) are defined as

$$I = min(S, d), \qquad \text{and } F_I(s) = \begin{cases} F_S(s), & s < d \\ 1, & s \geq d \end{cases}, \tag{3.2}$$

$$R = max(S - d, 0), \text{ and } F_R(s) = F_S(s + d).$$

Proposition 3.1. *[14] The expected values of costs of insurer and reinsurer, their variances and correlation coefficient with respect to retention level d are given as*

$$\mathbb{E}[I(d)] = \mathbb{E}[S] - \mathbb{E}[R(d)], \tag{3.3}$$

$$\mathbb{E}[R(d)] = \int_d^\infty [1 - F_S(s)]ds, \tag{3.4}$$

$$\mathbb{V}[I(d)] = \mathbb{V}[S] - \mathbb{V}[R(d)] - 2Cov[I(d), R(d)], \tag{3.5}$$

$$\mathbb{V}[R(d)] = 2\int_d^\infty s[1 - F_S(s)]ds + \mathbb{E}[R(d)](-2d - \mathbb{E}[R(d)]), \tag{3.6}$$

$$\rho(I(d), R(d)) = \frac{\mathbb{E}[R(d)](d - \mathbb{E}[S] + \mathbb{E}[R(d)])}{\sqrt{\mathbb{V}[R(d)]\left(\mathbb{V}[S] + \mathbb{E}[R(d)](d + \mathbb{E}[S]) - 2\int_d^\infty s[1 - F_S(s)]ds\right)}}. \tag{3.7}$$

The correlation coefficient between the insurer and the reinsurer specified in Eq. (3.7) is a purely d-dependent function; thus, the retenion level which maximizes the correlation coefficient results in the best option for the insurer and the reinsurer.

For a stop-loss contract type with both retention, d, and maximum, m, offers the cost partition for the insurer and the reinsurer, which is given as

$$I(d, m) = min(S, d) + max(S - m, 0), \tag{3.8}$$

$$R(d, m) = min(m - d, max(S - d, 0)). \tag{3.9}$$

The distribution functions for the costs of insurer and reinsurer in this contract type

(Case II) are

$$F_I(s) = \begin{cases} F_S(s), & s < d \\ F_S(s+m-d), & s \geq d, \end{cases},$$
$$F_R(s) = \begin{cases} F_S(s+d), & s < m-d \\ 1, & s \geq m-d, \end{cases}, \tag{3.10}$$

respectively. Using the same methodology as in Case I, the expressions of the expected costs, variances and correlation coefficient are obtained in Proposition 3.2.

Proposition 3.2. *[14] The expected values of costs of insurer and reinsurer, their variances and correlation coefficient with respect to retention level d and maximum m are*

$$\mathbb{E}[I(d,m)] = \mathbb{E}[S] - \mathbb{E}[R(d,m)], \tag{3.11}$$

$$\mathbb{E}[R(d,m)] = \mathbb{E}[R(d)] - \mathbb{E}[R(m)], \tag{3.12}$$

$$\mathbb{V}[I(d,m)] = \mathbb{V}[S] - \mathbb{V}[R(d,m)] - 2Cov[I(d,m), R(d,m)], \tag{3.13}$$

$$\begin{aligned} \mathbb{V}[R(d,m)] &= \mathbb{V}[R(d)] - \mathbb{V}[R(m)] \\ &\quad + 2\mathbb{E}[R(m)](\mathbb{E}[R(d)] - \mathbb{E}[R(m)] + d - m) \end{aligned} \tag{3.14}$$

$$\rho(I(d,m), R(d,m)) = \frac{Cov[I(d), R(d)] - (2d-m)\mathbb{E}[R(m)]}{\sqrt{\mathbb{V}[R(d,m)](\mathbb{V}[S] - \mathbb{V}[R(d,m)] - 2Cov[I(d,m), R(d,m)])}}. \tag{3.15}$$

where $\mathbb{E}[R(.)]$ and $\mathbb{V}[R(.)]$ are mentioned in Propositon 3.1. The term in Eq. (3.15), $\rho(I(d,m), R(d,m))$, is a function determined by the bounds agreed upon the contracts. The derivations related to the losses distributed Normal, Gamma, and translated Gamma are presented in [14]. However, Pareto, Gamma, and Inverse Gamma are the most common distributions for loss amounts in the literature, [9] and [47], because of the following characteristics: (i) the Pareto distribution captures the large losses since it has very tick tail; (ii) the fact that Gamma distribution is closed under convolution and right-skewed makes it infinitely divisible and applicable for extreme claims; (iii) the heavy-tail of Inverse Gamma is useful to analyse larger claims explicitly.

Furthermore, Pareto and Inverse Gamma have a comparably heavy tail than Gamma. The statiscal properties of Gamma and Inverse Gamma are better than Pareto, for instance, if a random variable Y has a distibution Gamma with parameters a and b, then $\frac{1}{Y}$ is distributed by Inverse Gamma with parameters a and $\frac{1}{b}$.

The analytical formulations are derived for the expected value, variance and the correlation coefficient under both contract types (Case I and Case II) in this chapter as well.

3.1.1.1 Aggregate claims with Pareto distribution

Suppose that the total costs of claims, S, has Pareto distribution with the shape parameter a and the scale parameter b where $a, b \in \mathbb{R}^+$. The expected costs and the variance of the insurer and their covariance for Case I and Case II are derived and presented below.

Proposition 3.3. *Under the assumption that $S \sim$ Pareto(a, b), the expected costs and the variances of the insurer and the reinsurer under Case I with respect to retention level d are*

$$\mathbb{E}[I(d)] = \frac{b\big(a - (b/d)^{(a-1)}\big)}{a-1}, \tag{3.16}$$

$$\mathbb{E}[R(d)] = \frac{b^a d^{1-a}}{a-1}, \tag{3.17}$$

$$\mathbb{V}[I(d)] = \frac{ab^2 - 2a(a-2)b^a d^{1-a}[d-b] + (a-2)b^{a+1}d^{2-2a}[b^{a-1}-2]}{(a-1)^2(a-2)}, \tag{3.18}$$

$$\mathbb{V}[R(d)] = \frac{b^a d^{(2-a)}\Big[2 - (b/d)^a(a-2)\Big]}{(a-1)^2(a-2)}, \tag{3.19}$$

$$Cov[I(d), R(d)] = \frac{ab^a d^{1-a}(d-b) + b^a d^{(2-a)}\Big[(b/d)^a - 1\Big]}{(a-1)^2}, \tag{3.20}$$

respectively.

Proposition 3.4. *Under the assumption that $S \sim$ Pareto(a, b), the expected costs and the variances of the insurer and the reinsurer under Case II with respect to retention level d and the maximum level m are*

$$\mathbb{E}[I(d,m)] = \frac{a^2b - ab - b^a[d^{1-a} - m^{1-a}]}{a-1}, \tag{3.21}$$

$$\mathbb{E}[R(d,m)] = \frac{b^a}{a-1}\Big[d^{1-a} - m^{1-a}\Big], \tag{3.22}$$

$$\begin{aligned}\mathbb{V}[I(d,m)] = &-\frac{2b^a d m^{1-a}}{a-1} + \frac{b^{2a}m^{2(1-a)}\Big[2d^{2(1-a)} - 1\Big]}{(a-1)^2} \\ &+ \frac{b^a d^{1-a}\Big[2(1-a)d + 2b^a - d(b/d)^a\Big] + 2b^{a-+1}d^{1-a}\Big[a - b^{a-1}d^{1-a}\Big]}{(a-1)^2} \\ &+ \frac{ab^2 - 2b^a\Big[d^{2-a} - m^{2-a}\Big]}{(a-1)^2(a-2)},\end{aligned} \tag{3.23}$$

$$\begin{aligned}\mathbb{V}[R(d,m)] = &\frac{b^{2a}}{(a-1)^2}\Big[(m^{1-a} - d^{1-a})^2 - 2(m^{2(1-a)} + d^{1-a})\Big] \\ &+ \frac{2b^a}{(a-1)^2(a-2)}\Big[d^{2-a} - m^{2-a} + (a-1)(a-2)m^{1-a}(d-m)\Big],\end{aligned} \tag{3.24}$$

$$Cov[I(d,m), R(d,m)] = \frac{(2d-m)b^a m^{1-a}}{a-1} + \frac{b^a d^{1-a}}{(a-1)^2}\Big[a(d-b) + d^{1-a}(b^a - d^a)\Big], \tag{3.25}$$

respectively.

3.1.1.2 Aggregate claims with Gamma distribution

Suppose that the aggregate costs of claims, S, has Gamma distribution with the shape parameter a and the scale parameter b where $a, b \in \mathbb{R}^+$. The expected costs and the variance of the insurer and their covariance for Case I and Case II are derived and presented below.

The derived expressions in Propositions 3.5 and 3.6 require the functions of the upper and lower incomplete gamma, $\Gamma(s,x)$, $\gamma(s,x)$, $x > 0$ and the gamma, $\Gamma(s)$, which are defined as

$$\Gamma(s,x) = \int_x^\infty t^{s-1}e^{-t}\,dt, \;\; \gamma(s,x) = \int_0^x t^{s-1}e^{-t}\,dt, \;\; \Gamma(x) = \int_0^\infty t^{s-1}e^{-t}\,dt. \tag{3.26}$$

In short, the relation between the incomplete gamma functions and gamma function can be written as

$$\Gamma(s,x)+\gamma(s,x)=\Gamma(x).$$

Proposition 3.5. *Under the assumption that $S \sim$ Gamma(a,b), the expected costs and the variances of the insurer and the reinsurer under Case I with respect to retention level d are*

$$\mathbb{E}[I(d)] = \frac{(ab+d)\Gamma(a,bd) - b\Gamma(a+1,bd) + ab\gamma(a,bd)}{\Gamma(a)}, \tag{3.27}$$

$$\mathbb{E}[R(d)] = \frac{1}{\Gamma(a)}\Big[b\Gamma(a+1,bd) - d\Gamma(a,bd)\Big], \tag{3.28}$$

$$\begin{aligned}\mathbb{V}[I(d)] &= ab^2 + \mathbb{E}[R(d)]\Big(2d + \mathbb{E}[R(d)]\Big) \qquad (3.29)\\ &\quad + \frac{\Gamma(a,bd)}{\Gamma(a)}\Big[2abd(b^{a+1}-1) - d^2(2b^{a+1}+1)\Big]\\ &\quad - \frac{b^2\Gamma(a+1,bd)}{\Gamma(a)} - 2\left(\frac{1}{\Gamma(a)}\Big[b\Gamma(a+1,bd) - d\Gamma(a,bd)\Big]\right)^2, \qquad (3.30)\end{aligned}$$

$$\begin{aligned}\mathbb{V}[R(d)] &= \mathbb{E}[R(d)]\Big(-2d - \mathbb{E}[R(d)]\Big) \qquad (3.31)\\ &\quad + \frac{1}{\Gamma(a)}\Big[b^2\Gamma(a+1,bd) - d^2\Gamma(a,bd)\Big],\end{aligned}$$

$$\begin{aligned}Cov[I(d),R(d)] &= \left(\frac{1}{\Gamma(a)}\Big[b\Gamma(a+1,bd) - d\Gamma(a,bd)\Big]\right)^2 \qquad (3.32)\\ &\quad - \frac{d\Gamma(a,bd)}{\Gamma(a)}\Big[(d-ab)(b^{a+1}d^{a-1}-1)\Big],\end{aligned}$$

respectively.

Proposition 3.6. *Under the assumption that $S \sim$ Gamma(a, b), the expected costs and the variances of the insurer and the reinsurer under Case II with respect to retention level d and the maximum level m are*

$$\mathbb{E}[I(d,m)] = \frac{\Big[ab - 2(b^2-1)d\Big]\Gamma(a,bd) + \Big[ab - 2(b^2-1)m\Big]\Gamma(a,bm)}{2\Gamma(a)} + \frac{ab\Big(\gamma(a,bd) + \gamma(a,bm)\Big) + (bd)^a e^{-bd} + (bm)^a e^{-bm}}{2\Gamma(a)}, \tag{3.33}$$

$$\mathbb{E}[R(d,m)] = \frac{b^2-1}{\Gamma(a)}\Big[d\Gamma(a,bd) - m\Gamma(a,bm)\Big] - \frac{b^a}{\Gamma(a)}\Big[d^a e^{-bd} - m^a e^{-bm}\Big], \tag{3.34}$$

$$\begin{aligned}\mathbb{V}[I(d,m)] = {} & ab^2 + \mathbb{E}[R(d,m)]\Big[\mathbb{E}[R(d,m)] + 2ab\Big] \\ & - \frac{1}{\Gamma(a)}\Big[b^2(\Gamma(a+2,bd) - \Gamma(a+2,bm)) + 2b(m-d)\Gamma(a+1,bd)\Big] \\ & + \frac{1}{\Gamma(a)}\Big[(m^2+2dm)\Gamma(a,bd)\Big] \\ & - 2\Big(\mathbb{E}[R(d,m)] - \frac{1}{\Gamma(a)}\Big[b\Gamma(a+1,bm) - d\Gamma(a,bm)\Big]\Big)^2,\end{aligned} \tag{3.35}$$

$$\begin{aligned}\mathbb{V}[R(d,m)] = {} & \frac{1}{\Gamma(a)}\Big[b^2(\Gamma(a+2,bd) - \Gamma(a+2,bm)) - d^2\Gamma(a,bd) - m^2\Gamma(a,bm)\Big] \\ & + \mathbb{E}[R(d,m)]\Big[-\mathbb{E}[R(d,m)] - 2d\Big],\end{aligned} \tag{3.36}$$

$$\begin{aligned}Cov[I(d,m), R(d,m)] = {} & \Big(\mathbb{E}[R(d,m)] - \frac{1}{\Gamma(a)}\Big[b\Gamma(a+1,bm) - d\Gamma(a,bm)\Big]\Big)^2 \\ & + \frac{m-d}{\Gamma(a)}\Big[b\Gamma(a+1,bd) - d\Gamma(a,bd)\Big] + \mathbb{E}[R(d,m)](d-ab),\end{aligned} \tag{3.37}$$

respectively.

3.1.1.3 Aggregate claims with Inverse Gamma distribution

Suppose that the total costs of claims, S, has Inverse Gamma distribution with the shape parameter a and the scale parameter b where $a, b \in \mathbb{R}^+$. The expected costs and the variance of the insurer and their covariance for Case I and Case II are derived and presented below.

Proposition 3.7. *Under the assumption that $S \sim$ IG(a, b), the expected costs and the*

variances of the insurer and the reinsurer under Case I with respect to retention level d are

$$\mathbb{E}[I(d)] = \frac{b\Big[\Gamma(a,b/d) - (a-1)\gamma(a-1,b/d)\Big] + \gamma(a,b/d)\Big[1+(a-1)d\Big]}{(a-1)\Gamma(a)} \tag{3.38}$$

$$\mathbb{E}[R(d)] = \frac{1}{\Gamma(a)}\Big[b\gamma(a-1,b/d) - d\gamma(a,b/d)\Big], \tag{3.39}$$

$$\begin{aligned}\mathbb{V}[I(d)] = {} & \frac{b^2}{(a-1)^2(a-2)} + \Big(\mathbb{E}[R(d)]\Big)^2 \\ & + \frac{b^2\gamma(a-2,b/d) + 2(bd-1)\gamma(a-1,b/d) + (2-d^2)\gamma(a,b/d)}{\Gamma(a)} \\ & - 2\left[\frac{1}{\Gamma(a)}[b\gamma(a-1,b/d) - d\gamma(a,b/d)]\right]^2,\end{aligned} \tag{3.40}$$

$$\begin{aligned}\mathbb{V}[R(d)] = {} & \frac{1}{\Gamma(a)}\Big[b^2\gamma(a-2,b/d) - 2db\gamma(a-1,b/d) + d^2\gamma(a,b/d)\Big] \\ & - \Big(\mathbb{E}[R(d)]\Big)^2,\end{aligned} \tag{3.41}$$

$$\begin{aligned}Cov[I(d),R(d)] = {} & \left[\frac{1}{\Gamma(a)}\Big[b\gamma(a-1,b/d) - d\gamma(a,b/d)\Big]\right]^2 \\ & + \frac{1}{\Gamma(a)}\left[\Gamma(a,b/d) - \Gamma(a-1,b/d) + (b-d)\left(d - \frac{b}{a-1}\right)\right],\end{aligned} \tag{3.42}$$

respectively.

Proposition 3.8. *Under the assumption that $S \sim IG(a,b)$, the expected costs and the variances of the insurer and the reinsurer under Case II with respect to retention level d and the maximum level m are*

$$\mathbb{E}[I(d,m)] = \frac{b}{a-1} - \frac{b^a}{\Gamma(a)}\Big[d^{1-a}e^{-b/d} - m^{1-a}e^{-m/d}\Big] \tag{3.43}$$
$$- \frac{1}{\Gamma(a)}\Big[(b-d)\gamma(a-1,b/d) - (b-m)\gamma(a-1,b/m)\Big],$$
$$\mathbb{E}[R(d,m)] = \frac{1}{\Gamma(a)}\Big[(b-d)\gamma(a-1,b/d) - (b-m)\gamma(a-1,b/m)\Big] \tag{3.44}$$
$$+ \frac{b^a}{\Gamma(a)}\Big[d^{1-a}e^{-b/d} - m^{1-a}e^{-m/d}\Big],$$
$$\mathbb{V}[I(d,m)] = \frac{b^2}{(a-1)^2(a-2)} - m^2 + d^2 + \mathbb{E}[R(d,m)]\Big[\mathbb{E}[R(d,m)] - \frac{2b}{a-1}\Big] \tag{3.45}$$
$$- \frac{2(m-d)}{\Gamma(a)}\left[\frac{1}{\Gamma(a)}[b\Gamma(a+1,bm) - m\Gamma(a,bm)]\right]$$
$$+ \sum_{k=0}^{\infty}\frac{(-1)^k(m^{2-a-k} - d^{2-a-k})}{k!(a+k)(2-a-k)},$$
$$\mathbb{V}[R(d,m)] = m^2 - d^2 - \sum_{k=0}^{\infty}\frac{(-1)^k(m^{2-a-k} - d^{2-a-k})}{k!(a+k)(2-a-k)} \tag{3.46}$$
$$+ \mathbb{E}[R(d,m)]\Big[-\mathbb{E}[R(d,m)] - 2d\Big],$$
$$Cov[I(d,m),R(d,m)] = \Big(\mathbb{E}[R(d,m)] - \frac{1}{\Gamma(a)}\Big[b\Gamma(a+1,bm) - m\Gamma(a,bm)\Big]\Big)^2 \tag{3.47}$$
$$= \frac{m-d}{\Gamma(a)}\left[\frac{1}{\Gamma(a)}[b\Gamma(a+1,bm) - m\Gamma(a,bm)]\right]$$
$$+ \mathbb{E}[R(d,m)]\left(d - \frac{b}{a-1}\right),$$

respectively.

The functions of incomplete gamma and gamma functions given in Eqs. (3.26) are used in Propositions 3.7 and 3.8. Combining with the exposure curves, the analytical derivations for Pareto, Gamma, and Inverse Gamma under Case I and Case II are our main tools to find the optimal values of retention, maximum , and premimum values in the contract agreement between the insurer and the reinsurer. A summary of these derivations is presented in the following Tables 3.1 and 3.2), as well as the sketches of some propositions in Appendix A.1.

Table 3.1: The derivations of the statistics under Case I

	Pareto	Gamma	Inverse Gamma
$\mathbb{E}[R(d)]$	$\frac{b^a d^{1-a}}{a-1}$	$\frac{1}{\Gamma(a)}[b\Gamma(a+1,bd) - d\Gamma(a,bd)]$	$\frac{1}{\Gamma(a)}[b\gamma(a-1,b/d) - d\gamma(a,b/d)]$
$\mathbb{V}[R(d)]$	$\frac{b^a d^{(2-a)}[2-(b/d)^a(a-2)]}{(a-2)(a-1)^2}$	$\mathbb{E}[R(d)](-2d - \mathbb{E}[R(d)])$ $+ \frac{1}{\Gamma(a)}[b^2\Gamma(a+1,bd) - d^2\Gamma(a,bd)]$	$\frac{1}{\Gamma(a)}[b^2\gamma(a-2,b/d) - 2db\gamma(a-1,b/d) + d^2\gamma(a,b/d)]$ $-(\mathbb{E}[R(d)])^2$
$Cov[I(d),R(d)]$	$\frac{ab^a d^{1-a}[d-b] + b^a d^{(2-a)}[(b/d)^a - 1]}{(a-1)^2}$	$\left(\frac{1}{\Gamma(a)}[b\Gamma(a+1,bd) - d\Gamma(a,bd)]\right)^2$ $-\frac{d\Gamma(a,bd)}{\Gamma(a)}[(d-ab)(b^{a+1}d^{a-1}-1)]$	$\left[\frac{1}{\Gamma(a)}[b\gamma(a-1,b/d) - d\gamma(a,b/d)]\right]^2$ $+\frac{1}{\Gamma(a)}\left[\Gamma(a,b/d) - \Gamma(a-1,b/d) + (b-d)\left(d - \frac{b}{a-1}\right)\right]$

Table 3.2: The derivations of the statistics under Case II

	Pareto	Gamma	Inverse Gamma
$\mathbb{E}[R(d,m)]$	$\frac{b^a}{a-1}[d^{1-a} - m^{1-a}]$	$\frac{b^2-1}{\Gamma(a)}[d\Gamma(a,bd) - m\Gamma(a,bm)]$ $-\frac{b^a}{\Gamma(a)}[d^a e^{-bd} - m^a e^{-bm}]$	$\frac{1}{\Gamma(a)}[(b-d)\gamma(a-1,b/d) - (b-m)\gamma(a-1,b/m)]$ $+\frac{b^a}{\Gamma(a)}[d^{1-a}e^{-b/d} - m^{1-a}e^{-m/d}]$
$\mathbb{V}[R(d,m)]$	$\frac{b^{2a}}{(a-1)^2}[(m^{1-a}-d^{1-a})^2 - 2(m^{2(1-a)}+d^{1-a})]$ $+\frac{2b^a}{(a-1)^2(a-2)}\left[d^{2-a} - m^{2-a} + (a-1)(a-2)m^{1-a}(d-m)\right]$	$\frac{1}{\Gamma(a)}[b^2(\Gamma(a+2,bd) - \Gamma(a+2,bm)) - d^2\Gamma(a,bd) - m^2\Gamma(a,bm)]$ $+\mathbb{E}[R(d,m)][-\mathbb{E}[R(d,m)] - 2d]$	$m^2 - d^2 - \sum_{k=0}^{\infty}\frac{(-1)^k(m^{2-a-k} - d^{2-a-k})}{k!(a+k)(2-a-k)}$ $+\mathbb{E}[R(d,m)][-\mathbb{E}[R(d,m)] - 2d]$
$Cov[I(d,m),R(d,m)]$	$\frac{(2d-m)b^a m^{1-a}}{a-1}$ $+\frac{b^a d^{1-a}}{(a-1)^2}[a(d-b) + d^{1-a}(b^a - d^a)]$	$(\mathbb{E}[R(d,m)] - \frac{1}{\Gamma(a)}[b\Gamma(a+1,bm) - d\Gamma(a,bm)])^2$ $+\frac{m-d}{\Gamma(a)}[b\Gamma(a+1,bd) - d\Gamma(a,bd)] + \mathbb{E}[R(d,m)(d-ab)$	$(\mathbb{E}[R(d,m)] - \frac{1}{\Gamma(a)}[b\Gamma(a+1,bm) - m\Gamma(a,bm)])^2$ $=\frac{m-d}{\Gamma(a)}\left[\frac{1}{\Gamma(a)}[b\Gamma(a+1,bm) - m\Gamma(a,bm)]\right]$ $+\mathbb{E}[R(d,m)]\left(d - \frac{b}{a-1}\right)$

3.2 Premium Shares using Exposure Curves

For the case of per risk, exposure rating is associated to risk profiles based on previous observation. A risk band is a summary of similar sized risks in the same risk category. For the rating, risks in a single band are regarded homogeneous; therefore, they can be modeled using a single loss distribution function. Our aim is to achieve acceptable partition of the specific risk between the insurer and the reinsurer by using the exposure rating and the risk band, which is carried out in two phases. To begin, by employing a convenient loss ratio, we estimate the risk premiums as a ratio of earned premium. Secondly, the risk premiums are transferred to a reinsurer with respect to the retention and the maximum, which necessitates the use of a loss distribution function. Furthermore, for a analogous risk types involved in large portfolios, the correct loss distribution function is derived, which are called exposure curves ($G(.)$) and evaluate the ratio of risk premiums in terms of a predetermined deductible and maximum.

The exposure curves under Case I and Case II are derived in the form of analytical expressions using the selected distribution on the aggregate claim amounts.

The aggregate claims has a range over $\mathbb{R}^+$; however, it is important to modify the aggregate claims using the maximum possible loss, M, in order to obtain a realistic approach. For this reason, let X be a new random variable with the distribution function $F_X(.)$ and X is defined as $X = \frac{S}{M}$.

The ratio between the insurer's expected loss and the expected aggregate loss is defined as, [6],

$$G(k) = \frac{\int_0^k [1 - F(x)]dx}{\int_0^\infty [1 - F(x)]dx}, \tag{3.48}$$

where $k = \frac{d}{M}$. In fact, Eq. (3.48) is adjusted for Case I as

$$G(k) = 1 - \frac{\int_k^\infty [1 - F(x)]dx}{\mathbb{E}[X]}. \tag{3.49}$$

The exposure curves under Case II are derived and we present the expressions as below.

Proposition 3.9. *The exposure curve with respect to the limits $k = \frac{d}{M}$ and $l = \frac{m}{M}$ is*

$$G(k,l) = 1 - \frac{\int_k^\infty [1-F(x)]dx - \int_l^\infty [1-F(x)]dx}{\int_0^\infty [1-F(x)]dx}. \tag{3.50}$$

The usage of exposure curves, $G(.)$, which matches $G(k)$ and $G(k,l)$ for the contract types Case I and Case II, respectively, partites the risk premium ($P(.)$) between the insurer and the reinsurer. The premium of insurer and reinsurer, which are denoted by ($PI(.)$) and ($PR(.)$), respectively are found for two cases as

$$PI(.) = G(.)P, \quad PR(.) = (1-G(.))P, \tag{3.51}$$

Under this partition, the loss ratios of insurer and reinsurer become

$$PIr(.) = \frac{\mathbb{E}[I(.)]}{PI(.)}, \tag{3.52a}$$

$$PRr(.) = \frac{\mathbb{E}[R(.)]}{PR(.)}, \tag{3.52b}$$

respectively.

The maximum possible loss adjustment on the upper limit is employed on the distribution of $X = \frac{S}{M}, M > 0$, where S has the selected distribution under the assumptions of Pareto(a,b), Gamma(a,b), and IG(a,b). Then, X has the distributions

$$X \stackrel{d}{=} \text{Pareto}\left(a, \frac{b}{M}\right), \; X \stackrel{d}{=} \text{Gamma}\left(a, \frac{b}{M}\right), \text{ and } X \stackrel{d}{=} \text{IG}\left(a, \frac{b}{M}\right)$$

with distribution functions

$$F_X^{\text{P}}(x) = 1 - \frac{b}{M\,x}, \; F_X^{\text{G}}(x) = \frac{\gamma(a, \frac{b}{M}x)}{\Gamma(a)}, \text{ and } F_X^{\text{IG}}(x) = \frac{\Gamma(a, \frac{b/M}{x})}{\Gamma(a)},$$

respectively.

Proposition 3.10. *Suppose that X has the distributions Pareto$(a, b/M)$, Gamma$(a, b/M)$, and IG$(a, b/M)$. In Case I, the exposure curves ($G_P(k)$, $G_G(k)$, $G_{IG}(k)$) for these distributions are*

$$G_P(k) = \frac{ak^{a-1} - (bM)^{a-1}}{ak^{a-1}}, \tag{3.53}$$

$$G_G(k) = \frac{\gamma(a+1, \frac{b}{M}k)}{\Gamma(a)} - \frac{kM}{ab}\left(1 - \frac{\gamma(a, \frac{b}{M}k)}{\Gamma(a)}\right), \tag{3.54}$$

$$G_{IG}(k) = \frac{(a-1)\Gamma(a-1, \frac{b}{Mk})}{\Gamma(a)} - \frac{kM(a-1)}{b}\frac{[\Gamma(a, \frac{b}{Mk}) - \Gamma(a)]}{\Gamma(a)}, \tag{3.55}$$

respectively, where $k = \frac{d}{M}$.

Proposition 3.11. *Suppose that* X *has the distributions Pareto*$(a, b/M)$*, Gamma*$(a, b/M)$*, and IG*$(a, b/M)$*. In Case II, the exposure curves (*$G_P(k,l)$*,* $G_G(k,l)$*,* $G_{IG}(k,l)$*) for these distributions are*

$$G_P(k,l) = \frac{aM^{a-1} - b^{a-1}(k^{1-a} - l^{1-a})}{aM^{a-1}}, \tag{3.56}$$

$$\begin{aligned} G_G(k,l) = 1 &+ \frac{\gamma(a+1, \frac{b}{M}k)}{\Gamma(a)} - \frac{\gamma(a+1, \frac{b}{M}l)}{\Gamma(a)} + \frac{(k-l)M}{ab} \\ &- k\frac{\gamma(a, \frac{b}{M}k)}{\Gamma(a)} + l\frac{\gamma(a, \frac{b}{M}l)}{\Gamma(a)}, \end{aligned} \tag{3.57}$$

$$\begin{aligned} G_{IG}(k,l) = 1 &- \frac{(a-1)\left[\Gamma(a-1, \frac{b}{Ml}) - \Gamma(a-1, \frac{b}{Mk})\right]}{\Gamma(a)} \\ &+ \frac{M(a-1)}{b}\frac{[k\Gamma(a, \frac{b}{Mk}) - l\Gamma(a, \frac{b}{Ml})]}{\Gamma(a)} + \frac{(k-l)M(a-1)}{b}, \end{aligned} \tag{3.58}$$

respectively, where $k = \frac{d}{M}$ *and* $l = \frac{m}{M}$.

3.3 The Optimization of d and m

Our aim is to find the values of the retention d and the maximum m, which maximize the dependence between the insurer and the reinsurer with the minimum cost to assure the plausible business. On the other hand, loss ratios of both parties are also affected by the values of d and m. For this reason, our approach to finding the optimal values maximizing the correlation between the expected costs attaining the loss ratios of both to be as close as to each other. In other words, the optimal d and m find the reasonable risk relation between parties for a reasonable debate on the loss and the premium share.

The optimization problem, which maximizes the correlation between the costs of insurer and the reinsurer while the loss ratios of parties are equivalent to each other are conveyed as

$$\begin{aligned} \text{Case I:} \quad \max_{d} \quad & \rho(I(d), R(d)) \\ \text{s.t.} \quad & PI_r(d) - PR_r(d) = 0 \\ & d > 0, \end{aligned} \tag{3.59}$$

$$\text{Case II:} \quad \max_{d,m} \quad \rho(I(d,m), R(d,m))$$
$$\text{s.t.} \quad PI_r(d,m) - PR_r(d,m) = 0 \tag{3.60}$$
$$d > 0, \quad m > 0, \quad m > d.$$

The loss ratios $PI_r(d)$ and $PR_r(d)$ can be rewritten as $\frac{\mathbb{E}[I(d)]}{PG(k)}$ and $\frac{\mathbb{E}[R(d)]}{P(1-G(k))}$, respectively, and the constraint in Eq. (3.59) turns into

$$\mathbb{E}[R(d)]G(k) = \frac{\mathbb{E}[S]}{2}$$

Correspondingly, the term representing the constraint in Eq. (3.60) facilitates to

$$\mathbb{E}[R(d,m)]G(k,l) = \frac{\mathbb{E}[S]}{2}$$

where $k = \frac{d}{M}$, $l = \frac{m}{M}$ and M is the maximum possible loss.

The problems in Eqs. (3.59, 3.60) are rephrased as

$$\text{Case I:} \quad \max_{d} \quad \rho(I(d), R(d))$$
$$\text{s.t.} \quad \mathbb{E}[R(d)]G(k) - \frac{\mathbb{E}[S]}{2} = 0 \tag{3.61}$$
$$d > 0,$$

$$\text{Case II:} \quad \max_{d,m} \quad \rho(I(d,m), R(d,m))$$
$$\text{s.t.} \quad \mathbb{E}[R(d,m)]G(k,l) - \frac{\mathbb{E}[S]}{2} = 0 \tag{3.62}$$
$$d > 0, \quad m > 0, \quad m > d.$$

In order to obtain the tractable solutions for the optimization problem, which do not have closed form, we require numerical methods. For this reason, we introduce two algorithms, Algorithm (1) and Algorithm (2), which are used to achieve optimal values for Case I and Case II contract types, respectively.

In these algorithms, the possible retention and maximum levels are considered in the interval of $[m \times M, M]$ and the loss amounts are generated by the proposed loss distribution. Searching of the maximum correlation between the parties and checking

whether the contraints in Eqs. (3.61) and (3.62) are satisfied provides the optimal values. Furthermore, the small choice of the partition length Δ of interval $[m \times M, M]$ enhances the robustness of the optimization problem.

Algorithm 1: Case I: optimal $d^\star$

Consider the partition of the interval $[m \times M, M]$ as

$m \times M = d_0 < d_1 < \ldots < d_i < d_{i+1} < \ldots < d_n = M$ such that n many equidistant subintervals are obtained where $m \times M$ and M are minimium and maximum possible losses, respectively.

Let $\Delta = d_{i+1} - d_i$.

Let tol be a chosen small tolerance number.

for $i \leftarrow n$ **by** Δ **do**

  while $\mathbb{E}[R(d_i)]G(\frac{d_i}{M}) - \frac{\mathbb{E}[S]}{2} < tol$ **do**

    Calculate $\rho(d_i) = \rho(I(d_i), R(d_i))$

  end

end

Choose the maximum correlation $\rho(I(d_i), R(d_i))$ which is satisfied by $d_i = d^\star$.

Algorithm 2: Case II: optimal $d^\star$ and $m^\star$

Consider the partitions of the interval $[m \times M, M]$ as

$m \times M = d_0 < d_1 < \ldots < di < d_{i+1} < \ldots < d_n = M$ and

$m \times M = m_0 < m_1 < \ldots < m_j < m_{j+1} < \ldots < m_n = M$ such that n many equidistant subintervals are obtained where $m \times M$ and M are minimium and maximum possible losses, respectively.

Let $\Delta = d_{i+1} - d_i = m_{j+1} - m_j$.

Let tol be a chosen small tolerance number.

```
for i ← n by Δ do
    for j ← n by Δ do
        while E[R(d_i, m_j)]G(d_i/M, m_j/M) − E[S]/2 < tol & m_j > d_i do
            Calculate ρ(d_i, m_j) = ρ(I(d_i, m_j), R(d_i, m_j))
        end
    end
end
```

Choose the maximum correlation $\rho(I(d_i, m_j), R(d_i, m_j))$ which is satisfied by $d_i = d^\star$ and $m_j = m^\star$.

3.4 Numerical Illustrations

Based on the aggregate losses drawn from the selected distributions, we establish exposure curves in order to express the applications of the proposed methodology. We choose the parameters of these distributions, which produce the same expected and variance values. This results in obtaining rational foundation from which to compare loss distribution and their exposure curves. Thus, the parameters of each distributions, which are Pareto$(3.2361, 1.3820)$, Gamma$(4, 0.5)$, IG$(6, 10)$, generate $\mathbb{E}[S] = 2$ and $\mathbb{V}[S] = 1$.

We resolve the levels of optimal retention and maximum with respect to the highest correlation between the costs of insurer and reinsurer, which have the impacts on the mean and variance values, partition of premium, and loss ratios simultaneously. For Case I and Case II, we summarize the results in Table 3.3 and Table 3.4 under tle

assumptions of selected distributions.

For **Case I**, in Table 3.3, the optimal retention levels are near 2 and close to each other under each distribution although it can be marked that Gamma distribution assumption yields the highest correlation. The premium shares of insurer and reinsurer are maximum in Pareto and Gamma, respectively. We also see that the loss ratios of insurer and reinsurer are obtained as same values, which are achieved their minumum in Gamma, whereas the shares of the premium for insurer and reinsurer are gained under different distributions. We deduce that the expected loss is lower for parties in Gamma as well. The selected distributions' tail nature is noticeable since our simulation includes the interval of minimum and maximum losses generated by proposed distributions. In Fig. 3.2a, the Gamma distribution has a confined interval with respect to others.

For **Case II**, simulations form a surface, which is not tractable. We clarify this problem by fixing the retention level to the optimal value, which enables us for searching for optimal maximum level and for investigating the effects of chane in m upon the correlation coefficient and loss ratios. Table 3.4 indicates that Pareto distribution yields the maximum correlation, which is the same situation in Case I. The maximum m level is achieved under Pareto distribution; however, Gamma distribution provides the maximum premium and preimum ratios. Furhermore, due to the fact that the commitments for the reinsurer rises according to the increase in the maximum level, we expect that the correlation tendency with respect to maximum levels become horizontal, which is also indicated in Fig. 3.2b. In other words, the adequate high cap levels do not impose on the depedence between parties.

Table 3.3: Case I: optimal retention values

	Pareto	**Gamma**	**InvGamma**
Max Correlation	0.3629	**0.4740**	0.4202
Optimal Retention ($d^\star$)	**2.2171**	**2.0996**	**2.1605**
Premium (P)	4.0416	**4.1859**	4.0626
$PI(d^\star)$	3.6076	3.4545	3.4641
$PR(d^\star)$	0.4340	0.7314	0.5985
$PI_r(d^\star)$	0.4948	**0.4748**	0.4923
$PR_r(d^\star)$	0.4948	**0.4748**	0.4923

Table 3.4: Case II: optimal retention and maximum values

	Pareto	**Gamma**	**InvGamma**
Max Correlation	**0.4412**	0.4346	0.4361
Optimal Retention ($d^\star$)	**3.5164**	**2.9214**	**3.1017**
Optimal Maximum ($m^\star$)	**9.1544**	**5.0814**	**6.0517**
Premium (P)	4.0810	**4.1149**	4.0916
$PI_r(d^\star,m^\star)$	0.4901	**0.4860**	0.4889
$PR_r(d^\star,m^\star)$	0.4901	**0.4860**	0.4889

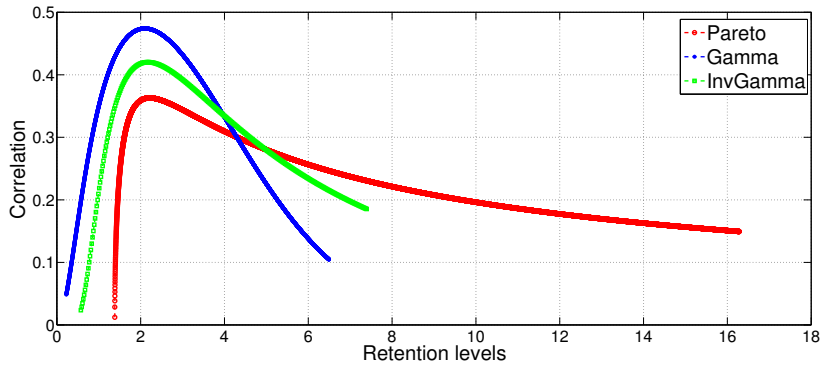

(a) Case I

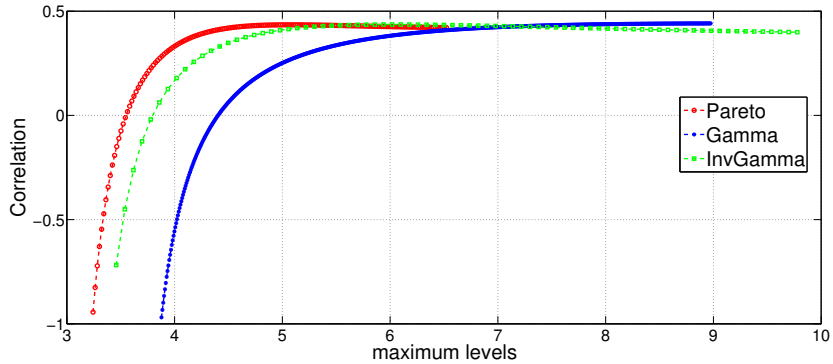

(b) Case II

Figure 3.2: The risk share between insurer and reinsurer

The derived exposure curve function, which represents the behavior of premium share between parties for Case I, is presented in Figs. 3.3a, 3.3c, and 3.3e. The charge for the insurer is increased by the raise in the retention level, which matches up to a higher premium share in favor of insurer's side. In contrast, this diminishes the reinsurer's cost, which causes a lesser premium share for the reinsurer's side. The exposure curves according to the change in m values under Case II are shown in Figs. 3.3b, 3.3d, and 3.3f, which indicate the ratio of reinsurer's premium share. The increase in

maximum level results in the larger costs for the reinsurer, which is the reason for the rise of reinsurer's premium share ratio. On the other hand, the decline in the insurer's cost leads to the decrease the premium gained by the insurer.

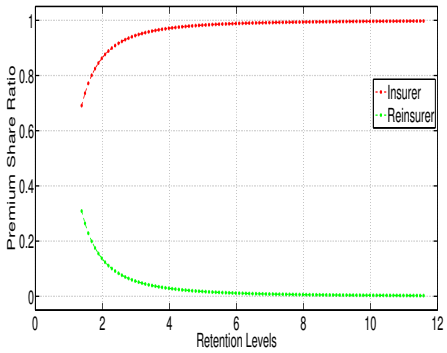

(a) Pareto: Case I

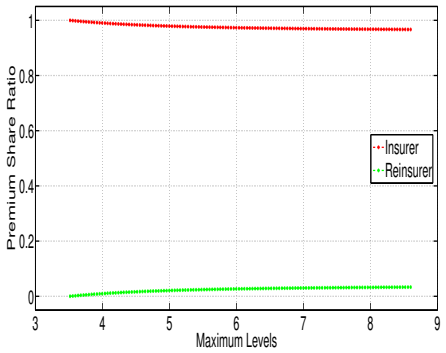

(b) Pareto: Case II

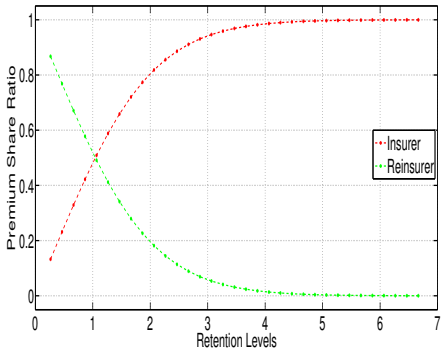

(c) Gamma: Case I

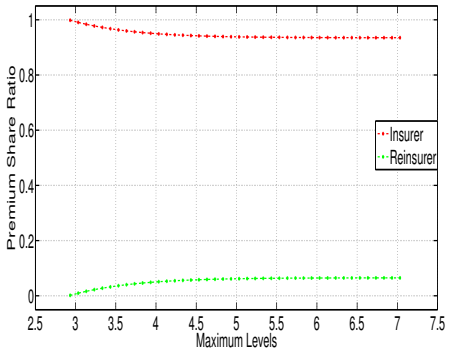

(d) Gamma: Case II

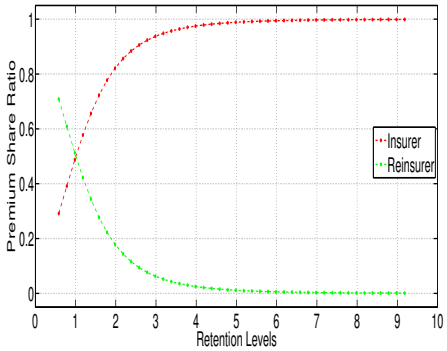

(e) Inverse Gamma: Case I

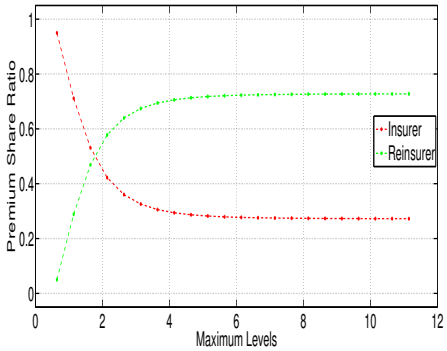

(f) Inverse Gamma: Case II

Figure 3.3: Case I and Case II: the exposure curves of parties under the selected distributions

The risk measures VaR and CVaR, which are associated with the requirements of reserve and capital, are considered for the assessment of each parties' maximal risk. For insurer and reinsurer, the VaR and CVaR values in terms of certain α (confidence

level) values under selected distributions are displayed in Table 3.5. According to the calculations that take $d^\star$ into account, we demonstrate that the increase on the values of α causes the declines in the difference between VaR and CVaR values for insurer and reinsurer under Gamma distribution. Futhermore, Gamma distribution yields the highest correlation between parties in Case I, which is additional sign for the optimal retention, $d^\star$, maximizing the correlation between parties and detecting the state of equilibrium between parties' loss ratios. Moreover, $d^\star$ is also confirmed when we consider the risk measures VaR and CVaR for insurer and reinsurer.

Table 3.5: Case I: VaR and CVaR of the parties for optimal d

α	Risk measure	**Pareto**	**Gamma**	**InvGamma**
0.90	VaR$_I$	2.2171	2.0996	2.1605
	CVaR$_I$	2.2171	2.0996	2.1605
	VaR$_R$	0.5990	1.2410	1.0130
	CVaR$_R$	5.8055	2.9455	6.5825
0.95	VaR$_I$	2.2171	2.0996	2.1605
	CVaR$_I$	2.2171	2.0996	2.1605
	VaR$_R$	1.2720	1.7780	1.6680
	CVaR$_R$	6.1420	3.2140	6.9100
0.99	VaR$_I$	2.2171	2.0996	2.1605
	CVaR$_I$	2.2171	2.0996	2.1605
	VaR$_R$	3.5350	2.9290	3.4530
	CVaR$_R$	7.2735	3.7895	7.8025

Table 3.6: VaR and CVaR according to the chosen loss distributions

α	Risk measure	**Pareto**	**Gamma**	**InvGamma**
0.975	VaR	4.3208	4.3860	4.5450
	CVaR	6.2540	5.0695	5.8206
0.99	VaR	5.7350	5.0290	5.6130
	CVaR	8.2972	5.6892	7.0823
0.995	VaR	7.1048	5.6879	6.5340
	CVaR	10.2891	6.1462	8.1793

The VaR and CVaR values under certain α values and selected distributions, which are computed according to the simulated aggregate claims, are presented in Table 3.6. For comparing our findings in Case II, the expected values ($\mathbb{E}[I_v]$, $\mathbb{E}[I_{cv}]$, $\mathbb{E}[R_v]$, $\mathbb{E}[R_{cv}]$) and the alterion based on the variances ($\frac{\mathbb{V}[I]}{\mathbb{V}[I_v]}$, $\frac{\mathbb{V}[R]}{\mathbb{V}[R_v]}$, $\frac{\mathbb{V}[I]}{\mathbb{V}[I_{cv}]}$, $\frac{\mathbb{V}[R]}{\mathbb{V}[R_{cv}]}$) for insurer and

reinsurer with respect to VaR and CVaR are obtained in Table 3.7. As an example demonstrated in Table 3.7, for insurer and reinsurer successively, the expected costs ($\mathbb{E}[I]$, $\mathbb{E}[R]$) are 1.9325 and 0.0675; whereas the same quantities in case of VaR ($\mathbb{E}[I_v]$,$\mathbb{E}[R_v]$) become 1.9718 and 0.0283 and for CVaR are ($\mathbb{E}[I_{cv}]$, $\mathbb{E}[R_{cv}]$) 1.9447 and 0.0555 under Pareto with $\alpha = 0.975$. The values in Table 3.7 are found by taking $m^\star$ as its corresponding optimal value exhibited in Table 3.4. Gamma distribution, which provides the lowest loss ratios as a result of our optimization algorithms, generates the closest approximation; therefore, is more appropriate when we consider VaR and CVaR risk measures. Additionally, the lowest variance change is obtained under Gamma distribution for all α values.

Table 3.7: The relative variances and expected costs if $m^\star$ is considered as VaR and CVaR

	Pareto			**Gamma**			**InvGamma**		
α	0.975	0.99	0.995	0.975	0.99	0.995	0.975	0.99	0.995
$\mathbb{E}[I]$	1.9325	1.9325	1.9325	1.8771	1.8771	1.8771	1.8990	1.8990	1.8990
$\mathbb{E}[I_v]$	1.9718	1.9489	1.9394	1.8881	1.8881	1.8772	1.8990	1.8990	1.8990
$\mathbb{E}[I_{cv}]$	1.9447	1.9347	1.9304	1.8771	1.8734	1.8720	1.9008	1.8940	1.8914
$\mathbb{E}[R]$	0.0675	0.0675	0.0675	0.1230	0.1230	0.1230	0.1010	0.1010	0.1010
$\mathbb{E}[R_v]$	0.0283	0.0509	0.0607	0.1120	0.1120	0.1229	0.0801	0.0974	0.1038
$\mathbb{E}[R_{cv}]$	0.0555	0.0654	0.0696	0.1228	0.1265	0.1277	0.0992	0.1060	0.1087
$\frac{\mathbb{V}[I]}{\mathbb{V}[I_v]}$	0.5948	0.7516	0.8748	1.0983	1.0983	1.0181	0.8319	0.9647	1.0301
$\frac{\mathbb{V}[I]}{\mathbb{V}[I_{cv}]}$	0.7672	0.9408	1.0372	0.9994	1.0224	1.0274	0.9819	1.0547	1.0893
$\frac{\mathbb{V}[R]}{\mathbb{V}[R_v]}$	10.1959	2.4040	1.4443	1.3478	1.3478	0.9166	2.0096	1.1293	0.9046
$\frac{\mathbb{V}[R]}{\mathbb{V}[R_{cv}]}$	1.8431	1.1537	0.8700	1.0033	0.8909	0.8549	1.0639	0.8297	0.7496

3.5 Discussion

The aim of this chapter is to analyse optimal premium share between the insurer and the reinsurer using the exposure curves under certain aggregate loss distribution. We achieve the optimal premium in terms of the level of dependence- correlation coefficient between the costs of insurer and reinsurer under an optimization scheme. The main contribution of this chapter to the literature is to obtain the analytical derivations of the exposure curves under Pareto, Gamma, and Inverse Gamma distributions under

the standard deviation premium principle. This enables researchers to understand the pricing behavior. Using the Monte Carlo simulations and the proposed approach in this chapter, we also determine that under which of the distributions the maximum correlation, the highest premium, and the smaller expected loss are observed with respect to the conditions on the reinsurance contract in terms of retention level and/or maximum level. Furthermore, we compare the optimized values based on the proposed approach with the values that minimize the total risks of parties with respect to VaR and CVaR risk measures. The outcomes indicate that the optimized solution that maximizes the correlation between parties and equates their loss ratios is close enough to the VaR and CVaR values with high α levels for all selected distributions under Case I and Case II. Among the others, Gamma distribution is more convenient when compared the others, which is the situation that we obtain by our proposed methodology.

CHAPTER 4

STOCHASTIC STOP-LOSS REINSURANCE AND EXPOSURE CURVES VIA GEOMETRIC BROWNIAN MOTION MODEL

This chapter presents the analytical derivations of the costs of insurer and reinsurer if the losses follow Geometric Brownian Motion model with time-varying parameters. The time-dependent exposure curves which determine the fair premium share between parties are derived under stochastic behavior of the losses. Moreover, the time-varying parameters of the model are estimated using maximum likelihood estimators (MLE) dynamically. The simulation and the forecasts of the loss amounts, the costs of parties, and the exposure curves are demonstraded as well.

Assume that the loss $X^G(t)$ satisfies the following stochastic differential equation (SDE) on the probability space $(\Omega, \mathcal{F}, \mathbb{P})$ and the contract issued for this random loss is written over the time period $[0, T]$:

$$dX_t^G = \mu X_t^G dt + \sigma X_t^G dW_t, \tag{4.1}$$

where the parameters μ and σ are constants, and W_t is one-dimensional Brownian motion.

The solution of SDE in Eq. (4.1) is known to be given as

$$X_t^G = X_0^G e^{(\mu - \sigma^2/2)t + \sigma W_t}.$$

The model in the discrete-time is built on a finite probability space $(\Omega, \mathcal{F}, \mathbb{P})$ equipped with a filtration, i.e., an increasing sequence of σ-algebras in $\mathcal{F}$ partitioned as $\mathcal{F}_0$, $\mathcal{F}_1$,

$\mathcal{F}_2, \ldots, \mathcal{F}_n$. That is, $\mathcal{F}_n$ represents the information at time n and is called as σ-algebra of events up to time n.

The n-many equidistant subintervals, which is the partition of the period $[0, T]$, is considered as $0 = t_0 < t_1 < \ldots < ti < t_{i+1} < \ldots < t_n = T$ and let $\Delta t = t_{i+1} - t_i$. The discrete-time solution of the SDE at t_{i+1} can be written as

$$X^G_{t_{i+1}} = X^G_{t_i} e^{(\mu(i) - \sigma(i)^2/2)\Delta t + \sigma(i)(W(t_{i+1}) - W(t_i))}, \tag{4.2}$$

where $\mu(i)$ and $\sigma(i)$ are the constant parameters governing the period between $[t_i, t_{i+1}]$. Moreover, we assume that the time-varying parameters, $\mu(i)$ and $\sigma(i)$, are independent.

According to this loss model setup, the costs of the insurer and the reinsurer are derived.

4.1 The Expected Costs Derivations

One of the important issues in a reinsurance contract is to decide at which retention level will be an agreeable selection maximizing the profit of both parties. The tools such as exposure curves help us determine an approximate partition of the premium as well as the loss amount. On the other hand, especially for the possibility of having catastrophic risks, reinsurers are reluctant to agree on taking the whole amount exceeding the retention. This is regularized by setting a cap (maximum) value on the claims from above. Therefore, a stop-loss contract may have either agreement based on only retention or both retention and cap. We consider both cases under Case I and Case II abbreviations for simplicity, respectively.

4.1.1 Case I: Retention

Suppose that the insurer and the reinsurer agreed on a predetermined retention level d. The costs at time t under the probability measure $\mathbb{P}$ can be written as

$$
\begin{aligned}
I(t, X_t^G, d) &= \min(X_t^G, d), \\
R(t, X_t^G, d) &= \max(X_t^G - d, 0).
\end{aligned}
\tag{4.3}
$$

The expected costs of insurer and reinsurer in an unspecified time frame within a contract year are collected in Theorem 4.1.

Theorem 4.1. *The expected costs of the reinsurer and insurer at time t with respect to the retention level d are*

$$
\begin{aligned}
\mathbb{E}[R(t, X_t^G, d)] &= X_0^G\, e^{\mu t}\Phi(E_{1d}) - d\Phi(E_{2d}), \\
\mathbb{E}[I(t, X_t^G, d)] &= X_0^G\, e^{\mu t}(1 - \Phi(E_{1d})) + d\Phi(E_{2d}),
\end{aligned}
\tag{4.4}
$$

respectively, where

$$
\begin{aligned}
\Phi(x) &= \int_{-\infty}^{x} \frac{1}{\sqrt{2\pi}} e^{-\frac{t^2}{2}}\, dt, \\
E_{2d} &= \frac{ln\left(\frac{X_0^G}{d}\right) + (\mu - \frac{\sigma^2}{2})t}{\sigma\sqrt{t}}, \quad \textit{and} \\
E_{1d} &= E_{2d} + \sigma\sqrt{t}.
\end{aligned}
$$

Proof. *The proof is sketched in Appendix A.2*

As we consider the time-varying impact on the expected losses, we define analogously, the costs at time t_i under the same probability measure is given as

$$
\begin{aligned}
I(t_i, X_{t_i}^G, d) &= \min(X_{t_i}^G, d), \\
R(t_i, X_{t_i}^G, d) &= \max(X_{t_i}^G - d, 0).
\end{aligned}
\tag{4.5}
$$

Using Theorem 4.1, Corollary 4.2 is established for the discrete-time model to achieve the expected costs terms for insurer and reinsurer with respect to the filtration $\mathcal{F}$.

Corollary 4.2. *The expected costs of the reinsurer and insurer at the time t_{i+1} with respect to the filtration $\mathcal{F}_{t_i}$ and the retention, d, are*

$$
\begin{aligned}
\mathbb{E}[R(t_{i+1}), X_{t_{i+1}}^G, d)|\mathcal{F}_{t_i}] &= X_{t_i}^G e^{\mu(i)\Delta t}\Phi(E_{1id}) - d\Phi(E_{2id}), \\
\mathbb{E}[I(t_{i+1}), X_{t_{i+1}}^G, d|\mathcal{F}_{t_i})] &= X_{t_i}^G e^{\mu(i)\Delta t}(1 - \Phi(E_{1id})) + d\Phi(E_{2id}),
\end{aligned}
\tag{4.6}
$$

respectively. Here,

$$E_{2id} = \frac{ln\left(\frac{X_{t_i}^G}{d}\right) + (\mu(i) - \frac{\sigma(i)^2}{2})\Delta t}{\sigma(i)\sqrt{\Delta t}}, \quad \textit{and}$$
$$E_{1id} = E_{2id} + \sigma(i)\sqrt{\Delta t},$$

where $\Phi(x)$ is defined in Theorem 4.1.

4.1.2 Case II: Retention and Maximum

Assume that the agreement between insurer and reinsurer is based on the predetermined retention level d and the maximum level m. The parties' costs, which depend on the time t, the loss X_t^G, d, and m, are written as

$$\begin{aligned} I(t, X_t^G, d, m) &= \min(X_t^G, d) + \max(X_t^G - m, 0), \\ R(t, X_t^G, d, m) &= \min(m - d, \max(X_t^G - d, 0)). \end{aligned} \tag{4.7}$$

According to the costs separation and the model in Eq. (4.1), the derivations of expected costs are obtained.

Theorem 4.3. *The expected costs of the insurer and reinsurer at time t with respect to the retention level d and the maximum level m are*

$$\begin{aligned} \mathbb{E}[I(t, X_t^G, d, m)] &= X_0^G e^{\mu t}[1 + \Phi(E_{1m}) - \Phi(E_{R1d})] + d\Phi(E_{2d}) - m\Phi(E_{2m}), \\ \mathbb{E}[R(t, X_t^G, d, m)] &= X_0^G e^{\mu t}[\Phi(E_{1d}) - \Phi(E_{1m})] - d\Phi(E_{2d}) + m\Phi(E_{2m}), \end{aligned} \tag{4.8}$$

respectively, where

$$E_{2m} = \frac{ln\left(\frac{X_0^G}{m}\right) + (\mu - \frac{\sigma^2}{2})t}{\sigma\sqrt{t}}, \quad \textit{and} \;\; E_{1m} = E_{2m} + \sigma\sqrt{t},$$

$\Phi(x)$, E_{1d}, and E_{2d} are the same as defined in Theorem 4.1.

Proof. The proof is sketched in Appendix A.2.

In the discrete-time t_i, the costs of both parties are expressed as

$$\begin{aligned} I(t_i, X^G_{t_i}, d, m) &= \min(X^G_{t_i}, d) + \max(X^G_{t_i} - m, 0), \\ R(t_i, X^G_{t_i}, d, m) &= \min(m - d, \max(X^G_{t_i} - d, 0)). \end{aligned} \tag{4.9}$$

We also derive the expected costs under Case II for both parties under the discrete-time model with the filtration $\mathcal{F}$ as the following Corrollaries 4.2 and 4.4.

Corollary 4.4. *The expected costs of the insurer and reinsurer at the time t_{i+1} with respect to the filtration $\mathcal{F}_{t_i}$, the retention, d, and the maximum, m, are*

$$\begin{aligned} \mathbb{E}[I(t_{i+1}, X^G_{t_{i+1}}, d, m)|\mathcal{F}_{t_i}] &= X^G_{t_i} e^{\mu(i)\Delta t}[1 + \Phi(E_{1im}) - \Phi(E_{1id})] \\ &\quad + d\Phi(E_{2id}) - m\Phi(E_{2im}), \\ \mathbb{E}[R(t_{i+1}, X^G_{t_{i+1}}, d, m)|\mathcal{F}_{t_i}] &= X^G_{t_i} e^{\mu(i)\Delta t}[\Phi(E_{1id}) - \Phi(E_{1im})] \\ &\quad - d\Phi(E_{2id}) + m\Phi(E_{2im}), \end{aligned} \tag{4.10}$$

respectively, where

$$E_{2im} = \frac{ln\left(\frac{X^G_{t_i}}{m}\right) + (\mu(i) - \frac{\sigma(i)^2}{2})\Delta t}{\sigma(i)\sqrt{\Delta t}}, \quad \textit{and} \;\; E_{1im} = E_{2im} + \sigma(i)\sqrt{\Delta t},$$

$\Phi(x)$, E_{1id}, and E_{2id} are defined in Corollary 4.2.

The derivations in Corrollaries 4.2 and 4.4 are obtained based on Theorems 4.1 and 4.3; thus, we skip the proofs for them as we give the proofs for their related theorems.

4.2 Time-Varying Frame in Exposure Curves

The allocation of risks together with the premium share for insurer and reinsurer are achieved by employing the exposure curves. The risk for loss alters by time elapsing, which is especially the case when natural catastrophes are considered; thus, the mean of losses varies over time. This is another indicator that the exposure curves need to take the time influence into account. For this reason, we modify the exposure curves proposed by [6] under Case I and Case II in both time-dimensional and SDE-type loss distribution assumptions and derive the corresponding analytical forms.

Definition 4.1. *The exposure curves for reinsurer and insurer under Case I are defined as*

$$\begin{aligned} G_R(t,d) &= \frac{\mathbb{E}[R(t,X_t^G,d)]}{\mathbb{E}[X_t^G]} \\ &= \Phi(E_{1d}) - \frac{d}{X_0^G} e^{-\mu t}\Phi(E_{2d}), \\ G_I(t,d) &= 1 - G_R(t,d), \end{aligned} \tag{4.11}$$

respectively.

Definition 4.2. *The exposure curves for reinsurer and insurer at time t_{i+1} with respect to filtration $\mathcal{F}$ under Case I are expressed as*

$$\begin{aligned} G_R(t_{i+1},d) &= \frac{\mathbb{E}[R(t_{i+1},X_{t_{i+1}}^G,d)|\mathcal{F}_{t_i}]}{\mathbb{E}[X_{t_{i+1}}^G|\mathcal{F}_{t_i}]} \\ &= \Phi(E_{1id}) - \frac{d}{X_{t_i}^G} e^{-\mu(i)\Delta t}\Phi(E_{2id}), \\ G_I(t_{i+1},d) &= 1 - G_R(t_{i+1},d), \end{aligned} \tag{4.12}$$

respectively.

Definition 4.3. The exposure curves for reinsurer and insurer under Case II are defined as

$$\begin{aligned} G_R(t,d,m) &= \frac{\mathbb{E}[R(t,X_t^G,d,m)]}{\mathbb{E}[X_t^G]} \\ &= \Phi(E_{1d}) - \Phi(E_{1m}) + e^{-\mu t}\left[\frac{m}{X_0^G}\Phi(E_{2m}) - \frac{d}{X_0^G}\Phi(E_{2d})\right], \\ G_I(t,d,m) &= 1 - G_R(t,d,m), \end{aligned} \tag{4.13}$$

respectively.

Definition 4.4. *The exposure curve under Case II for reinsurer and insurer at time t_{i+1} with respect to filtration $\mathcal{F}$ are expressed as*

$$\begin{aligned} G_R(t_{i+1},d,m) &= \frac{\mathbb{E}[R(t_{i+1},X_{t_{i+1}}^G,d,m)|\mathcal{F}_{t_i}]}{\mathbb{E}[S(t_{i+1})|\mathcal{F}_{t_i}]} \\ &= \Phi(E_{1id}) - \Phi(E_{1im}) + e^{-\mu(i)\Delta t}\left[\frac{m}{X_{t_i}^G}\Phi(E_{2im}) - \frac{d}{X_{t_i}^G}\Phi(E_{2id})\right], \\ G_I(t_{i+1},d,m) &= 1 - G_R(t_{i+1},d,m), \end{aligned} \tag{4.14}$$

respectively.

The parameters μ and σ of the proposed loss model should be estimated in accord with the derivations given in this section.

4.3 Parameter Estimation under Time-Varying Frame

The models developed under the SDE assumption do not produce good solutions for parameter estimation; therefore, we calibrate the parameters using real-life data by employing a a dynamic maximum likelihood estimation method in order to incorporate the time-varying effects on the parameters at each discritized time interval. The real-life data contains a large portfolio (approx. 1 million) compulsory traffic insurance (MTPL) policyholders in Turkey for the year 2006. The reasons for using MTPL data are listed as follows: (i) The real-life data which is accessible covers all MTPL policies in Turkey in 2006, (ii) The claim history is exceptional as in 2006 severe weather conditions and flood experienced in Istanbul causing extreme payments for insurance and reinsurance companies. Additionally, Istanbul and its vicinity, which is the highly populated and industrial region in Turkey, can be taken as a good representative for Turkey's MTPL picture. (ii) The data owner and source, TRAMER (Traffic Insurance Information Center), does not permit the use of its data due to confidentiality purposes. For this reason, the extension of the application to later years is not possible. On the other hand, we are confident that the methodology introduced here can find its applicability to any other non-life branches.

We prepare the data as aggregate daily losses, which provides 365 observations for 2006 and forms equally distant time subintervals with each length of 1-day. Fig. 4.1a exemplifies the daily loss, which shows a rising movement that is more incessant behavior until half of the year and then depreciates its increasing rate. This structure in the data also confirms our methodologies for examining loss, costs, and exposure curves at time-varying aspects. As being observed, the range in the loss is very large (maximum loss is 5,738,647 TL); therefore, we rescale using min-max data transformation.

Suppose that L_i denotes the aggregate daily claim at time t_i for $i = 0, 1, \ldots, 365$. Then min-max transformation whose graph is shown in Fig. 4.1b becomes

$$TL(i) = \frac{L(i) - \min(L(i))}{\max(L(i)) - \min(L(i))},$$

where $TL(i)$ denotes the transformed data at time t_i for $i = 0, 1, \ldots, 365$.

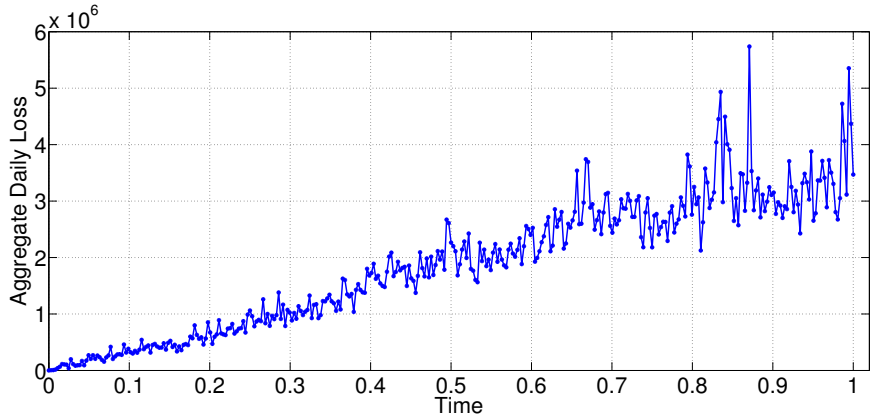

(a) Original data

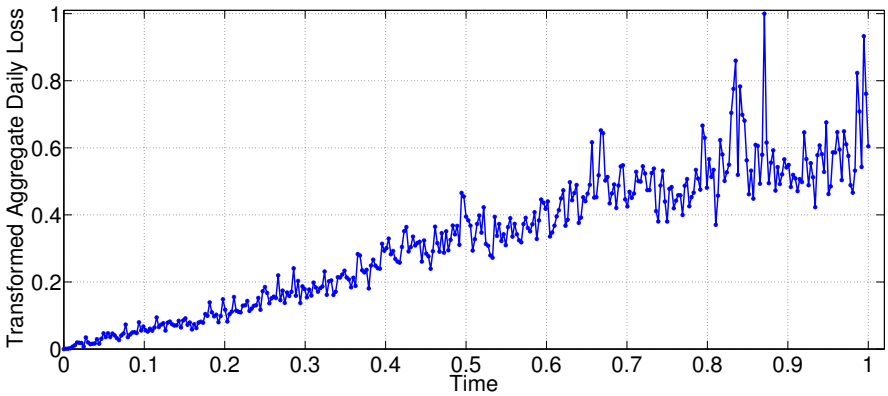

(b) Transformed Data

Figure 4.1: Aggregate daily claims for the compulsory traffic insurance data

Based on the loss distribution expressed in terms of SDE, we derive the corresponding estimates for the parameters $\hat{\mu}$ and $\hat{\sigma}$ using DMLE.

$$\begin{aligned}\bar{S}(i) :&= \ln\left(\frac{X^G_{t_{i+1}}}{X^G_{t_i}}\right)\\ &= \left(\mu(i) - \frac{\sigma(i)^2}{2}\right)\Delta t + \sigma(i)W(\Delta t).\end{aligned}$$

Since $W(\Delta t) \stackrel{d}{=} \sqrt{\Delta t}Y$ where $Y \sim N(0,1)$, $\bar{S}(i) \sim N\left(\left(\mu(i) - \frac{\sigma(i)^2}{2}\right)\Delta t, \sigma(i)^2\Delta t\right)$.

Define the log-transformed data as $LTL(i) := \ln\left(\frac{TL(i+1)}{TL(i)}\right)$. Equating $LTL(i)$ to $\bar{S}(i)$ and using the maximum likelihood estimator (MLE) of $\bar{S}(i)$ for each $[t_i, t_{i+1}]$ produce the results for calibrated parameters $\hat{\mu}(i)$ and $\hat{\sigma}(i)$ in $[t_i, t_{i+1}]$. Then, the MLE of $\bar{S}(i)$ is found as

$$\begin{aligned} \hat{\mu}_{\text{MLE}} &= \frac{1}{i+1}\sum_{j=0}^{i+1}\bar{S}(j) = \left(\mu(i) - \frac{\sigma(i)^2}{2}\right)\Delta t, \\ \hat{\sigma}_{\text{MLE}} &= \sqrt{\frac{1}{i+1}\sum_{j=0}^{i+1}(\bar{S}(j) - \hat{\mu}_{\text{MLE}})^2} = \sqrt{\sigma(i)^2\Delta t}, \end{aligned} \tag{4.15}$$

whose solution yields the estimates of parameters for the specified time interval expressed as

$$\begin{aligned} \hat{\sigma}(i) &= \frac{\sqrt{\frac{1}{i+1}\sum_{j=0}^{i+1}(\bar{S}(j) - \frac{1}{i+1}\sum_{j=0}^{i+1}\bar{S}(j))^2}}{\sqrt{\Delta t}}, \\ \hat{\mu}(i) &= \frac{\frac{1}{i+1}\sum_{j=0}^{i+1}\bar{S}(j) + \frac{\frac{1}{i+1}\sum_{j=0}^{i+1}(\bar{S}(j) - \frac{1}{i+1}\sum_{j=0}^{i+1}\bar{S}(j))^2}{2}}{\Delta t}. \end{aligned} \tag{4.16}$$

As a subsequent of the calibration of parameters, we perform a simulation analysis in order to justify our proposed model. The parameters $\mu(i)$ and $\sigma(i)$ for $i = 0, 1, \ldots, 365$ are calculated using Eq. 4.16 over $100,000$ Monte Carlo (MC) simulations. We displays the DMLE fit's performance regarding to the transformed observations in Fig. 4.2. In the graph, the line represents the simulation results while the dots are for the real observations.

MAPE(%) and RMSE values are calculated in order to determine the performance of the estimates through simulations. It is found that MAPE is around to be 1.5177%, whereas RMSE yields a value of 0.0734 for transformed data. It is also important to note that these performance measures estimated using the original data remain unchanged for MAPE but produces large values in RMSE as the original data includes extreme values.

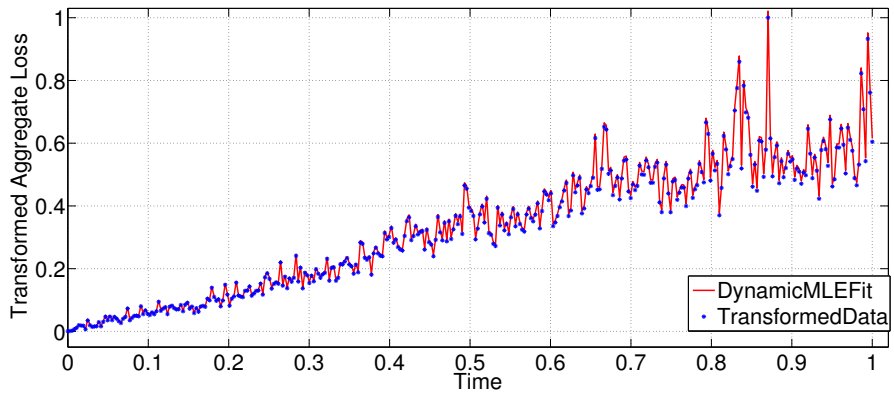

Figure 4.2: Comparison of Geometric Brownian motion model with time-varying parameters and transformed data

4.4 Application to MPTL Data

As a result of examination of possible retention and cap levels, we choose retention and cap values as $d = 0.3$ and $m = 0.7$ according to the levels having the lowest MAPE and RMSE in simulations. We simulate the expected costs and the exposure curves for insurer and reinsurer separately by considering the analytical derivations and the calibrated estimates.

4.4.1 Simulations for expected costs

Fig. 4.3 indicates the costs' behavior of parties in a position to real claim amount for Case I with $d = 0.3$ by using Corollary 4.2. When the aggregate daily loss (dashed blue color) exceeds the retention level, the insurer's expected cost (green line) stays constant with an insignificant deviation around the retention level (black horizontal line) until the middle of the policy year. The expected cost of the reinsurer (red line) is deemed to be zero until the aggregate claim exceeds the retention level, which is expected from the contract agreement.

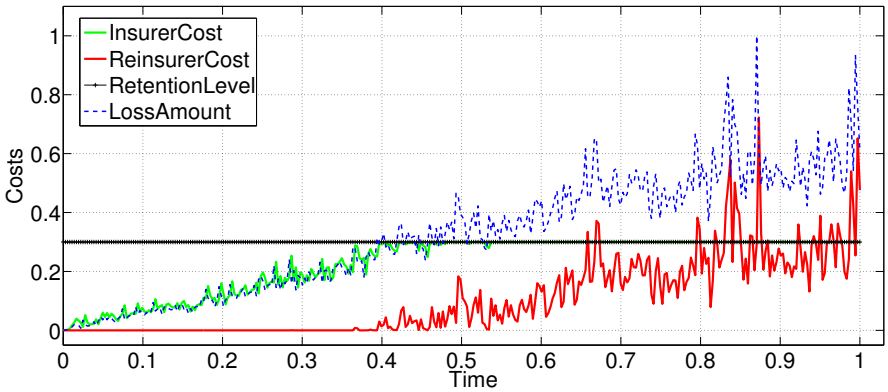

Figure 4.3: Case I: the expected costs

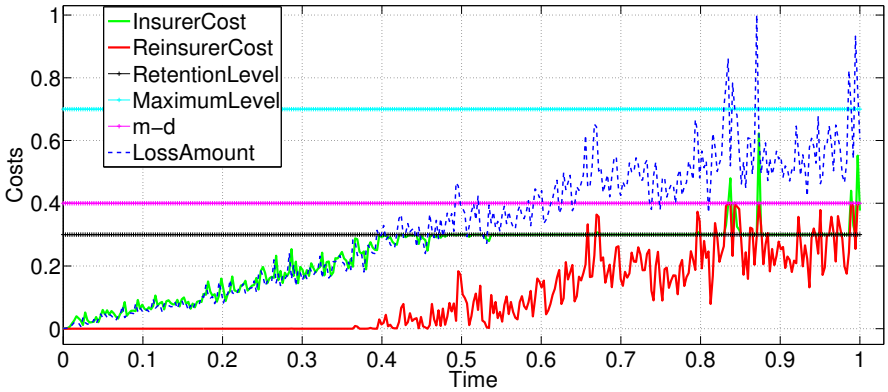

Figure 4.4: Case II: the expected costs

Based on the real claim amounts, Fig. 4.4 shows the costs' behavior of the parties under Case II with $d = 0.3$ and $m = 0.7$ by using Corollary 4.4. When the claim amount is between the retention level and the maximum level (cyan horizontal line), insurer's expected costs (green line) remains constant with an insignificant deviation around the retention level (black horizontal line), which is also the same in Case I.

Using Corollary 4.4, the costs' behavior of the parties according to real claim amounts for Case II with $d = 0.3$ and $m = 0.7$ is shown in Fig. 4.4. It can be seen that when the loss amount is higher than the retention level and smaller than the maximum level (cyan horizontal line), the expected costs of the insurer (green line) remains constant with an insignificant deviation around the retention level (black horizontal line) as in Case I. When the loss amount is higher than the maximum level, the expected cost of the reinsurer remains constant with an insignificant deviation around the level $m - d = 0.4$ (pink horizontal line). These small deviations between d and $m - d$ can

be expected as the simulations are done based on estimated parameters.

4.4.2 Simulations for exposure curves

The time-dependent exposure curves are simulated by the following Definitions 4.2 and 4.4 for Case I and Case II, respectively.

Based on the simulated expected costs given in Fig. 4.3, we study the behavior of exposure curves under Case I, given in Fig. 4.5a. In a position to the expected claims in time, we see that the insurer's costs remain below the retention level until the loss reaches the retention level. For this reason, the exposure curve suggests the premium to be shared in such a way that the insurer collects all the premium (green line) until the loss exceeds the retention level. After this, the losses above the retention level set the cost of the insurer constant at the retention level, and the cost of the reinsurer starts inclining (red line), resulting in the share of the reinsurer in the premium to be increased as expected. Thus, Fig. 4.5a represents the fair division between the parties while time elapses.

In Case II, in addition to the maximum level, the simulations depict that the higher the costs from m, the less the reinsurer pays as the amount corresponds to the difference $m - d$. This reduces the risks of the reinsurer by decreasing its costs. Thus, when both types of contracts are compared, one can expect that the share of the premium for the reinsurer is lower in Case II than its share Case I. This leads reinsurer's premium share is lower in Case II, as can be seen from Figs. 4.5a and 4.5b. The fair partition of the premium between two parties within a policy year is represented in Fig. 4.5b.

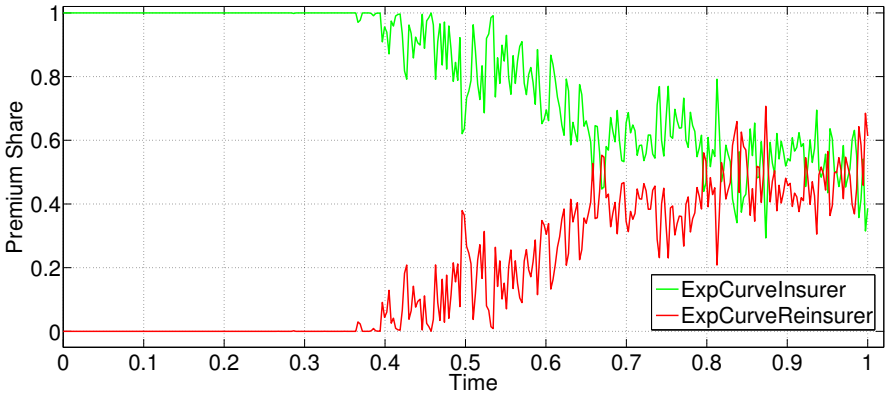

(a) Case I

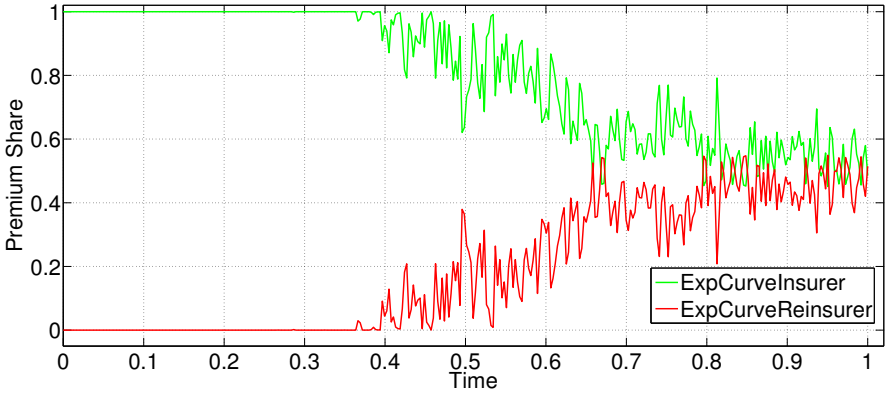

(b) Case II

Figure 4.5: The exposure curves: (a) Case I, (b) Case II

4.5 Forecasting the losses, costs and exposure curves

Due to the random occurrences of the aggregate daily loss at any time t, we aim to forecast the aggregate claims, expected costs, and premium share within the remaining time in a policy year based on the analytical derivations and the estimated parameters obtained using real-life data. To do so, we employ two methods at which one encounters the time effect, whereas the other is easier to implement and does not require any constraints. We use the method of cubic spline extrapolation and dynamic ARIMA models. Since we estimate the time-varying parameters which fit the data appropriately, we end up with again a time series composed of parameters for daily and weekly units. The performance of the daily time unit is found to be more accurate. Processing the forecasting on the time-varying parameters rather than the original data has advantages such as (ii) the performance of forecasting is found to be

much better than applying these methods to the data itself directly, (ii) the analytical results are to be preserved and incorporated.

4.5.1 Using cubic spline extrapolation

The forecasting algorithm using cubic spline extrapolation depends on system updates. In other words, we update the data after finding the extrapolated parameters using the estimated parameters. Here, we set the first 300 days as training and the rest as test data to measure the forecasting performance. Therefore, the estimated parameters of $\hat{\mu}$ and $\hat{\sigma}$ for forecasting are found based on these 300 observations. We consider system updates having one day time unit. These updates basically refer to daily forecasts with replacement, if updates are one day. The forecast of the loss amounts is based on the forecast of the time-varying parameters, $\hat{\mu}$, and $\hat{\sigma}$, which are considered a time series. The algorithm of the method is presented in Algorithm 3.

Algorithm 3: cubic spline extrapolation with system updates

```
Let nmo and tn be the number of observed data points and the number of
  training data points, respectively ;
Set u as the system updates;
for j ← tn to nmo by 1 do
    fit cubic spline function to j many data points;
    extrapolate a data point and save it for forecasting;
    if j − tn + 1 (mod u) ≠ 0 then
        use extrapolated data instead of (j + 1)^th data of original one;
    else
        replace all the extrapolated data with the original data;
    end
end
```

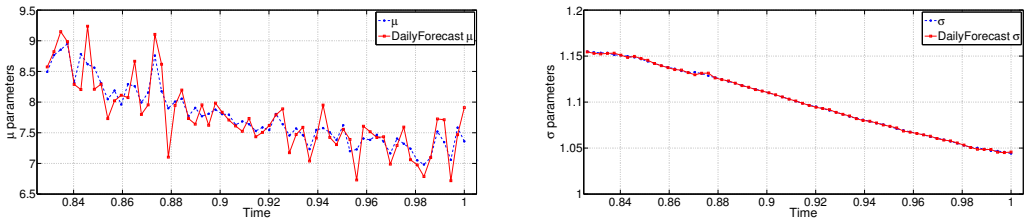

(a) Daily $\hat{\mu}$ forecast (b) Daily $\hat{\sigma}$ forecast

Figure 4.6: The parameter forecasts: cubic spline extrapolation

Figs. 4.6a and 4.6b expose the forecasted $\hat{\mu}$ and $\hat{\sigma}$ and estimated values according to daily updates, respectively. Cubic spline forecasted and estimated values of $\hat{\sigma}$ follow better fit compared to $\hat{\mu}$. Both of the estimates decay by the time, and this is captured by the forecasted values as well. Although $\hat{\mu}$ parameters are volatile, this method is good enough to obtain daily forecasts.

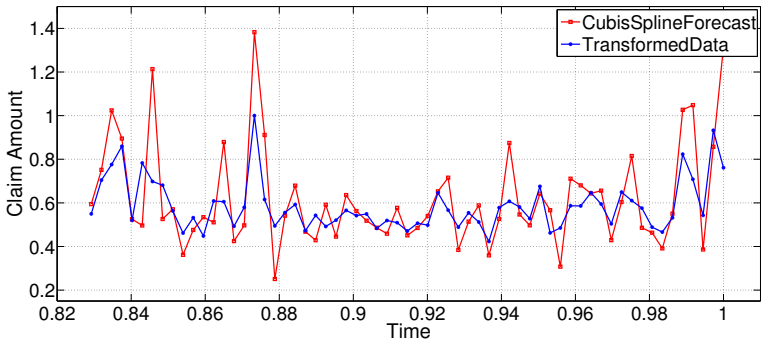

(a) Claim amount

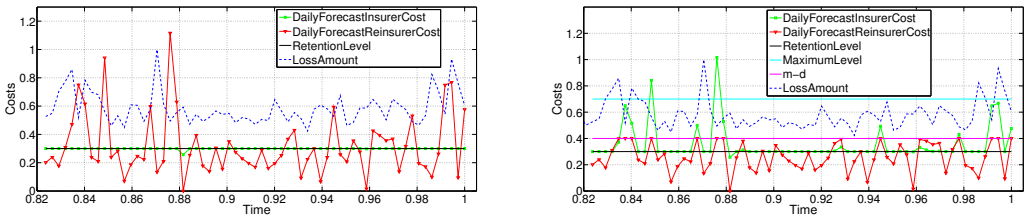

(b) The costs under Case I (c) The costs under Case II

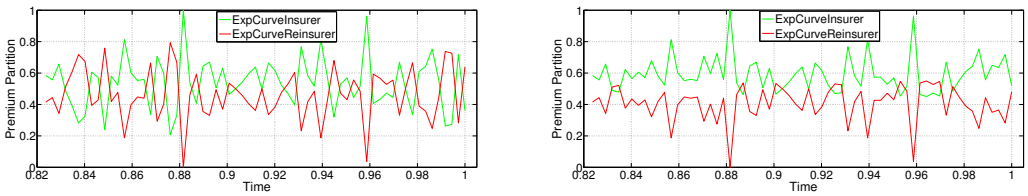

(d) The exposure curves: Case I (e) The exposure curves: Case II

Figure 4.7: Daily forecasts: cubic spline exptrapolation

Plugging in the forecasted parameters to the analytical derivations, we obtain aggregate loss, costs, and exposure curves illustrated in Figs. 4.7a, 4.7b, 4.7c, 4.7d, and 4.7e. We see that the cubic spline extrapolation captures the relatively more stable losses but not good enough for the extreme losses yielding the cubic spline method to be a good choice when extreme claims are not expected. In Figs. 4.7b and 4.7c under both Case I, and Case II, the forecasted costs are captured better within the constraints (retention level and cap value). On the extreme claims, the parties' costs are not captured; however, when the claim amounts are higher than the retention level and the maximum level in Case I and in Case II, respectively, the cubic spline extrapolation satisfies the contracts' offers, which are that the insurer should pay the costs of only the retention level amount for Case I and the reinsurer should pay the costs of only the difference between maximum and retention levels for Case II. The fair share of the premium between parties by using time-dependent exposure curves is given in Figs. 4.7d and 4.7e for Case I and Case II under the circumstances that we take the forecasted loss amounts in our estimation. Therefore, a good performance in forecasting the time-dependent exposure curves is a result of a good performance in forecasting the loss. The accuracy of the fits is measured by MAPE (20.01%) and RMSE (0.1881), whose values show efficiency in implementing the cubic spline method in forecasts.

4.5.2 Using dynamic ARIMA

Our aim is to forecast the loss amounts, the parties' costs, and their exposure curves by using daily system update. However, to keep the dynamic behavior of the forecasting to enhance the performance, we use ARIMA and forecast by searching the trend in the data of the estimated parameters that are considered as time series in this study. Similar to the first cubic spline approach, we split the data as training and test. At this point, to analyze the influence of the number of observations (tn) included in the training set, which can have an impact on the model performance, we set two options: (i) 200 and (ii) 300 observations for training sets which are chosen randomly. Dynamic ARIMA algorithm to forecast given time series depends on trend search in train data, and then this search should be expanded by adding a test data point to train the new set. However, to ensure the dynamic structure, we consider a sliding pattern

to create a new set.

In forecasting by using cubic spline extrapolation, we find that the weekly updates' performance is poor compared to the daily updates. In the ARIMA trend search algorithm above, we may change the updates easily; however, although weekly updates in the ARIMA trend search gives a better performance than the weekly updates in cubic spline extrapolation (% change in MAPEs of ARIMA is 20 % less than the one with cubic spline). The algorithm of the process is given in Algorithm 4.

Algorithm 4: dynamic ARIMA with trend search

```
Let nmo and tn be the number of observed data points and the number of
  training data points, respectively.
Fit ARIMA to tn many data points, i.e., to train data.
Find best fitted ARIMA order (p, d, q) where p is the number of
  autoregressive terms, d is the number of nonseasonal differences needed for
  stationarity, and q is the number of lagged forecast errors in the prediction
  equation.
Forecast a data point and save it;
for j ← tn to nmo by 1 do
    Exclude the first data point from the train data and add the first data of the
      test data to the last of train data;
    Set this data as new train data;
    Exclude the first data of the test data and set it as test data;
    Fit ARIMA to new train data;
    Find best fitted ARIMA order (p, d, q);
    Forecast a data point and save it.
end
```

We use the same approach as in the cubic spline forecasting, i.e., we first apply dynamic ARIMA with trend search on the estimated time-varying parameters, $\hat{\mu}$, and $\hat{\sigma}$. Figs. 4.8a, 4.8b, 4.8c, and 4.8d compare the forecasted $\hat{\mu}$ and $\hat{\sigma}$ variates, and estimated ones according to daily updates for both train data with 200 and 300 time units, respectively. Forecasted $\hat{\sigma}$ shows a similar pattern as in the cubic spline case, whereas $\hat{\mu}$ with the dynamic ARIMA method captures volatility in the parameter better, especially with a sample size of 200. This is due to short time memory being carried with

the information more than a large sample under a sliding frame setup.

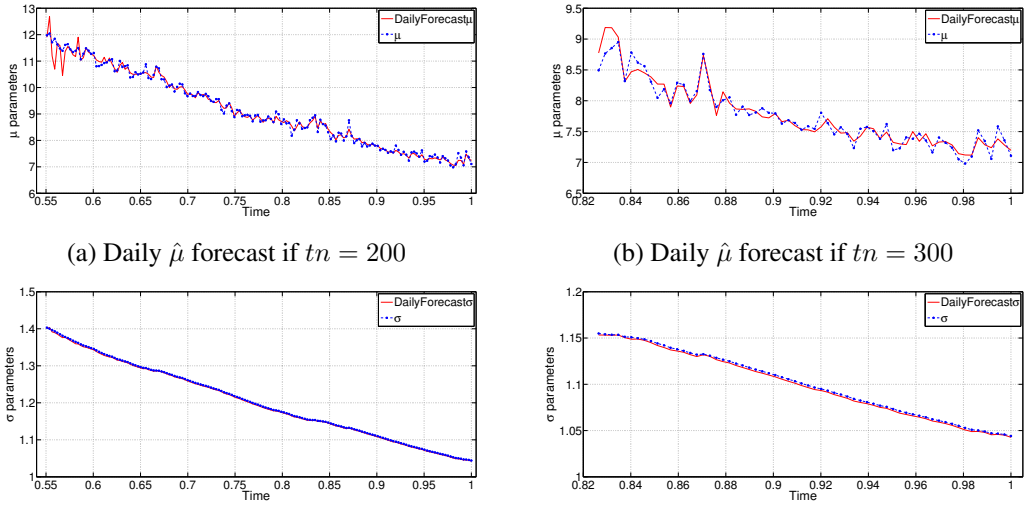

(a) Daily $\hat{\mu}$ forecast if $tn = 200$

(b) Daily $\hat{\mu}$ forecast if $tn = 300$

(c) Daily $\hat{\sigma}$ forecast if $tn = 200$

(d) Daily $\hat{\sigma}$ forecast if $tn = 300$

Figure 4.8: The parameter forecasts: dynamic ARIMA

Based on these forecasts, the proposed variables are forecasted, whose results are illustrated in Figs. 4.9c, 4.9d, 4.9e, and 4.9f, and show the daily forecast of the parties' costs under Case I and Case II. The performance of the cost forecasts under both Case I and Case II is directly affected by the forecasts of the loss amounts. As in the cubic spline extrapolation method, when a better performance in the loss amounts forecast is obtained, better results in the forecasting parties' costs are achieved. A fair and suitable share of the premium depends on the exposure curves. Figs. 4.9g, 4.9h, 4.9i, and 4.9j show the forecasted time-dependent exposure curves under Case I, and Case II. The curves are suitable when we consider the forecasted loss amounts. Moreover, the risks of the insurer and the reinsurer are reflected according to the contract types (Case I and Case II) in the forecasted curves. The algorithm to forecasts daily loss amounts results in a better forecast when we use the shorter length of the training data set; however, when we compare Figs. 4.9a and 4.9b, we see that the extreme losses are captured by the algorithm if $tn = 300$. Although the overall results are better if $tn = 200$, the algorithm does not catch the extreme losses contrary to the situations of $tn = 300$. The efficiency measures for $tn = 200$, MAPE (7.44%) and RMSE (0.0530), show that dynamic ARIMA with trend search yield slightly good performance with respect to $tn = 300$ (MAPE(9.03%) and RMSE (0.0771)), but much better results compared to cubic spline method.

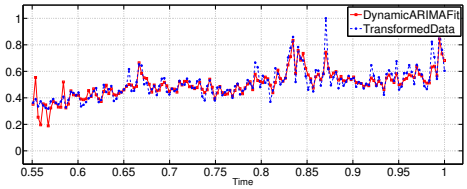

(a) The claim amounts if $tn = 200$

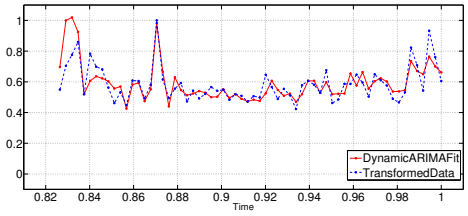

(b) The claim amounts if $tn = 300$

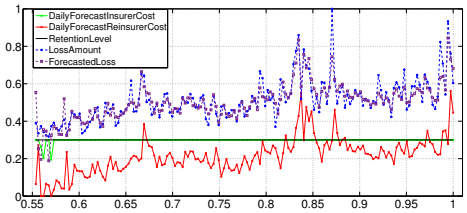

(c) The expected costs if $tn = 200$: Case I

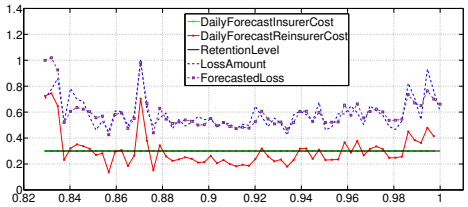

(d) The expected costs if $tn = 300$: Case I

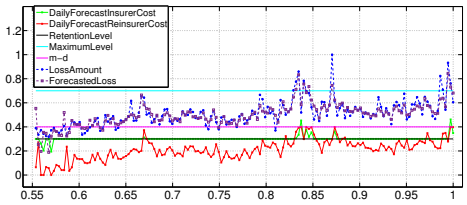

(e) The expected costs if $tn = 200$: Case II

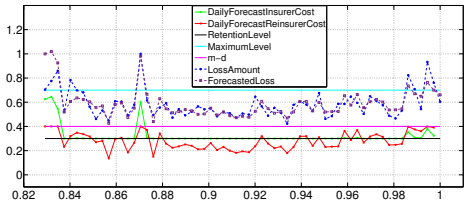

(f) The expected costs if $tn = 300$: Case II

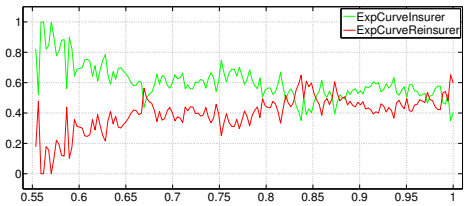

(g) The exposure curves if $tn = 200$

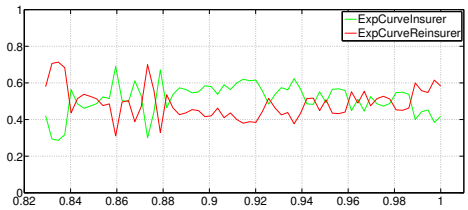

(h) The exposure curves if $tn = 300$

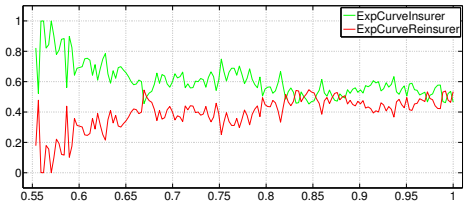

(i) The exposure curves if $tn = 200$

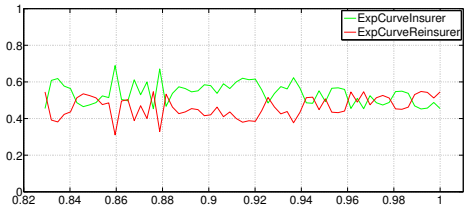

(j) The exposure curves if $tn = 300$

Figure 4.9: Daily forecasts: dynamic ARIMA

4.6 Discussion

With the stop-loss arrangement, the insurer and reinsurer begin a business in which the costs of the parties and the fair distribution of the premium are the primary con-

siderations. The goal of this chapter is to propose a stochastic model, specifically a geometric Brownian motion with time-varying parameters, to describe the behavior of actuarial claim amounts. The dynamics of stop-loss contracts are investigated under policy period, retention level, and retention-cap levels, with the assumption that claim amounts follow a stochastic model. Analytical derivations of the costs and exposure curves are found for both continuous-time and discrete-time models. The real-life data is used to validate the model and dynamically estimate the time-varying parameters using the maximum likelihood estimator to achieve the parameters governing the small and equidistant time intervals. The fit results are sufficient to demonstrate that the model's application to the real data set is appropriate. Based on our analytical derivations and estimated parameters, we present simulations of expected parties' costs and exposure curves. Furthermore, we forecast loss amounts, expected costs, and exposure curves using cubic spline extrapolation and dynamic ARIMA family models. Moreover, we investigate the performances of daily and weekly updates in cubic spline extrapolation, as well as the performances of the length of the train data set with daily updates in dynamic ARIMA models, in order to capture the future behavior of claim amounts and develop a better understanding of the effects of length of train data on claim forecasts in a short term period prediction. The parties can reinvest or start a new business by utilizing this property.

CHAPTER 5

TIME DEPENDENT STOP-LOSS REIUNSURANCE AND EXPOSURE CURVES VIA STOCHASTIC JUMP DIFFUSION

This chapter presents the analytical derivations of the costs of insurer and reinsurer if the losses follow stochastic Pareto and Beta jump diffusion model with time-varying parameters. The time-dependent exposure curves which determine the fair premium share between parties are derived under stochastic jump diffusion behavior of the losses. Moreover, the time-varying parameters of the model are estimated using moment matching estimator (MME) and maximum likelihood estimators (MLE) dynamically. The simulation and the forecasts of the loss amounts, the costs of parties, and the exposure curves are demonstraded as well.

In this chapter, a difference is made in the use of notation for the retention level. This is because d we will use for the down jump is the same as the retention level. In order not to contradict the general literature usage for down symbol d, the retention level for this chapter is characterized by k.

Suppose that the loss $X^J(t)$ satisfies the following stochastic differential equation (SDE) with jumps on the probability space $(\Omega, \mathcal{F}, \mathbb{P})$ and the contract is valid for this random loss over period $[0, T]$:

$$dX^J(t) = X^J(t-)\left(\mu dt + \sigma dW(t) + \sum_{j=u,d}(V^j_{N^j(t)} - 1)dN^j(t)\right), \tag{5.1}$$

where μ and σ are the drift and volatility terms, $W(t)$ is a standard Brownian motion (Wiener process), V^j is the jump magnitude, and $N^j(t)$ are independent Poisson

process with intensity parameters λ^j. Here, $j = u, d$ represent up- and down- jumps, respectively.

Furthermore, the up-jump magnitude (V^u) and the down-jump magnitude (V^d) are distributed Pareto(ν_u) and Beta$(\nu_d, 1)$ with density functions

$$f_{V^u}(x) = \frac{\nu_u}{x^{\nu_u+1}},\ V^u \geq 1, \quad f_{V^d}(x) = \nu_d x^{\nu_d-1},\ \ 0 < V^d < 1,$$

respectively.

All jumps are assumed independent, which results in a mixture of Pareto-Beta distributions for jump magnitudes.

The explicit solution for Eq. (5.1) is obtained by using the Doléans-Dade formula as,[33],

$$X^J(t) = X^J(0)e^{(\mu-\sigma^2/2)t+\sigma W(t)} \prod_{j=u,d} V^j(N^j(t)), \tag{5.2}$$

where

$$\prod_{j=u,d} V^j(N^j(t)) = \begin{cases} 1 & \text{if } N^j(t) = 0, \\ \prod_{i=1}^{N^j(t)} V_i^j & \text{if } N^j(t) = 1, 2, 3, \ldots . \end{cases} \tag{5.3}$$

Our aim is to add time-varying parameters to Pareto-Beta jump diffusion (PBJD) defined above. For this reason, we investigate the model in discrete-time to analyze its behavior and compare it with our claims data.

On a finite probability space $(\Omega, \mathcal{F}, \mathbb{P})$ equipped with a filtration, the model in the discrete-time is built. Consider increasing sequence of σ-algebras in $\mathcal{F}$ partitioned as $\mathcal{F}_0$, $\mathcal{F}_1$, $\mathcal{F}_2$, $\ldots$, $\mathcal{F}_n$, i.e., $\mathcal{F}_n$ can be taken as the information available at time n and is called as σ- algebra of events up to time n.

The time period $[0, T]$ is partitioned as n-many equidistant subintervals such that $0 = t_0 < t_1 < \ldots < ti < t_{i+1} < \ldots < t_n = T$ and let $\Delta t = t_{i+1} - t_i$. The discrete-time solution of the SDE at t_{i+1} can be written as

$$X^J(t_{i+1}) = X^J(t_i)e^{(\mu(i)-\sigma(i)^2/2)\Delta t+\sigma(i)(W(t_{i+1})-W(t_i))} \prod_{j=u,d} V_i^j(N^j(\Delta t)), \tag{5.4}$$

where

$$\prod_{j=u,d} V_i^j(N^j(\Delta t)) = \begin{cases} 1 & \text{if } N^j(\Delta t) = 0, \\ V_i^j & \text{if } N^j(\Delta t) = 1. \end{cases}$$

In Eq. (5.4), we define the jump magnitudes V_i^j distributed Pareto$(\nu_u(i))$ and Beta$(\nu_d(i), 1)$ at time t_i for $j = u, d$, respectively. In other words, we consider up- and down- jump magnitudes are varying during the period $[0, T]$. Moreover, the drift and diffusion parameters, $\mu(i)$ and $\sigma(i)$, are also considered as time-varying. On the other hand, the Poisson parameters, λ_u and λ_d are taken as constant.

Eq. (5.4) is obtained using the independent increment property of Brownian motion and Poisson process, i.e.,

$$W(t_{i+1}) - W(t_i) \stackrel{d}{=} W(\Delta t) \text{ and } N^j(t_{i+1}) - N^j(t_i) \stackrel{d}{=} N^j(\Delta t).$$

According to this loss model setup, the probability density function of log-return process in discrete-time and the costs of insurer and reinsurer are derived.

5.1 The Log-Return Process in Discrete-Time

The log-return process of the explicit solution in Eq. (5.4) becomes

$$\begin{aligned} Z(t_i) := \ln\left(\frac{X^J(t_{i+1})}{X^J(t_i)}\right) &= (\mu(i) - \sigma(i)^2/2)\Delta t \\ &\quad + \sigma(i)W(\Delta t) + Y_i^u N^u(\Delta t) + Y_i^d N^d(\Delta t), \end{aligned} \tag{5.5}$$

where $\ln(V_i^j) = Y_i^j$ for $j = u, d$ and $i = 0, 1, 2, \ldots$, whose up-jump and down-jump magnitudes (V_i^u, V_i^d) within $[t_i, t_{i+1}]$ follow Pareto$(\nu_u(i))$ and Beta$(\nu_d(i), 1)$, respectively.

The density of Z_{t_i} in Eq. (5.5) is obtained as

$$\begin{aligned} f_{Z(t_i)}(z) =& \mathbb{P}(uu=0,\lambda_u)\mathbb{P}(dd=0,\lambda_d)f_{0|0}(z) + \mathbb{P}(uu=0,\lambda_u)f_{0|1}(z) \\ &+ \mathbb{P}(dd=0,\lambda_d)f_{1|0}(z) \\ =& e^{-(\lambda_u+\lambda_d)}f_{0|0}(z) + e^{-\lambda_u}f_{0|1}(z) + e^{-\lambda_d}f_{1|0}(z) \end{aligned} \tag{5.6}$$

by modifiying the derivations from [35] into the discrete-time model. Here, $\mathbb{P}(x,\lambda)$ refers to the density of Poisson distribution. Also, $f_{0|0}(z)$ represents the conditional density of $Z(t_i)$ for the case $uu=0$, $dd=0$, i.e., no up- and down-jumps, such that $Z(t_i) = \left(\mu(i) - \dfrac{\sigma(i)^2}{2}\right)\Delta t + \sigma(i)W(\Delta t)$. In other words,

$$Z(t_i) \sim N\left(\left(\mu(i) - \tfrac{\sigma(i)^2}{2}\right)\Delta t, \sigma(i)^2\Delta t\right).$$

For simplicity in the following terms, let $s := \Delta t$.

The next term, $f_{0|1}(z)$ is the conditional density of $Z(t_i)$ when $uu=0$, $dd=1$, i.e., no up-jump and a down-jump, with

$$\begin{aligned} f_{0|1}(z) &= \frac{\nu_d(i)}{\sqrt{2\pi s\sigma(i)^2}} \underbrace{\int_{-\infty}^{0} e^{\nu_d(i)x - \frac{1}{2s\sigma(i)^2}\left(z-x-\mu(i)s+\frac{1}{2}\sigma(i)^2 s\right)^2} dx}_{=:I_1(i)}, \\ &= \nu_d(i) e^{-v_d(i)\left(\frac{\sigma(i)^2 s}{2}(\nu_d(i)+1)+z-\mu(i)s\right)} \Phi(0;\alpha_1(i),\beta_1(i)^2) \end{aligned}$$

where

$$\begin{aligned} I_1(i) &= e^{-v_d(i)\left(\frac{\sigma(i)^2 s}{2}(\nu_d(i)+1)+z-\mu(i)s\right)} \sigma(i)\sqrt{2\pi s}\ \Phi(0;\alpha_1(i),\beta_1(i)^2), \\ \alpha_1(i) &= z + \frac{\sigma(i)^2 s}{2} - \mu(i)s + \nu_d(i)\sigma(i)^2 s, \quad \beta_1(i) = \sigma(i)\sqrt{s}, \text{ and} \end{aligned}$$

$\Phi(0;\alpha_1(i),\beta_1(i)^2)$ is the value of normal cdf with mean $\alpha_1(i)$ and variance $\beta_1(i)^2$ at 0.

Finally, $f_{1|0}(z)$ represents the conditional density of $Z(t_i)$ for the case $uu=1$, $dd=0$, i.e., an up-jump and no down-jump, having the form

$$\begin{aligned} f_{1|0}(z) &= \frac{\nu_u(i)}{\sqrt{2\pi s\sigma(i)^2}} \underbrace{\int_{0}^{\infty} e^{-\nu_u(i)x - \frac{1}{2s\sigma(i)^2}\left(z-x-\mu(i)s+\frac{1}{2}\sigma(i)^2 s\right)^2} dx}_{=:I_2(i)}, \\ &= \nu_u(i) e^{-v_u(i)\left(\frac{\sigma(i)^2 s}{2}(\nu_u(i)-1)-z+\mu(i)s\right)} \left[1 - \Phi(0;\alpha_2(i),\beta_2(i)^2)\right] \end{aligned}$$

where

$$I_2(i) = e^{-v_u(i)\left(\frac{\sigma(i)^2 s}{2}(\nu_u(i)-1)-z+\mu(i)s\right)}\sigma(i)\sqrt{2\pi s}\,[1-\Phi(0;\alpha_2(i),\beta_2(i)^2)],$$

$$\alpha_2(i) = z + \frac{\sigma(i)^2 s}{2} - \mu(i)s - \nu_u(i)\sigma(i)^2 s, \quad \beta_2(i) = \sigma(i)\sqrt{s}, \text{ and}$$

$\Phi(0;\alpha_2(i),\beta_2(i)^2)$ is the value of Normal cdf with mean $\alpha_2(i)$ and variance $\beta_2(i)^2$ at 0.

The density of $Z(t_i)$ in Eq.(5.6) is the weighted sum of mixture of Normal, Pareto, and Beta distributions. The proofs for $f_{0|1}(z)$ and $f_{1|0}(z)$ are given in Appendix A.2.

5.2 Expected Costs Derivations

One of the important issues in a reinsurance contract is to decide on which retention level will be a mutually agreed choice maximizing the profits of insurer and reinsurer. In this respect, exposure curves are handful tools to depict an approximate premium partition as well as its corresponding loss amount. Reinsurers, on the other hand, may also set a cap (maximum) value on the claims to keep their costs under control as a prevention against catastrophic losses. Therefore, aggrements in a stop-loss contract may have either only retention or both a retention and a cap. We consider these two contract types separately and denote each as Case I and Case II, respectively.

5.2.1 Case I: Retention

We assume that the parties (insurer and reinsurer) agree on a predetermined retention level k. The costs at discrete-time t_i under the probability measure $\mathbb{P}$ can be written as

$$\begin{aligned} I(t_i, X^J(t_i), k) &= \min(X^J(t_i), k), \\ R(t_i, X^J(t_i), k) &= \max(X^J(t_i) - k, 0). \end{aligned} \tag{5.7}$$

The expected claims, Eq. (5.8), the costs of reinsurer, Eq. (5.9), and the costs of insurer, Eq. (5.10), under Case I are shown as follows:

$$\mathbb{E}[X^J(t_{i+1})|\mathcal{F}_{t_i}] = \mathbb{E}[X^J(t_i)e^{Z(t_i)}] = \int_{-\infty}^{\infty} X^J(t_i)e^z f_{Z(t_i)}(z)\,dz, \tag{5.8}$$

$$
\begin{aligned}
\mathbb{E}[R(t_{i+1}, X^J(t_{i+1}), k)|\mathcal{F}_{t_i}] &= \mathbb{E}[\max(X^J(t_{i+1}) - k, 0)|\mathcal{F}_{t_i}] \\
&= \mathbb{E}[\max(X^J(t_i)e^{Z(t_i)} - k, 0)] \\
&= \underbrace{\int_{-\infty}^{\infty} \max(X^J(t_i)e^z - k, 0) f_{Z(t_i)}(z)\, dz}_{\text{for } z > \ln\left(\frac{k}{X^J(t_i)}\right) := E_{1i},\ \max(X^J(t_i)e^z - k, 0) \neq 0} \\
&= \int_{E_{1i}}^{\infty} (X^J(t_i)e^z - k) f_{Z(t_i)}(z)\, dz \\
&= \int_{E_{1i}}^{\infty} X^J(t_i)e^z\, f_{Z(t_i)}(z)\, dz - k \int_{E_{1i}}^{\infty} f_{Z(t_i)}(z)\, dz,
\end{aligned}
\tag{5.9}
$$

$$
\begin{aligned}
\mathbb{E}[I(t_{i+1}, X^J(t_{i+1}), k)|\mathcal{F}_{t_i}] &= \mathbb{E}[X^J(t_i)e^{Z(t_i)}] - \mathbb{E}[\max(X^J(t_i)e^{Z(t_i)} - k, 0)] \\
&= \int_{-\infty}^{E_{1i}} X^J(t_i)e^z f_{Z(t_i)}(z)\, dz + k \int_{E_{1i}}^{\infty} f_{Z(t_i)}(z)\, dz.
\end{aligned}
\tag{5.10}
$$

The solutions to the integrals in Eqs. (5.8-5.10) require numerical methods to obtain a closed form analytical solution. The estimations are obtained using the summation on the indexing sets over the intervals of endpoints in the integrals are highlighted in Proposition 5.1.

Proposition 5.1. *The expected claims, costs of reinsurer and insurer at the time t_{i+1} with respect to the filtration $\mathcal{F}_{t_i}$ and the retention, k, are*

$$
\mathbb{E}[X^J(t_{i+1})|\mathcal{F}_{t_i}] = \lim_{N_{max}\to\infty} X^J(t_i) \sum_{j=0}^{N_a} e^{a_j} f_{Z(t_i)}(a_j)\, \Delta a, \tag{5.11}
$$

$$
\mathbb{E}[R(t_{i+1}, X^J(t_{i+1}), k)|\mathcal{F}_{t_i}] = \lim_{N_{max}\to\infty} \sum_{j=0}^{N_b} \left[X^J(t_i)e^{b_j} - k\right] f_{Z(t_i)}(b_j)\, \Delta b, \tag{5.12}
$$

$$
\mathbb{E}[I(t_{i+1}, X^J(t_{i+1}), k)|\mathcal{F}_{t_i}] = \mathbb{E}[X^J(t_{i+1})|\mathcal{F}_{t_i}] - \mathbb{E}[R(t_{i+1}, X^J(t_{i+1}), k)|\mathcal{F}_{t_i}], \tag{5.13}
$$

respectively. Here,

$$
\{a_0 = -N_{max}; a_1 = a_0 + \Delta a, \ldots; a_j = a_0 + j\Delta a, \ldots; a_{N_a} = N_{max}\},
$$

$$
\{b_0 = E_{1i}; b_1 = b_0 + \Delta b, \ldots; b_j = b_0 + j\Delta b, \ldots; b_{N_b} = N_{max}\},
$$

where $\Delta a = a_j - a_{j-1}$, $\Delta b = b_j - b_{j-1}$ *for each* $j \in \{1, 2, \ldots, max(N_a, N_b)\}$ *and*

$$E_{1i} = ln\left(\frac{k}{X^J(t_i)}\right),\ i = 0, 1, 2, \ldots\ .$$

5.2.2 Case II: Retention and Maximum

Suppose that the parties agreed on the prespecified retention level k and the maximum level m, in $[0, T]$ which remains the same in each discrete-time t_i. The costs under the probability measure $\mathbb{P}$ are expressed as

$$\begin{aligned} I(t_i, X^J(t_i), k, m) &= \min(X^J(t_i), k) + \max(X^J(t_i) - m, 0), \\ R(t_i, X^J(t_i), k, m) &= \min(m - k, \max(X^J(t_i) - k, 0)). \end{aligned} \tag{5.14}$$

Given the expected cost remains to be the same as in Eq. (5.8), the costs of insurer and reinsurer under Case II are expressed in Eqs. (5.15) and (5.16), respectively.

$$\begin{aligned} &\mathbb{E}[I(t_{i+1}, X^J(t_{i+1}), k, m)|\mathcal{F}_{t_i}] \\ &\quad = \mathbb{E}[\max(X^J(t_{i+1}) - m, 0)|\mathcal{F}_{t_i}] + \mathbb{E}[\min(X^J(t_{i+1}), k)|\mathcal{F}_{t_i}] \\ &\quad = \mathbb{E}[\max(X^J(t_i)e^{Z(t_i)} - m, 0)] + \mathbb{E}[\min(X^J(t_i)e^{Z(t_i)}, k)] \\ &\quad = \int_{E_{2i}}^{\infty} X^J(t_i)e^z\ f_{Z(t_i)}(z)\ dz - m\int_{E_{2i}}^{\infty} f_{Z(t_i)}(z)\ dz + \int_{-\infty}^{E_{1i}} X^J(t_i)e^z f_{Z(t_i)}(z)\ dz \\ &\quad + k\int_{E_{1i}}^{\infty} f_{Z(t_i)}(z)\ dz, \end{aligned} \tag{5.15}$$

where

$$\begin{aligned} \mathbb{E}[\max(X^J(t_i)e^{Z(t_i)} - m, 0)] &= \underbrace{\int_{-\infty}^{\infty} \max(X^J(t_i)e^z - m, 0) f_{Z(t_i)}(z)\ dz}_{\text{for } z > \ln\left(\frac{m}{X^J(t_i)}\right) := E_{2i},\ \max(X^J(t_i)e^z - m, 0) \neq 0} \\ &= \int_{E_{2i}}^{\infty} (X^J(t_i)e^z - m) f_{Z(t_i)}(z)\ dz \\ &= \int_{E_{2i}}^{\infty} X^J(t_i)e^z\ f_{Z(t_i)}(z)\ dz - m\int_{E_{2i}}^{\infty} f_{Z(t_i)}(z)\ dz, \end{aligned}$$

$$\mathbb{E}[\min(X^J(t_i)e^{Z(t_i)}, k)] = \underbrace{\int_{-\infty}^{\infty} \min(X^J(t_i)e^z, k) f_{Z(t_i)}(z)\, dz}_{\text{for } \ln\left(\frac{k}{X^J(t_i)}\right)=E_{1i},\ \min(X^J(t_i)e^z,k)=k}$$
$$= \int_{-\infty}^{E_{1i}} X^J(t_i)e^z f_{Z(t_i)}(z)\, dz + k \int_{E_{1i}}^{\infty} f_{Z(t_i)}(z)\, dz.$$

$$\begin{aligned}
&\mathbb{E}[R(t_{i+1}, X^J(t_{i+1}), k, m)|\mathcal{F}_{t_i}] \\
&= \mathbb{E}[X^J(t_i)e^{Z(t_i)}] - \mathbb{E}[\max(X^J(t_i)e^{Z(t_i)} - m, 0)] - \mathbb{E}[\min(X^J(t_i)e^{Z(t_i)}, k)] \\
&= \int_{-\infty}^{\infty} X^J(t_i)e^z f_{Z(t_i)}(z)\, dz - \int_{E_{2i}}^{\infty} X^J(t_i)e^z\, f_{Z(t_i)}(z)\, dz + m \int_{E_{2i}}^{\infty} f_{Z(t_i)}(z)\, dz \\
&- \int_{-\infty}^{E_{1i}} X^J(t_i)e^z f_{Z(t_i)}(z)\, dz - k \int_{E_{1i}}^{\infty} f_{Z(t_i)}(z)\, dz.
\end{aligned} \tag{5.16}$$

Implementing numerical estimations for the integrals in (5.15-5.16), we derive the expected values as introduced in Proposition 5.2.

Proposition 5.2. *The expected costs of insurer and reinsurer at the time t_{i+1} with respect to the filtration $\mathcal{F}_{t_i}$, the retention, k, and the maximum, m, are*

$$\begin{aligned}
\mathbb{E}[I(t_{i+1}, X^J(t_{i+1}), k)|\mathcal{F}_{t_i}] = &\lim_{N_{max}\to\infty} \sum_{j=0}^{N_c} \left[X^J(t_i)e^{c_j} - m\right] f_{Z(t_i)}(c_j)\, \Delta c \\
&+ \sum_{j=0}^{N_g} X^J(t_i)e^{g_j} f_{Z(t_i)}(g_j)\, \Delta g + k \sum_{j=0}^{N_h} f_{Z(t_i)}(h_j)\, \Delta h,
\end{aligned} \tag{5.17}$$

$$\mathbb{E}[R(t_{i+1}, X^J(t_{i+1}), k, m)|\mathcal{F}_{t_i}] = \mathbb{E}[X^J(t_{i+1})|\mathcal{F}_{t_i}] - \mathbb{E}[I(t_{i+1}, X^J(t_{i+1}), k, m)|\mathcal{F}_{t_i}], \tag{5.18}$$

respectively. Here,

$$\{c_0 = E_{2i}, c_1 = c_0 + \Delta c, \ldots, c_j = c_0 + j\Delta c, \ldots, c_{N_c} = N_{max}\},$$
$$\{g_0 = -N_{max}, g_1 = g_0 + \Delta g, \ldots, g_j = g_0 + j\Delta g, \ldots, g_{N_g} = E_{1i}\},$$
$$\{h_0 = E_{2i}, h_1 = h_0 + \Delta h, \ldots, h_j = h_0 + j\Delta h, \ldots, h_{N_h} = N_{max}\},$$

where $\Delta c = c_j - c_{j-1}$, $\Delta g = g_j - g_{j-1}$, $\Delta h = h_j - h_{j-1}$ for each $j \in \{1, 2, \ldots, max(N_c, N_g, N_h)\}$ and

$$E_{1i} = ln\left(\frac{k}{X^J(t_i)}\right),\ \ E_{2i} = ln\left(\frac{m}{X^J(t_i)}\right),\ i = 0, 1, 2, \ldots\ .$$

5.3 Time Varying Frame in Exposure Curves

The exposure curves are used to allocate risks between insurers and reinsurers, allowing us also to determine their premium share. While we assume that the risk of loss behavior changes over time due to natural disasters, so do the average losses. In that case, the exposure curves should also be adopted to capture the time influence. For this aim, we derive the analytical forms of exposure curves by modifying Bernegger's model [6] under time-dimensional and SDE-type loss distribution assumptions for Case I and Case II.

Definition 5.1. *The exposure curves for Case I for the reinsurer and insurer at time t_{i+1} with respect to filtration $\mathcal{F}$ are defined as*

$$\begin{aligned} G_R(t_{i+1}, d) &= \frac{\mathbb{E}[R(t_{i+1}, X^J(t_{i+1}), k)|\mathcal{F}_{t_i}]}{\mathbb{E}[X^J(t_{i+1})|\mathcal{F}_{t_i}]} \\ &= \lim_{N_{max}\to\infty} \frac{\sum_{j=0}^{N_b}\left[X^J(t_i)e^{b_j} - k\right] f_{Z(t_i)}(b_j)\,\Delta b}{X^J(t_i)\sum_{j=0}^{N_a} e^{a_j} f_{Z(t_i)}(a_j)\,\Delta a}, \\ G_I(t_{i+1}, k) &= 1 - G_R(t_{i+1}, k), \end{aligned} \tag{5.19}$$

respectively. Here,

$$\{a_0 = -N_{max}, a_1 = a_0 + \Delta a, \ldots, a_j = a_0 + j\Delta a, \ldots, a_{N_a} = N_{max}\},$$
$$\{b_0 = E_{1i}, b_1 = b_0 + \Delta b, \ldots, b_j = b_0 + j\Delta b, \ldots, b_{N_b} = N_{max}\},$$

where $\Delta a = a_j - a_{j-1}$, $\Delta b = b_j - b_{j-1}$ for each $j \in \{1, 2, \ldots, max(N_a, N_b)\}$ and

$$E_{1i} = ln\left(\frac{k}{X^J(t_i)}\right),\ i = 0, 1, 2, \ldots\ .$$

Definition 5.2. *The exposure curves for Case II for the insurer and reinsurer at time t_{i+1} with respect to filtration $\mathcal{F}$ are expressed as*

$$\begin{aligned} G_I(t_{i+1}, k, m) &= \frac{\mathbb{E}[I(t_{i+1}, X^J(t_{i+1}), k, m)|\mathcal{F}_{t_i}]}{\mathbb{E}[X^J(t_{i+1})|\mathcal{F}_{t_i}]} \\ &= \lim_{N_{max}\to\infty}\left(\frac{\sum_{j=0}^{N_c}\left[X^J(t_i)e^{c_j} - m\right] f_{Z(t_i)}(c_j)\,\Delta c}{X^J(t_i)\sum_{j=0}^{N_a} e^{a_j} f_{Z(t_i)}(a_j)\,\Delta a} + \frac{\sum_{j=0}^{N_g} X^J(t_i)e^{g_j} f_{Z(t_i)}(g_j)\,\Delta g}{X^J(t_i)\sum_{j=0}^{N_a} e^{a_j} f_{Z(t_i)}(a_j)\,\Delta a}\right. \\ &\qquad \left. + k\frac{\sum_{j=0}^{N_h} f_{Z(t_i)}(h_j)\,\Delta h}{X^J(t_i)\sum_{j=0}^{N_a} e^{a_j} f_{Z(t_i)}(a_j)\,\Delta a}\right), \\ G_R(t_{i+1}, k, m) &= 1 - G_I(t_{i+1}, k, m), \end{aligned} \tag{5.20}$$

respectively. Here,

$$\{a_0 = -N_{max}, a_1 = a_0 + \Delta a, \ldots, a_j = a_0 + j\Delta a, \ldots, a_{N_a} = N_{max}\},$$
$$\{c_0 = E_{2i}, c_1 = c_0 + \Delta c, \ldots, c_j = c_0 + j\Delta c, \ldots, c_{N_c} = N_{max}\},$$
$$\{g_0 = -N_{max}, g_1 = g_0 + \Delta g, \ldots, g_j = g_0 + j\Delta g, \ldots, g_{N_g} = E_{1i}\},$$
$$\{h_0 = E_{2i}, h_1 = h_0 + \Delta h, \ldots, h_j = h_0 + j\Delta h, \ldots, h_{N_h} = N_{max}\},$$

where $\Delta a = a_j - a_{j-1}$, $\Delta c = c_j - c_{j-1}$, $\Delta g = g_j - g_{j-1}$, $\Delta h = h_j - h_{j-1}$ *for each* $j \in \{1, 2, \ldots, max(N_a, N_c, N_g, N_h)\}$ *and*

$$E_{1i} = ln\left(\frac{k}{X^J(t_i)}\right), \quad E_{2i} = ln\left(\frac{m}{X^J(t_i)}\right), \; i = 0, 1, 2, \ldots .$$

After defining the expressions for the insurer and reinsurer, and assuming that the stochastic loss defined in Eq. (5.1) is influenced by random jumps Eq. (5.4), we focus on the estimation of parameters, μ, σ, ν_u and ν_d using MTPL data set.

5.4 Parameter Estimation under Time-Varying Frame

We calibrate the model parameter considering an application to the real data, which is Turkey's compulsory traffic insurance (MTPL) claims occurred in the calendar year 2006. The parameter estimation structure consists of three parts. We first find the jump times using the geometric Brownian motion model with time-varying parameters whose fit performance is found to be very good [31]. Next, our aim is to find the parameter of jump magnitudes using the dynamic moment matching estimation (DMME) for each time unit. After estimating parameters for the jump part of the process, we use these parameters to eliminate the jumps from the data. Then remaining structure of the PBJD process becomes suitable for dynamic maximum likelihood estimation (DMLE) for the drift and the volatility parameters for each time unit under the framework of the geometric Brownian Motion model. The outcomes of the study is found to capture the real MTPL loss data.

To validate the proposed model and analytical derivations, a real-life data set consisting of approximately 1 million entries in the portfolio of compulsory traffic insurance (MTPL) in Turkey in one policy year is employed. To calibrate the parameters ($\mu(i)$,

$\sigma(i)$, $\nu_u(i)$ and $\nu_d(i)$) of the proposed model, we use maximum likelihood and moment matching estimations under a dynamic structure to contribute the time-varying impact on the parameters at each time partition. MATLAB is the software employed in all numerical applications. The data set with aggregate daily losses provides 365 observations for the year 2006 (Figure 4.1a). We choose equidistant time intervals of 1-day length. Figure 4.1a shows that the daily losses have an increasing trend throughout the period, but show volatile structure by the half of the year. The volatile period shows a sharpe inrease and decrease; however, the up and down extreme variations differ from each others and the excessive alterations in succesive time points for the data show different characteristics in the different periods. This pattern also confirms our assumption on using a PBJD process. Since the range of loss amounts is very high (minimum $= 270$ TL, maximum $= 5,738,647$ TL), we rescale the original losses ($L(i),\ i = 1, .., 365$) using min-max transformation ($TL(i)$).

5.4.1 The detection of jump time and its parameters

We use the properties of geometric Brownian Motion model with time-varying parameters to detect the jump time [31]. The calibration results using geometric Brownian Motion on original and transformed data sets yields the same MAPE for both, but, lower RMSE for the transformed data. Then, by the help of a risk measure, tail value at risk (TVaR), we detect jump times to either directions. The proposed GBM model is given as

$$X^G_{t_{i+1}} = X^G_{t_i} e^{\left(\mu_G(i) - \frac{\sigma_G(i)^2}{2}\right)\Delta t + \sigma_G(i)(W(t_{i+1}) - W(t_i))}, \tag{5.21}$$

where $\mu_G(i)$ and $\sigma_G(i)$ are the calibrated constant parameters governing the period between $[t_i, t_{i+1}]$.

1) ***Up-jump time detection:*** If $X^G(t_{i+1}) \geq X^G(t_i)$, then we consider the discrete-time solution given in Eq. (5.4) and let

$$\begin{aligned} \bar{S}_u(i) :&= ln\left(\frac{X^G(t_{i+1})}{X^G(t_i)}\right) \\ &= \left(\mu_G(i) - \frac{\sigma_G(i)^2}{2}\right)\Delta t + \sigma_G(i)W(\Delta t). \end{aligned}$$

Since $W(\Delta t) \stackrel{d}{=} \sqrt{\Delta t} Y$ where $Y \sim N(0,1)$,

$$\bar{S}_u(i) \sim N\left(\left(\mu_G(i) - \frac{\sigma_G(i)^2}{2}\right)\Delta t, \sigma_G(i)^2 \Delta t\right).$$

Thefore, the right TVaR of $\bar{S}_u(i)$ is given by

$$\text{TVaR}_\alpha(\bar{S}_u(i)) = \left(\mu_G(i) - \frac{\sigma_G(i)^2}{2}\right)\Delta t + \sigma_G(i)\sqrt{\Delta t}\frac{\phi(\Phi^{-1}(\alpha))}{1-\alpha},$$

where $\phi(.)$ and $\Phi^{-1}(.)$ are the standard Normal density function and quantile, respectively.

Definition 5.3. *The t_i's are stated to be up-jump times if*

$$\textit{TVaR}_\alpha(\bar{S}_u(i)) < X^G(t_{i+1}), \tag{5.22}$$

where α is close to 1.

2) ***Down-jump time detection:*** If $X^G(t_{i+1}) < X^G(t_i)$, then we consider

$$\begin{aligned}\bar{S}_d(i) :&= ln\left(\frac{X^G(t_i)}{X^G(t_{i+1})}\right) = -\bar{S}_u(i)\\ &= -\left(\mu_G(i) - \frac{\sigma_G(i)^2}{2}\right)\Delta t - \sigma_G(i)W(\Delta t).\end{aligned}$$

Since $W(\Delta t) \stackrel{d}{=} \sqrt{\Delta t} Y$ where $Y \sim N(0,1)$,
$-\bar{S}_d(i) \sim N\left(-\left(\mu_G(i) - \frac{\sigma_G(i)^2}{2}\right)\Delta t, \sigma_G(i)^2\Delta t\right)$.

The right TVaR of the random variable $\bar{S}_d(i)$ detects the down- jump times and is given by

$$\text{TVaR}_\alpha(\bar{S}_d(i)) = -\left(\mu_G(i) - \frac{\sigma_G(i)^2}{2}\right)\Delta t + \sigma_G(i)\sqrt{\Delta t}\frac{\phi(\Phi^{-1}(\alpha))}{1-\alpha}.$$

Definition 5.4. *The t_i's are stated to be down-jump times if*

$$\textit{TVaR}_\alpha(\bar{S}_d(i)) < X^G(t_{i+1}), \tag{5.23}$$

where α is close to 1.

Based on Definitions (5.3-5.4), on the data set we find the locations of jump times at which red and green colored points in Figure 5.1 represent the up- and down- jumps, respectively.

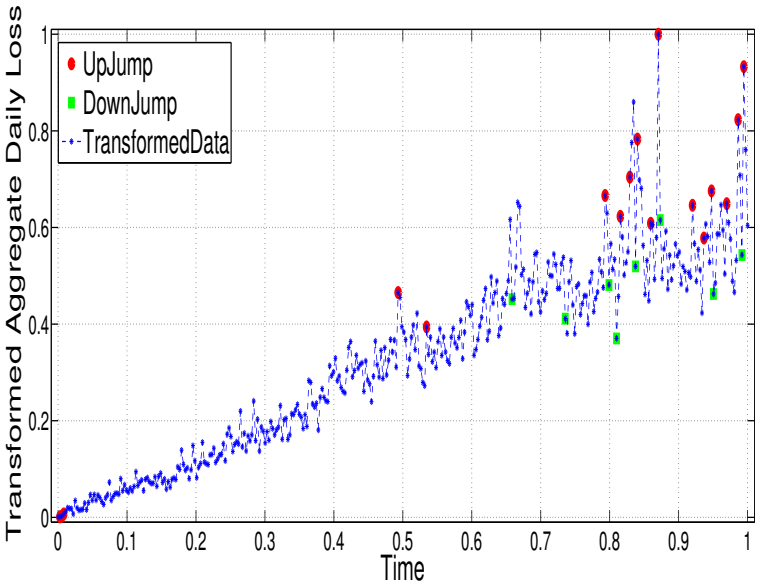

Figure 5.1: Jump times in transformed aggregate daily claims

The detected jumps, especially during the last quarter of the contract period Figure 5.1 is verifyable with the history, as in 2006 extreme floods caused large claims in Turkey [26]. The proposed approach proves to detect jump structure in the frame of PBJD assumptions.

Using MLE method, the *parameters of Poisson processes*, λ_u and λ_d, are estimated based on up-jump and down-jump times. Given

$$\mathbb{E}[N^u(T)] = \lambda_u T, \text{ and } \mathbb{E}[N^d(T)] = \lambda_d T,$$

we estimate $\hat{\lambda}_u = \frac{17}{365} = 0.0467$ and $\hat{\lambda}_d = \frac{8}{365} = 0.0220$.

Along with the detection of jump times, their magnitude have exposure on aggregate claims. The *up- and down-jump magnitudes* require the parameters $\nu_u(i)$ and $\nu_d(i)$ to be estimated due to the distributional assumptions on each $[t_i, t_{i+1}]$. To do so, the dynamic match of skewness and kurtosis of $X(t_i)$ for each $[t_i, t_{i+1}]$ with Δt is made.

Using the log-return process $Z(t_i)$ defined in Eq. (5.5), the skewness and kurtosis of $Z(t_i)$ become

$$
\begin{aligned}
\text{Skew}[Z(t_i)] &= \frac{6\left(\frac{\lambda_u}{\nu_u(i)^3} - \frac{\lambda_d}{\nu_d(i)^3}\right)}{\mathbb{V}[Z(t_i)]^{3/2}\sqrt{\Delta t}}, \\
\text{Kurt}[Z(t_i)] &= \frac{24\left(\frac{\lambda_u}{\nu_u(i)^4} - \frac{\lambda_d}{\nu_d(i)^4}\right)}{\mathbb{V}[Z(t_i)]^{2}\Delta t},
\end{aligned}
\tag{5.24}
$$

respectively. Here, the variance is $\mathbb{V}[Z(t_i)] = \left(\sigma(i)^2 + 2\frac{\lambda_u}{\nu_u(i)^2} + 2\frac{\lambda_d}{\nu_d(i)^2}\right)\Delta t$.

Let $\overline{\mathbb{V}}[LTL(i)]$, $\overline{\text{Skew}}[LTL(i)]$, and $\overline{\text{Kurt}}[LTL(i)]$ denote the sample variance, skewness, and kurtosis at each t_i, respectively.

Equating the sample estimates to the population parameters

$$
\begin{aligned}
6\left(\frac{\hat{\lambda}_u}{\nu_u(i)^3} - \frac{\hat{\lambda}_d}{\nu_d(i)^3}\right) &= \overline{\text{Skew}}[LTL(i)]\overline{\mathbb{V}}[LTL(i)]^{3/2}\sqrt{\Delta t}, \\
24\left(\frac{\hat{\lambda}_u}{\nu_u(i)^4} - \frac{\hat{\lambda}_d}{\nu_d(i)^4}\right) &= \overline{\text{Kurt}}[LTL(i)]\overline{\mathbb{V}}[LTL(i)]^{2}\Delta t
\end{aligned}
\tag{5.25}
$$

leads to

$$
\begin{aligned}
\hat{\lambda}_u\nu_d(i)^3 - \hat{\lambda}_d\nu_u(i)^3 - A_1(i)\nu_u(i)^3\nu_d(i)^3 &= 0, \\
\hat{\lambda}_u\nu_d(i)^4 + \hat{\lambda}_d\nu_u(i)^4 - A_2(i)\nu_u(i)^4\nu_d(i)^4 &= 0.
\end{aligned}
\tag{5.26}
$$

Defining

$$
A_1(i) = \frac{\overline{\text{Skew}}[LTL(i)]\overline{\mathbb{V}}[LTL(i)]^{3/2}\sqrt{\Delta t}}{6} \quad \text{and} \quad A_2(i)\frac{\overline{\text{Kurt}}[LTL(i)]\overline{\mathbb{V}}[LTL(i)]^{2}\Delta t}{24}
$$

and solving the systems of two equations and two unknowns using MATLAB programming in Eq. (5.26), $\hat{\nu_u}(i)$ and $\hat{\nu_d}(i)$ for each $[t_i, t_{i+1}]$ are estimated using dynamic moment matching method.

5.4.2 Determination of drift and volatility parameters

As the final step, we estimate the *drift and volatility parameters* using dynamic MLE (DMLE) with the contribution of sample estimates of $\hat{\lambda}_u$, $\hat{\lambda}_d$, $\hat{\nu_u}(i)$ and $\hat{\nu_d}(i)$ that construct the jump part of the proposed model.

Given the GBM model fit to log transformed returns, jump modified model with time-varying parameters has drawbacks in implementing the dynamic MLE method. For this reason, we first eliminate the influence of jumps form the series using Monte Carlo (MC) simulations. It should be noted that the jump influence on Eq. (5.2), which is explicitly given in Eq. (5.3), can be reduced easily. To achieve this, $100,000$ up- and down- jumps for each discrete-time period, i, are randomly generated and the resulting series, called JP, is used to create new series, CD, as follows

$$CD(i) = \frac{TL(i)}{JP(i)}, \quad i = 1, 2, \ldots, 365. \tag{5.27}$$

Consider the discrete-time solution of GBM given in Eq. (5.21) and let

$$\begin{aligned} \bar{K}(i) :&= \ln\left(\frac{X^G(t_{i+1})}{X^G(t_i)}\right) \\ &= \left(\mu(i) - \frac{\sigma(i)^2}{2}\right)\Delta t + \sigma(i)W(\Delta t). \end{aligned}$$

Since $W(\Delta t) \stackrel{d}{=} \sqrt{\Delta t}Y$ where $Y \sim N(0,1)$, $\bar{K}(i) \sim N\left(\left(\mu(i) - \frac{\sigma(i)^2}{2}\right)\Delta t, \sigma(i)^2\Delta t\right)$.

Similarly, writing $LCD(i) := ln\left(\frac{CD(i+1)}{CD(i)}\right)$, and then equating $LCD(i)$ to $\bar{K}(i)$, we obtain MLEs of $\bar{K}(i)$ for each $[t_i, t_{i+1}]$ as

$$\begin{aligned} \hat{\mu}_{\text{MLE}} &= \frac{1}{i+1}\sum_{j=0}^{i+1}\bar{K}(j) = \left(\mu(i) - \frac{\sigma(i)^2}{2}\right)\Delta t, \\ \hat{\sigma}_{\text{MLE}} &= \sqrt{\frac{1}{i+1}\sum_{j=0}^{i+1}(\bar{K}(j) - \hat{\mu}_{\text{MLE}})^2} = \sqrt{\sigma(i)^2\Delta t}, \end{aligned} \tag{5.28}$$

whose solutions yield the estimates of parameters for the specified time interval and expressed as

$$\begin{aligned} \hat{\sigma}(i) &= \frac{\sqrt{\frac{1}{i+1}\sum_{j=0}^{i+1}(\bar{K}(j) - \frac{1}{i+1}\sum_{j=0}^{i+1}\bar{K}(j))^2}}{\sqrt{\Delta t}}, \\ \hat{\mu}(i) &= \frac{\frac{1}{i+1}\sum_{j=0}^{i+1}\bar{K}(j) + \frac{\frac{1}{i+1}\sum_{j=0}^{i+1}(\bar{K}(j) - \frac{1}{i+1}\sum_{j=0}^{i+1}\bar{K}(j))^2}{2}}{\Delta t}. \end{aligned} \tag{5.29}$$

After the calibration of the parameters, the justification of the model is performed by $100,000$ MC simulations with the estimated parameters. Figure 5.2 shows that the DMLE (red line) is accurate to catch the jumps as well as it follows the pattern of transformed data (blue points). This is also justified by the estimates yielding low MAPE (1.4758%) and RMSE (0.0713) values.

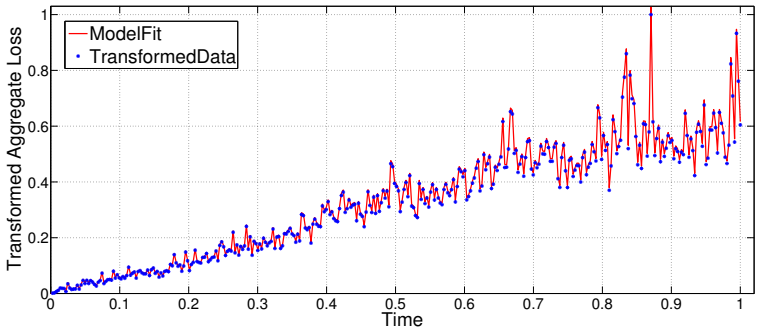

Figure 5.2: Loss estimates using PBJD with time-varying parameters (red lines) compared to transformed data (blue dots).

5.5 Appilcation to MPTL Data

In the model setup, for simplicity the values of retention and cap are assumed to be constant. As their value have an influence on the parameter estmates and findings, we aim to investigate for the values of k, m, which yield lowest MAPE and RMSE as in [32]. After experimenting with a variety of retention and cap values, we conclude $k = 0.3$ and $m = 0.7$ to be the best choice for this loss data. Based on these, the simulations are run to calculate the expected costs and exposure curves for the insurer and the reinsurer separately based on the analytical derivations and calibrated estimates proposed in this study.

As Propositions (5.1-5.2), Definitions (5.19-5.20) require the knowledge on end values of the paremeters, we need the probability density of log-return process. In discrete-time setup, it is observed that a sharp decrease is experienced after a closed interval of loss amount. This is an expected result, since the frequency of extreme values is not significant. We choose the time interval which has a jump to see the behavior of end points. Two examples of $f_{Z(t_i)}(.)$, $i = 316$, illustrated in Figures 5.3a-5.3b show varying scales. Further examinations show that $f_{Z(t_i)}(.)$ attains its minimum

value for each $i = 0, 1, \ldots, 365$ at different values for N_{max}, which is actually real minimum, 10^{-323}, for MATLAB. Thus, we take $N_{\text{max}} = 30$ to calculate the expected claims and the expected costs of insurer and reinsurer.

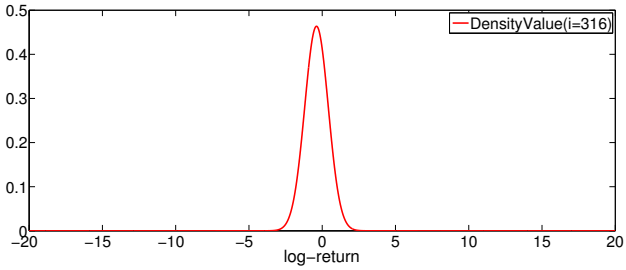

(a) Log-return density in a wider interval $(-20, 20)$ for $i = 316$

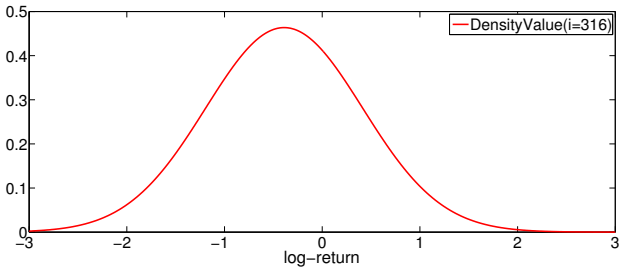

(b) Log-return density in a narrow interval $(-3, 3)$ for $i = 316$

Figure 5.3: Log-return density for one of the jump points at $i = 316$

5.5.1 Simulations for expected costs

Based on the outcome of Proposition 5.1 and implications from Figure 5.3, the partitions are choosen as

$$\{a_0 = -30, a_1 = a_0 + \Delta a, \ldots, a_j = a_0 + j\Delta a, \ldots, a_{N_a} = 30\},$$
$$\{b_0 = E_{1i}, b_1 = b_0 + \Delta b, \ldots, b_j = b_0 + j\Delta b, \ldots, b_{N_b} = 30\},$$

where $N_a = N_b = 100,000$ and $E_{1i} = \ln(\frac{k}{X^J(t_i)})$ are used to evaluate the expected costs of insurer and reinsurer. For Case I, Figure 5.4a depicts the behavior of costs for both parties in a position to real claim amount (blue line) for Case I with $k = 0.3$. It can be seen that the insurer's expected cost (green line) remains constant until the mid of the policy year with a slight variation around the deductible (black horizontal line) when the total daily loss (blue line) is higher than the deductible. The expected cost of the reinsurer (red line) is expected to be zero until the total loss exceeds the amount of deductible.

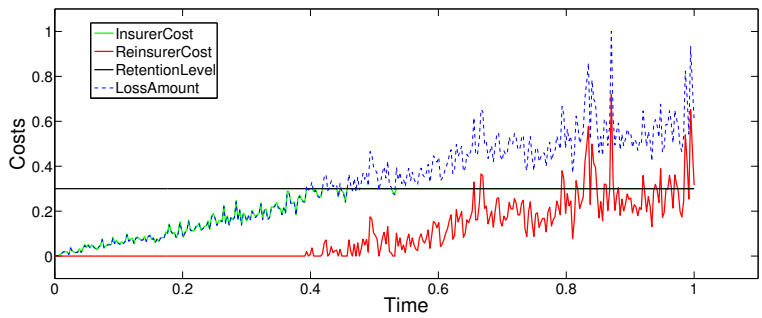

(a) Case I

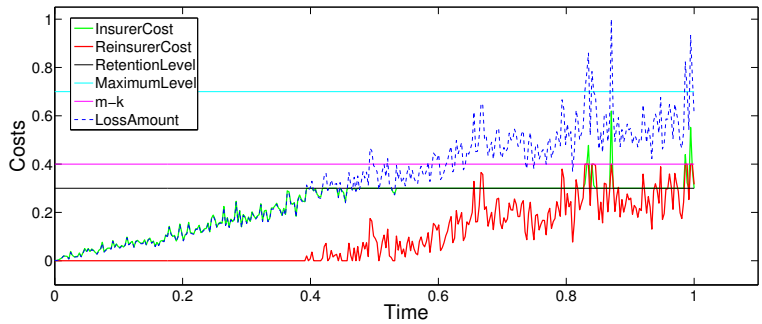

(b) Case II

Figure 5.4: The simulations on the expected costs

For Case II, the partitions given in Proposition 5.2 are

$$\{c_0 = E_{2i}, c_1 = c_0 + \Delta c, \ldots, c_j = c_0 + j\Delta c, \ldots, c_{N_c} = 30\},$$
$$\{g_0 = -30, g_1 = g_0 + \Delta g, \ldots, g_j = g_0 + j\Delta g, \ldots, g_{N_g} = E_{1i}\},$$
$$\{h_0 = E_{2i}, h_1 = h_0 + \Delta h, \ldots, h_j = h_0 + j\Delta h, \ldots, h_{N_h} = 30\},$$

where $N_c = N_g = N_h = 100,000$, $E_{1i} = \ln(\frac{k}{X^J(t_i)})$, and $E_{2i} = \ln(\frac{m}{X^J(t_i)})$ with $k = 0.3$ and $m = 0.7$. Figure 5.4b shows that the insurer's expected cost (green line) remains constant with a slight variation around the deductible (black horizontal line), as in Case I, when the claim amount is higher than the deductible and lower than the maximum amount (cyan horizontal line). If the loss amount is higher than the maximum value, the expected cost of the reinsurer remains constant with a slight deviation around the value $m - k = 0.4$ (pink horizontal line).

5.5.2 Simulation for exposure curves

Relative to expected losses over time, expsoure curves simulations are made based on Definitions (5.1-5.2). Figure 5.5a illustrates that the insurer's cost remains below the deductible until the loss reaches to k. For this reason, the exposure curve proposes to allocate the premium so that the insurer collects the entire premium (green line) until the loss exceeds the deductible. Thereafter, claims above k keep the insurer's cost constant at the deductible level, and the reinsurer's cost begins to decline (red line), causing the reinsurer's share of the premium to increase as expected. Thus, Figure 5.5a depicts the equitable allocation between the parties over time. On the other hand, the aggreeable share of the premium between parties for Case II is shown in Figure 5.5b. In adding the maximum level to the contract, we observe that the higher the difference between the loss amount and m, the lesser the reinsurer's proportional risks, since the reinsurer costs remains constant at $m - k$. Thus, comparing these cases, it can be expected that the reinsurer's share on the premium is lower in Case II than Case I.

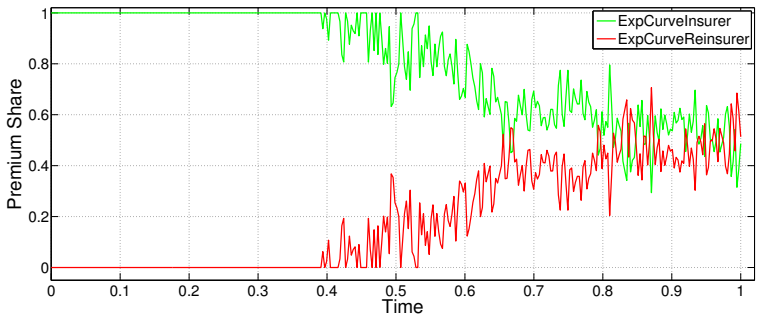

(a) Case I

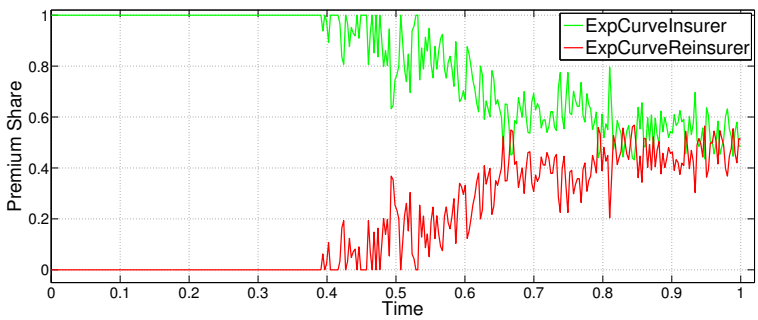

(b) CaseII

Figure 5.5: The simulated exposure curves

5.6 Forecasting the losses, costs and exposure curves

To forecast daily aggregate claims, we employ dynamic ARIMA models. Processing the forecasting regarding the time-varying parameters as opposed to the original data benefits such as (i) the performance of forecasting is found a lot better than using the dynamic ARIMA method to the data itself directly, (ii) the analytical derivations are to be maintained and integrated. As we estimate the parameters as a time series, we utilize some parts as training at which dynamic ARIMA algorithm is applied to forecast these times series. This behavior relies on trend search in train data; then, this search should be grown with the addition of the test data point to train the new set. The usage of dynamic structure in ARIMA with trend search causes a sliding pattern that is examined to establish a new set.

We select the lengths of train data and test data as 200 and 165 days, which are implemented in dynamic ARIMA algorithm in order to forecast the claim amounts, the costs of insurer and reinsurer, and the exposure curves. Figure 5.7 indicates the ARIMA forecast on claim amount the claim amount foreacast and the original test data, whose values show a good fit MAPE (9.75%) and RMSE (0.0783). It is shown that PBJD together with dynamic ARIMA trend search algorithm captures the behavior of claim amounts. Figures 5.6a and 5.6b demonstrate the forecasted costs of parties under Case I and Case II, repsectively. In Case I, the insurer pays only the retention level k, which is seen as the green line (insurer's costs) and it is coincident with the retention level (black horizontal line) and the reinsurer pays the rest of the claim amount in which its costs are expressed with red line. In Case II, the insurer pays only the retention level k if the claim amount is between the retention and maximum levels. On the other hand, if the claim amount is higher than maximum level m (cyan horizontal line), the reinsurer only pays the difference between the maximum and retention levels $m - k$ (purple horizontal line). The accomplishment of parties's costs forecasting is one of the outcomes of obtaining adequate forecasts for claim amounts. Figures 5.6c and 5.6d show the forecasts under the same setup. The share of insurer on the premium in Case I is less than its share in Case II since the costs of the insurer are more than its costs in Case II. The exposure curves of the parties provide a fair premium share between parties and this is our observations in exposure

curves forecasts simulations.

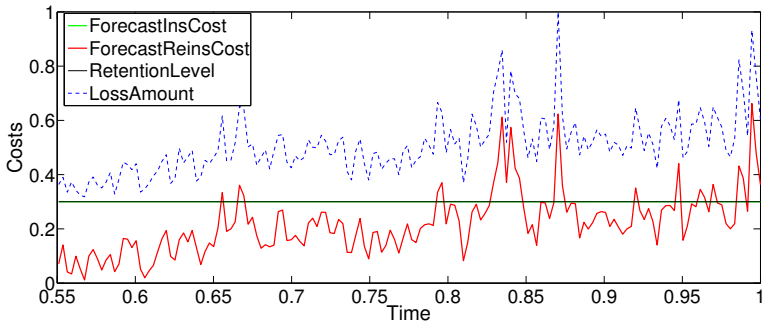

(a) Dynamic ARIMA costs forecasts under Case I

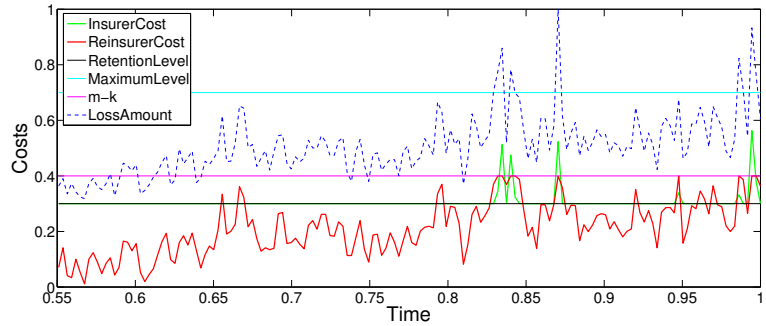

(b) Dynamic ARIMA costs forecasts under Case II

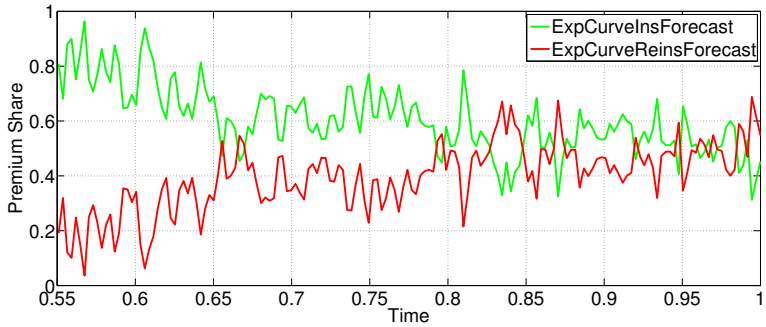

(c) Dynamic ARIMA exposure curve forecasts under Case I

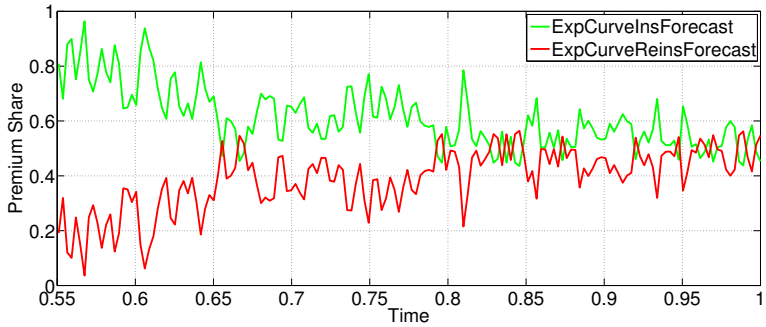

(d) Dynamic ARIMA exposure curve forecasts under Case II

Figure 5.6: The simulated focecasts of expected costs, and exposure curves

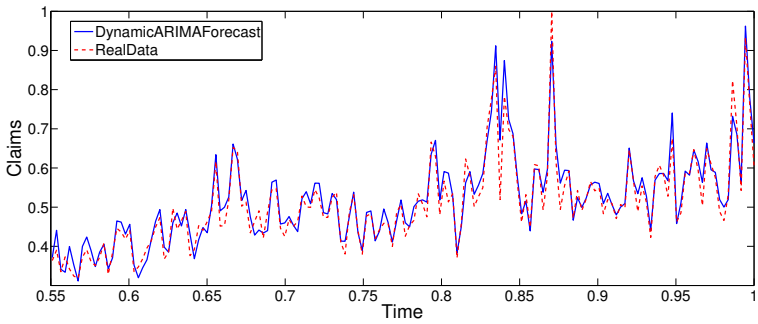

Figure 5.7: Dynamic ARIMA claim forecasts and the test data

5.7 Discussion

In the setting of a stochastic loss amount process with jump influence, this chapter investigates the impact of extreme losses on a stop-loss agreement between an insurer and a reinsurer. We assume that PBJD can capture extreme losses and investigate the models' validity on real-life data set. The analytical derivations for determining expected costs and premium shares via exposure curves are novel, and the verifications using Monte Carlo simulations based on data-driven calibrated parameters look promising as a tool for practitioners. The use of MTPL data in numerical analysis is new, and estimating time-varying parameters in two stages, dynamic moment matching estimation for the jump part $(\hat{\lambda}_u, \hat{\lambda}_d, \hat{\nu}_u(i), \hat{\nu}_d(i))$ and dynamic maximum-likelihood estimation for the continuous part $(\hat{\mu}(i), \hat{\sigma}(i))$, is shown to be effective for estimating aggregate losses. Forecasting is accomplished by implementing both dynamic structures of parameters in time and time dependence, which allows researchers and practitioners to predict daily aggregate claims for a policy year.

CHAPTER 6

CONCLUSION

Insurance markets are a necessary part of the world's economy. Due to the effects of the inreasing trend in world population, catastrophic events, and political and economical necessities on the insurance markets, the monetary obligations of companies in the market also rises significantly. For this reason, the reinsurance policies are playing a vital role to lighten the financial burden on the insurance companies. In this thesis, the stop-loss reinsurance, which is one of the commonly issued reinsurance types, is studied for two types of contracts: contracts with retention value (Case I) and contracts wtih both retention and cap values (Case II).

The issues required to set the retention and cap values agreed by the insurer and the reinsurer are the time-dependent structure of randomly changing losses, the change of the insurer and reinsurer's own costs over time according to these randomly changing losses and retention, cap values, and how their share on the premium appear to. The modeling of these random losses is one of the main elements of the thesis, and it is carried out by approaching it from three different perspectives. First, it is the examination of the losses, which are frequently used in the literature, under a prescribed distribution. We use Pareto, Gamma and Inverse Gamma distributions for modeling losses, since it is more convenient to examine actuarial losses under the heavy-tailed distributions which are commonly used in the literature. Secondly, we model the losses with one of stochastic models, Geometric Brownian Motion, since the distributional approach cannot give the time dependent behavior of the losses and the effects of time. Finally, we use a stochastic jump diffusion model, the Pareto-Beta jump diffusion model, to take into account the existence of large losses due to

extreme and catastrophic events such as floods, earthquakes, and wild fires. Furthermore, among these three methodologies, we examine the costs of the insurer and the reinsurer and find fair premium shares using the exposure curve.

In this thesis, the effectiveness of our methodologies are discussed with detailed analysis and derivations. The loss modeling of both distributional and stochastic aspects are analyzed comprehensively. Moreover, the costs of the insurer and reinsurer are derived analytically and the fair premium share between them are obtained analogously. For the aim of revealing the validity of our methodologies, especially the time-dependent structure of the stop-loss reinsurance analysis in terms of loss modeling, expected costs, the fair premium share under exposure curves, and the forecasting power, we apply our findings to a real-life data set containing compulsory traffic insurance claims (MTPL) from the Turkish insurance market. In these aspects, this thesis has theoretical and practical contributions to the insurance market and actuarial literature, as they are summarized below.

- We determine the optimal premium share between parties under the influence of exposure curves and certain aggregate loss distributions (Chapter 3). The optimal premimum is achieved for the level of correlation coefficient between the costs of parties, which is attained under an optimization scheme. The analytical expressions of exposure curves for the selected distributions (Pareto, Gamma, and Inverse Gamma) in terms of standard deviation premium principle are the main contributions to the literature, which guides the researchers to charactize the behavior of premium pricing. We use Monte Carlo simulations to determine the maximum correlation, the smaller expected costs, and the topmost premium under the constraintive conditions in terms of predetermined retention and cap levels. For a better undestanding of our proposed approach in this chapter, we minimize the total risks of the insurer and reinsurer under VaR and CVaR risk measures for the comparison purposes. The results display that, for all selected distributions under Case I and Case II, the optimized solutions of proposed approach is close to VaR and CVaR solutions. Furthermore, both solutions of VaR and CvaR, and our proposed methodogy, Gamma distribution is more suitable than the others.

- A stochastic model, specifically a geometric Brownian motion with time-varying parameters, in order to depict the loss behavior under a time-dependent structure is proposed (Chapter 4). We derive analytically the costs of parties and the exposure curves for continuous and discrete time frameworks. We use real-life data to validate the proposed approach in this chapter and to estimate dynamically the time-varying parameters with the maximum likelihood estimator, which are governing the small and equidistant time intervals. The fitting results of the proposed model is adequate. Based on the estimated parameters, we simulate the expected costs and the exposure curves of insurer and reinsurer and forecast claim amounts, expected costs, and exposure curves by considering time-varying parameters as time-series. Thus, we use cubic-spline extrapolation and ARIMA with trend search on these series in order to protect the structure of the stochastic model and our derivations of expected costs and exposure curves. Additionaly, we investigate the efficiency for daily and weekly updates in cubic spline forecasting and daily updates in ARIMA with trend search forecasting. Moreover, the performances of train data length on ARIMA with trend search forecast are obtained to achieve a better recognition forecasts in a short term period. This enables the insurer and the reinsurer to reinvest according to forecasts on the claim amounts, the expected costs, and how to share the premium using exposure curves and to rebalance their portfolios. The main contribution of this chapter to literature is to set up a time-dependent mechanism on a stop-loss reinsurance.

- We model the claim amounts with a stochastic jump diffusion model, specifically Pareto-Beta jump diffusion (PBJD) with time-varying parameters, in order to capture extreme losses and to keep the time influenced structure of losses (Chapter 5). We derive analytically the expected costs of parties and exposure curves to find fair premium share under PBJD, which is quite a novel approach and contribution to the literature. The calibration of parameters is obtained in two phases: dynamic moment matching estimation for the parameters in jump part and dynamic maximum-likelihood estimation for continous part, which are competent for estimating aggreagate losses and appears encouraging tool for practitioners. Additionally, we forecast the dailly aggregate claims, expected

costs of parties, and exposure curves for the share of premium for a contract period by considering ARIMA with trend search on a time-varying parameters in order to keep the structure of time-dependent structure of claim amounts via PBJD.

The results presented in the thesis will serve as a benchmark for time-dependent structure of loss modeling, the costs of parties, and premium pricing and its fair share via the exposure curves. Using the time dependent structure of our methodologies, the insurer and reinsurer can evaluate their position on the future loss amounts, the size of financial costs on their parts of responsibilities, fairly partition of the premium obtained using exposure curves, and the premium value according to the los amounts, their costs and share on the premium on a specific time interval decided by their own direction. This can help the practitioners to construct a reinvestment strategy and construct a portfolio to pay their reponsibilities and to make profit. In this perspective, as a future work, we aim to investigate the reserve scheme on a stop-loss contract by adding an optimal reinvestment strategy for the joint analysis of insurer and reinsurer under time-dependent mechanism presented in the thesis.

APPENDIX A

DERIVATIONS AND RELATED PROOFS

A.1 Proofs for Chapter 3

i) The proofs related to equations given in *Proposition (3.3)* and *Proposition (3.4)*:

$$\begin{aligned}\mathbb{E}(R(d)) &= \int_d^\infty (1 - F_S(s))ds \\ &= \int_d^\infty \frac{b^a}{s^a} ds = \frac{b^a d^{1-a}}{a-1}.\end{aligned} \tag{A.1}$$

Using Proposition 3.2, $\mathbb{E}[R(d,m)]$ is obtained by putting Eq. (A.1) into

$$\mathbb{E}[R(d,m)] = \mathbb{E}[R(d)] - \mathbb{E}[R(m)].$$

$$\begin{aligned}\mathbb{V}[R(d)] &= 2\int_d^\infty \frac{b^a}{s^{a-1}} ds + \mathbb{E}[R(d)](-2d - \mathbb{E}[R(d)]) \\ &= \frac{b^a d^{(2-a)}[2 - (b/d)^a(a-2)]}{(a-2)(a-1)^2}.\end{aligned} \tag{A.2}$$

Using Eq. (A.1), the covariance between I and R in Case I is found as

$$\begin{aligned}Cov[I(d), R(d)] &= \mathbb{E}(R(d))\left[d - \frac{ab}{a-1}\right] + \mathbb{E}(R(d))] \\ &= \frac{ab^a d^{1-a}[d-b] + b^a d^{(2-a)}[(b/d)^a - 1]}{(a-1)^2}.\end{aligned} \tag{A.3}$$

$$\mathbb{V}[R(d,m)] = \mathbb{V}[R(d)] - \mathbb{V}[R(m)] + 2\mathbb{E}[R(m)](\mathbb{E}[R(d)] - \mathbb{E}[R(m)] + d - m) \tag{A.4}$$

$$\begin{aligned}&= \frac{b^{2a}}{(a-1)^2}\Big[(m^{1-a} - d^{1-a})^2 - 2(m^{2(1-a)} + d^{1-a})\Big] \\ &+ \frac{2b^a}{(a-1)^2(a-2)}\Big[d^{2-a} - m^{2-a} + (a-1)(a-2)m^{1-a}(d-m)\Big].\end{aligned}$$

ii) The proofs related to equations given in *Proposition (3.5)* and *Proposition (3.6)*:

$$\begin{aligned}
\mathbb{E}[R(d)] &= \int_d^\infty (s-d)\frac{s^{a-1}e^{-\frac{s}{b}}}{b^a\Gamma(a)}ds \\
&= \int_d^\infty s\frac{s^{a-1}e^{-\frac{s}{b}}}{b^a\Gamma(a)}ds - d\int_d^\infty \frac{s^{a-1}e^{-\frac{s}{b}}}{b^a\Gamma(a)}ds \\
&= ab\int_d^\infty \frac{s^{a}e^{-\frac{s}{b}}}{b^{a+1}\Gamma(a+1)}ds - d\int_d^\infty \frac{s^{a-1}e^{-\frac{s}{b}}}{b^a\Gamma(a)}ds \\
&= ab(1-Ga(d;a+1,b)) - d(1-Ga(d;a,b)) \\
&= ab\frac{\Gamma(a+1,d)}{\Gamma(a+1)} - d\frac{\Gamma(a,d)}{\Gamma(a)}. \qquad \text{(A.5)}
\end{aligned}$$

Using Proposition 3.2, $\mathbb{E}[R(d,m)]$ is obtained by putting Eq. (A.5) into

$$\mathbb{E}[R(d,m)] = \mathbb{E}[R(d)] - \mathbb{E}[R(m)].$$

$$\begin{aligned}
&\mathbb{V}[R(d)] = \int_d^\infty (s-d)^2\frac{s^{a-1}e^{-\frac{s}{b}}}{b^a\Gamma(a)}ds - (\mathbb{E}[R(d)])^2 \\
&= \mathbb{E}[R(d)](-2d-\mathbb{E}[R(d)]) + (a+1)ab^2(1-Ga(d;a+2,b)) \\
&- d^2(1-Ga(d;a,b)) \\
&= \mathbb{E}[R(d)](-2d-\mathbb{E}[R(d)]) \qquad \text{(A.6)} \\
&+ \frac{1}{\Gamma(a)}[b^2\Gamma(a+1,bd) - d^2\Gamma(a,bd)].
\end{aligned}$$

Using Equation[A.5], the covariance between I and R in Case I is found as

$$\begin{aligned}
Cov[I(d),R(d)] &= \mathbb{E}(R(d))\,[d-ab] + \mathbb{E}(R(d))] \qquad \text{(A.7)} \\
&= \left[\frac{1}{\Gamma(a)}\Big[b\gamma(a-1,b/d) - d\gamma(a,b/d)\Big]\right]^2 \\
&+ \frac{1}{\Gamma(a)}\left[\Gamma(a,b/d) - \Gamma(a-1,b/d) + (b-d)\left(d-\frac{b}{a-1}\right)\right].
\end{aligned}$$

$$\begin{aligned}
\mathbb{V}[R(d,m)] =& \mathbb{V}[R(d)] - \mathbb{V}[R(m)] + 2\mathbb{E}[R(m)](\mathbb{E}[R(d)] - \mathbb{E}[R(m)] + d - m) \\
& \qquad \text{(A.8)} \\
=& 2\int_d^m s[1-F_S(s)]ds + \mathbb{E}[R(d,m)][-\mathbb{E}[R(d,m)] - 2d] \\
=& \frac{1}{\Gamma(a)}[b^2(\Gamma(a+2,bd) - \Gamma(a+2,bm)) - d^2\Gamma(a,bd) - m^2\Gamma(a,bm)] \\
&+ \mathbb{E}[R(d,m)][-\mathbb{E}[R(d,m)] - 2d].
\end{aligned}$$

The proof is obtained with a revision on

$$Cov[I(d,m), R(d,m)] = Cov[I(d), R(d)] - (2d-m)\mathbb{E}[R(m)$$

such that

$$\begin{aligned} Cov[I(d,m),R(d,m)] &= \mathbb{E}[R(d)](d - \mathbb{E}[S] + \mathbb{E}[R(d)]) - (2d-m)\mathbb{E}[R(m) \\ &= (\mathbb{E}[R(d,m)] - \frac{1}{\Gamma(a)}[b\Gamma(a+1,bm) - d\Gamma(a,bm)])^2 \\ &+ \frac{m-d}{\Gamma(a)}[b\Gamma(a+1,bd) - d\Gamma(a,bd)] + \mathbb{E}[R(d,m)(d-ab). \end{aligned} \tag{A.9}$$

iii) The proofs related to equations given in *Proposition (3.7)* and *Proposition (3.8)*:

$$\begin{aligned} \mathbb{E}[R(d)] &= \int_d^\infty (s-d)\frac{b^a}{\Gamma(a)}s^{-a-1}e^{-b/s}ds \\ &= \frac{b^a}{\Gamma(a)}\int_d^\infty s^{-a}e^{-b/s}ds - \frac{b^a d}{\Gamma(a)}\int_d^\infty s^{-a-1}e^{-b/s}ds \\ &= \frac{1}{\Gamma(a)}[b\gamma(a-1,b/d) - d\gamma(a,b/d)]. \end{aligned} \tag{A.10}$$

$\mathbb{E}[R(d,m)]$ is obtained by putting Eq. (A.10) into

$$\mathbb{E}[R(d,m)] = \mathbb{E}[R(d)] - \mathbb{E}[R(m)].$$

Using Eq. (A.10), the covariance between I and R in Case I is found as

$$\begin{aligned} Cov[I(d),R(d)] &= \mathbb{E}(R(d))\left[d - \frac{b}{a-1}\right] + \mathbb{E}(R(d))] \\ &= \left[\frac{1}{\Gamma(a)}\Big[b\gamma(a-1,b/d) - d\gamma(a,b/d)\Big]\right]^2 \\ &+ \frac{1}{\Gamma(a)}\left[\Gamma(a,b/d) - \Gamma(a-1,b/d) + (b-d)\left(d - \frac{b}{a-1}\right)\right]. \end{aligned} \tag{A.11}$$

Finding the second moment of the cost of reinsurer with respect to d is enough to estimate the variance. Thus,

$$
\begin{aligned}
\mathbb{E}[R(d)^2] &= \int_d^\infty (s-d)^2 \frac{b^a}{\gamma(a)} s^{-a-1} e^{-b/s} ds \qquad \text{(A.12)} \\
&= \frac{b^a}{\Gamma(a)} \left[\int_d^\infty s^{1-a} e^{-b/s} ds - 2d \int_d^\infty s^{-a} e^{-b/s} ds \right. \\
&\qquad \left. + d^2 \int_d^\infty s^{-1-a} e^{-b/s} ds \right] \\
&= \frac{1}{\Gamma(a)} [b^2 \gamma(a-2, b/d) - 2db\gamma(a-1, b/d) + d^2 \gamma(a, b/d)].
\end{aligned}
$$

$$
\begin{aligned}
\mathbb{V}[R(d,m)] &= \mathbb{V}[R(d)] - \mathbb{V}[R(m)] + 2\mathbb{E}[R(m)](\mathbb{E}[R(d)] - \mathbb{E}[R(m)] + d - m) \qquad \text{(A.13)} \\
&= 2\int_d^m s[1 - F_S(s)]ds + \mathbb{E}[R(d,m)][-\mathbb{E}[R(d,m)] - 2d] \\
&= m^2 - d^2 - \sum_{k=0}^{\infty} \frac{(-1)^k (m^{2-a-k} - d^{2-a-k})}{k!(a+k)(2-a-k)} \\
&+ \mathbb{E}[R(d,m)][-\mathbb{E}[R(d,m)] - 2d].
\end{aligned}
$$

A.2 Proofs for Chapter 4

Theorem 4.1:

Let $Z = \left(\mu - \frac{\sigma^2}{2}\right) t + \sigma W_t = \left(\mu - \frac{\sigma^2}{2}\right) t + \sigma\sqrt{t}Y$, where Y is distributed by standard normal. The linear transformation of normal random variables gives

$$
Z \sim N\left(\left(\mu - \frac{\sigma^2}{2}\right) t, \sigma^2 t\right).
$$

In other words, Z has distributed by normal with mean $\left(\mu - \frac{\sigma^2}{2}\right) t$ and variance $\sigma^2 t$. By Eq. (4.1),

$$
X_t^G = X_0^G e^{(\mu - \sigma^2/2)t + \sigma W_t} = X_0^G e^Z.
$$

Let $R_t = \max(X_t^G - d, 0)$ be the cost of reinsurer at time t where d is the predetermined retention level. The expected cost of the reinsurer at t can be written in terms of the integration using the density of Z as

$$\begin{aligned}\mathbb{E}[R_t] &= \mathbb{E}[\max(X_t^G - d, 0)] = \mathbb{E}[\max(X_0^G e^Z - d, 0)] \\ &= X_0^G \int_K^\infty e^z f_Z(z)dz - d\int_K^\infty f_Z(z)dz,\end{aligned} \tag{A.14}$$

where $K = \ln\left(\frac{d}{X_0^G}\right)$ and $f_Z(z) = \frac{1}{\sigma\sqrt{2\pi t}} e^{-\frac{((\mu-\sigma^2/2)t-z)^2}{2\sigma^2 t}}$.

We should solve the following integrals in Eq. (A.14) to obtain the expected cost of the reinsurer:

$$I_1 := \int_K^\infty e^z \frac{1}{\sigma\sqrt{2\pi t}} e^{-\frac{((\mu-\sigma^2/2)t-z)^2}{2\sigma^2 t}} dz, \quad I_2 := \int_K^\infty \frac{1}{\sigma\sqrt{2\pi t}} e^{-\frac{((\mu-\sigma^2/2)t-z)^2}{2\sigma^2 t}} dz.$$

The solution for I_1 is obtained as

$$\begin{aligned} I_1 &= e^{(\mu-\sigma^2/2)t} \int_{-\infty}^{E_{2d}} \frac{1}{\sqrt{2\pi}} e^{-(u^2/2 - u\sigma\sqrt{t})} du, \quad \left(\text{by substitution} \quad u = \frac{-z + (\mu-\sigma^2)t}{\sigma\sqrt{t}}\right), \\ &= e^{\mu t} \int_{-\infty}^{E_{1d}} \frac{1}{\sqrt{2\pi}} e^{-v^2/2} dv, \quad \left(\text{by substitution} \quad v = u + \sigma\sqrt{t}\right), \\ &= e^{\mu t} N_F(E_{1d}), \end{aligned} \tag{A.15}$$

where $N_F(x) = \int_{-\infty}^x \frac{1}{\sqrt{2\pi}} e^{-\frac{t^2}{2}} dt$, $E_{2d} = \frac{ln\left(\frac{X_0^G}{d}\right) + (\mu - \frac{\sigma^2}{2})t}{\sigma\sqrt{t}}$, and $E_{1d} = E_{2d} + \sigma\sqrt{t}$.

The solution for I_2 is obtained as

$$I_2 = \underbrace{\int_K^\infty \frac{1}{\sigma\sqrt{2\pi t}} e^{-\frac{((\mu-\sigma^2/2)t-z)^2}{2\sigma^2 t}} dz = N_F(E_{2d})}_{\text{by substitution} \quad u = \frac{-z+(\mu-\sigma^2)t}{\sigma\sqrt{t}}}. \tag{A.16}$$

Therefore, plugging the solutions of the integrals found in Eqs. (A.15) and (A.16) into Eq. (A.14) gives the expected cost of the reinsurer at t, which is found as

$$\mathbb{E}[R_t] = X_0^G e^{\mu t} N_F(E_{1d}) - dN_F(E_{2d}). \tag{A.17}$$

Since $X_t^G = X_0^G e^Z$,

$$\mathbb{E}[X_t^G] = X_0^G e^{\mu t}.$$

Since $I_t = \min(X_t^G, d)$ and $X_t^G = I_t + R_t$,

$$\mathbb{E}[\min(X_t^G, d)] = \mathbb{E}[I_t] = \mathbb{E}[X_t^G] - \mathbb{E}[R_t].$$

Therefore, the expected cost of the insurer at t is found as

$$\mathbb{E}[I_t] = X_0^G e^{\mu t}(1 - N_F(E_{1d})) + dN_F(E_{2d}). \tag{A.18}$$

Theorem 4.3:

We use the same methodology used in the proof of Theorem 4.1.

Let $I_t = \min(X_t^G, d) + \max(X_t^G - m, 0)$ be the cost of the insurer at time t where d and m are predetermined retention and maximum levels. The expected cost of the insurer at t is

$$\mathbb{E}[I_t] = \mathbb{E}[\min(X_t^G, d)] + \mathbb{E}[\max(X_t^G - m, 0)]. \tag{A.19}$$

$\mathbb{E}[\min(X_t^G, d)]$ is found in Theorem 4.1 as

$$\mathbb{E}[\min(X_t^G, d)] = X_0^G e^{\mu t}(1 - N_F(E_{1d})) + dN_F(E_{2d}). \tag{A.20}$$

Moreover, $\mathbb{E}[\max(X_t^G - m, 0)]$ is obtained using $\mathbb{E}[\max(X_t^G - d, 0)]$ given in Theorem 4.1. For this, we only need to substitute d with m. Therefore,

$$\mathbb{E}[\max(X_t^G - m, 0)] = X_0^G e^{\mu t} N_F(E_{1m}) - mN_F(E_{2m}), \tag{A.21}$$

where $E_{2m} = \frac{ln\left(\frac{X^G(0)}{m}\right) + (\mu - \frac{\sigma^2}{2})t}{\sigma\sqrt{t}}$ and $E_{1m} = E_{2m} + \sigma\sqrt{t}$.

Plugging Eqs. (A.20) and (A.21) into Eq. A.19, the cost of the insurer at t is found as

$$\mathbb{E}[I_t] = X_0^G e^{\mu t}[1 + N_F(E_{1m}) - N_F(E_{1d})] + dN_F(E_{2d}) - mN_F(E_{2m}). \tag{A.22}$$

Since $\mathbb{E}[R_t] = \mathbb{E}[X_t^G] - \mathbb{E}[I_t]$ where $\mathbb{E}[X_t^G] = X_0^G e^{\mu t}$, the cost of the reinsurer at t is

$$\mathbb{E}[R_t] = X_0^G e^{\mu t}[N_F(E_{1d}) - N_F(E_{1m})] - dN_F(E_{2d}) + mN_F(E_{2m}). \tag{A.23}$$

A.3 Proofs for Chapter 5

First, we fix time for $t_i = i$, then we obtain a solution for all i without loss of generality.

The conditional density of $Z(t_i)$ when no up-jump and a down-jump becomes

$$f_{0|1}(z) = \frac{\nu_d}{\sqrt{2\pi s\sigma^2}} \underbrace{\int_{-\infty}^{0} e^{\nu_d x - \frac{1}{2s\sigma^2}\left(z - x - \mu s + \frac{1}{2}\sigma^2 s\right)^2} dx,}_{=:I_1}$$

To solve I_1,

$$I_1(z) = \int_{-\infty}^{0} e^{\nu_d x - \frac{1}{2s\sigma^2}\left(z - x - \mu s + \frac{1}{2}\sigma^2 s\right)^2} dx := \int_{-\infty}^{0} e^{-K(x)}\, dx$$

where

$$K(x) = \frac{1}{2s\sigma^2}\left(z - x - \mu s + \frac{1}{2}\sigma^2 s\right)^2 - \nu_d x.$$

Our aim is to complete the square in $K(x)$ using

$$\frac{1}{2}\left(\frac{x - \alpha_1}{\beta_1}\right)^2 = \frac{x^2}{2\beta_1^2} - \frac{x\alpha_1}{\beta_1^2} + \frac{\alpha_1^2}{2\beta_1^2}. \tag{A.24}$$

$K(x)$ is obtained explicitly as

$$\frac{1}{2s\sigma^2}\left[x^2 + z^2 + \mu^2 s^2 + \frac{\sigma^4 s^2}{4} - 2xz - x\sigma^2 s + 2x\mu s + z\sigma^2 s - 2z\mu s - \mu\sigma^2 s\right] - \nu_d x.$$

The term with x^2 in $K(x)$ is denoted by

$$K_2(x) := \frac{x^2}{2\sigma^2 s}.$$

By equating the x^2 terms in Eq. (A.24) and $K_2(x)$, we obtain

$$\beta_1 = \sigma\sqrt{s},\ \sigma, s > 0.$$

The term with x in $K(x)$ is is denoted by

$$K_1(x) := x\left[\frac{-z}{\sigma^2 s} - \frac{1}{2} + \frac{\mu}{\sigma^2} - \nu_d\right].$$

By equating the x terms in Eq. (A.24) and $K_1(x)$, we obtain

$$\alpha_1 = z + \frac{\sigma^2 s}{2} - \mu s + \nu_d \sigma^2 s.$$

The term with x^0 in $K(x)$ is denoted by

$$K_0(x) := \frac{z^2}{2\sigma^2 s} + \frac{\mu^2 s}{2\sigma^2} + \frac{\sigma^2 s}{8} + \frac{z}{2} - \frac{z\mu}{\sigma^2} - \frac{\mu}{2}.$$

To complete the square in $K(x)$, we adjust $K_0(x)$ by

$$K_0(x) \pm \nu_d \left(\frac{\sigma^2 s}{2}(\nu_d + 1) + z - \mu s \right) = \frac{\alpha_1^2}{2\beta_1^2} - \nu_d \left(\frac{\sigma^2 s}{2}(\nu_d + 1) + z - \mu s \right).$$

Thus,

$$\begin{aligned} I_1(z) &= \int_{-\infty}^{0} e^{-K(x)}\, dx = e^{-\nu_d\left(\frac{\sigma^2 s}{2}(\nu_d+1)+z-\mu s\right)} \int_{-\infty}^{0} e^{-\frac{1}{2}\left(\frac{x-\alpha_1}{\beta_1}\right)^2}\, dx \\ &= e^{-\nu_d\left(\frac{\sigma^2 s}{2}(\nu_d+1)+z-\mu s\right)} \beta_1\sqrt{2\pi} \int_{-\infty}^{0} \frac{1}{\beta_1\sqrt{2\pi}} e^{-\frac{1}{2}\left(\frac{x-\alpha_1}{\beta_1}\right)^2} dx \\ &= e^{-\nu_d\left(\frac{\sigma^2 s}{2}(\nu_d+1)+z-\mu s\right)} \sigma\sqrt{2\pi s}\, \Phi(0; \alpha_1, \beta_1^2), \end{aligned}$$

where $\Phi(0; \alpha_1, \beta_1^2)$ is the value of the normal cdf with mean α_1 and variance β_1^2 at 0. Therefore,

$$f_{0|1}(z) = \frac{\nu_d}{\sqrt{2\pi s\sigma^2}} I_1 = \nu_d e^{-\nu_d\left(\frac{\sigma^2 s}{2}(\nu_d+1)+z-\mu s\right)}\, \Phi(0; \alpha_1, \beta_1^2).$$

The conditional density of $Z(t_i)$ when an up-jump and no down-jump becomes

$$f_{1|0}(z) = \frac{\nu_u}{\sqrt{2\pi s\sigma^2}} \underbrace{\int_0^{\infty} e^{-\nu_u x - \frac{1}{2s\sigma^2}\left(z-x-\mu s+\frac{1}{2}\sigma^2 s\right)^2} dx}_{=:I_2}.$$

To solve I_2,

$$I_2(z) = \int_0^{\infty} e^{-\nu_u x - \frac{1}{2s\sigma^2}\left(z-x-\mu s+\frac{1}{2}\sigma^2 s\right)^2} dx := \int_{-\infty}^{0} e^{-M(x)}\, dx$$

where

$$M(x) = \frac{1}{2s\sigma^2}\left(z - x - \mu s + \frac{1}{2}\sigma^2 s\right)^2 + \nu_u x.$$

Our aim is to complete the square in $M(x)$ using

$$\frac{1}{2}\left(\frac{x-\alpha_2}{\beta_2}\right)^2 = \frac{x^2}{2\beta_2^2} - \frac{x\alpha_2}{\beta_2^2} + \frac{\alpha_2^2}{2\beta_2^2}. \tag{A.25}$$

$M(x)$ is obtained explicitly as

$$\frac{1}{2s\sigma^2}\left[x^2 + z^2 + \mu^2 s^2 + \frac{\sigma^4 s^2}{4} - 2xz - x\sigma^2 s + 2x\mu s + z\sigma^2 s - 2z\mu s - \mu\sigma^2 s\right] + \nu_u x.$$

The term with x^2 in $M(x)$ is denoted by

$$M_2(x) := \frac{x^2}{2\sigma^2 s}.$$

By equating the x^2 terms in Eq. (A.25) and $M_2(x)$, we obtain

$$\beta_2 = \sigma\sqrt{s},\ \sigma, s > 0.$$

The term with x in $M(x)$ is denoted by

$$M_1(x) := x\left[\frac{-z}{\sigma^2 s} - \frac{1}{2} + \frac{\mu}{\sigma^2} + \nu_u\right].$$

By equating the x terms in Eq. (A.25) and $M_1(x)$, we obtain

$$\alpha_2 = z + \frac{\sigma^2 s}{2} - \mu s - \nu_u \sigma^2 s.$$

The term with x^0 in $M(x)$ is

$$M_0(x) := \frac{z^2}{2\sigma^2 s} + \frac{\mu^2 s}{2\sigma^2} + \frac{\sigma^2 s}{8} + \frac{z}{2} - \frac{z\mu}{\sigma^2} - \frac{\mu}{2}.$$

To complete the square in $M(x)$, we adjust $M_0(x)$ by

$$M_0(x) \pm \nu_u\left(\frac{\sigma^2 s}{2}(\nu_u - 1) - z + \mu s\right) = \frac{\alpha_2^2}{2\beta_2^2} - \nu_u\left(\frac{\sigma^2 s}{2}(\nu_u - 1) - z + \mu s\right).$$

Thus,

$$\begin{aligned} I_2(z) &= \int_0^\infty e^{-M(x)}\, dx = e^{-\nu_u\left(\frac{\sigma^2 s}{2}(\nu_u-1)-z+\mu s\right)} \int_{-\infty}^0 e^{-\frac{1}{2}\left(\frac{x-\alpha_2}{\beta_2}\right)^2}\, dx \\ &= e^{-\nu_u\left(\frac{\sigma^2 s}{2}(\nu_u-1)-z+\mu s\right)} \beta_2\sqrt{2\pi} \int_0^\infty \frac{1}{\beta_2\sqrt{2\pi}} e^{-\frac{1}{2}\left(\frac{x-\alpha_2}{\beta_2}\right)^2} dx \\ &= e^{-\nu_u\left(\frac{\sigma^2 s}{2}(\nu_u-1)-z+\mu s\right)} \sigma\sqrt{2\pi s}\,[1 - \Phi(0; \alpha_2, \beta_2^2)], \end{aligned}$$

where $\Phi(0; \alpha_2, \beta_2^2)$ is the value of the normal cdf with mean α_2 and variance β_2^2 at 0. Therefore,

$$f_{1|0}(z) = \frac{\nu_u}{\sqrt{2\pi s\sigma^2}} I_1 = \nu_u e^{-\nu_u\left(\frac{\sigma^2 s}{2}(\nu_u-1)-z+\mu s\right)}\,[1 - \Phi(0; \alpha_2, \beta_2^2)].$$

REFERENCES

[1] C. M. Ahn and H. E. Thompson, Jump-diffusion processes and the term structure of interest rates, The journal of finance, 43(1), pp. 155–174, 1988.

[2] G. Akarsu, *Reinsurance pricing using exposure curve of two dependent risks*, Master's thesis, Middle East Technical University, 2018.

[3] S. Asmussen, B. Højgaard, and M. Taksar, Optimal risk control and dividend distribution policies. example of excess-of loss reinsurance for an insurance corporation, Finance and Stochastics, 4(3), pp. 299–324, 2000.

[4] A. Balbás, B. Balbás, and A. Heras, Optimal reinsurance with general risk measures, Insurance: Mathematics and Economics, 44(3), pp. 374–384, 2009.

[5] V. Bally, L. Caramellino, R. Cont, F. Utzet, and J. Vives, *Stochastic integration by parts and functional Itô calculus*, Springer, 2016.

[6] S. Bernegger, The Swiss Re exposure curves and the MBBEFD distribution class1, ASTIN Bulletin: The Journal of the IAA, 27(1), pp. 99–111, 1997.

[7] J. Bi, Q. Meng, and Y. Zhang, Dynamic mean-variance and optimal reinsurance problems under the no-bankruptcy constraint for an insurer, Annals of Operations Research, 212(1), pp. 43–59, (2014).

[8] C. Bolancé, M. Guillen, and J. P. Nielsen, Kernel density estimation of actuarial loss functions, Insurance: Mathematics and Economics, 32(1), pp. 19–36, 2003.

[9] P. J. Boland, Statistical methods in general insurance, 2006.

[10] K. Borch, The optimal reinsurance treaty, ASTIN Bulletin: The Journal of the IAA, 5(2), pp. 293–297, 1969.

[11] J. Cai, Y. Fang, Z. Li, and G. E. Willmot, Optimal reciprocal reinsurance treaties under the joint survival probability and the joint profitable probability, Journal of Risk and Insurance, 80(1), pp. 145–168, 2013.

[12] J. Cai, C. Lemieux, and F. Liu, Optimal reinsurance from the perspectives of both an insurer and a reinsurer, ASTIN Bulletin: The Journal of the IAA, 46(3), pp. 815–849, 2016.

[13] J. Cai and K. S. Tan, Optimal retention for a stop-loss reinsurance under the VaR and CTE risk measures, ASTIN Bulletin: The Journal of the IAA, 37(1), pp. 93–112, 2007.

[14] A. Castañer and M. M. Claramunt, Optimal stop-loss reinsurance: a dependence analysis, Hacettepe Journal of Mathematics and Statistics, 45(2), pp. 497–519, 2016.

[15] K. C. Cheung, K. Sung, S. C. P. Yam, and S. P. Yung, Optimal reinsurance under general law-invariant risk measures, Scandinavian Actuarial Journal, 2014(1), pp. 72–91, 2014.

[16] S. Dedu and R. Ciumara, Restricted optimal retention in stop-loss reinsurance under VaR and CTE risk measures, Proc. Rom. Acad. Ser. A Math. Phys. Tech. Sci. Inf. Sci, 11(3), pp. 213–217, 2010.

[17] M. Denuit and C. Vermandele, Optimal reinsurance and stop-loss order, Insurance: Mathematics and Economics, 22(3), pp. 229–233, 1998.

[18] D. S. Dimitrova and V. K. Kaishev, Optimal joint survival reinsurance: An efficient frontier approach, Insurance: Mathematics and Economics, 47(1), pp. 27–35, 2010.

[19] Y. Fang and Z. Qu, Optimal combination of quota-share and stop-loss reinsurance treaties under the joint survival probability, IMA journal of Management Mathematics, 25(1), pp. 89–103, 2014.

[20] L. Gajek and D. Zagrodny, Insurer's optimal reinsurance strategies, Insurance: Mathematics and Economics, 27(1), pp. 105–112, 2000.

[21] M. Guerra and M. d. L. Centeno, Optimal reinsurance policy: The adjustment coefficient and the expected utility criteria, Insurance: Mathematics and Economics, 42(2), pp. 529–539, 2008.

[22] M. Hald and H. Schmidli, On the maximisation of the adjustment coefficient under proportional reinsurance, ASTIN Bulletin: The Journal of the IAA, 34(1), pp. 75–83, 2004.

[23] X. Hu, H. Yang, and L. Zhang, Optimal retention for a stop-loss reinsurance with incomplete information, Insurance: Mathematics and Economics, 65, pp. 15–21, 2015.

[24] M. Kaluszka, Mean-variance optimal reinsurance arrangements, Scandinavian Actuarial Journal, 2004(1), pp. 28–41, 2004.

[25] G. Kara, A. Özmen, and G.-W. Weber, Stability advances in robust portfolio optimization under parallelepiped uncertainty, Central European Journal of Operations Research, 27(1), pp. 241–261, 2019.

[26] G. Koç, T. Petrow, and A. H. Thieken, Analysis of the most severe flood events in Turkey (1960–2014): Which triggering mechanisms and aggravating pathways can be identified?, Water, 12(6), p. 1562, 2020.

[27] A. E. Kyprianou, *Introductory lectures on fluctuations of Lévy processes with applications*, Springer Science & Business Media, 2006.

[28] D. Lamberton and B. Lapeyre, *Introduction to stochastic calculus applied to finance*, CRC press, 2011.

[29] A. Lo and Z. Tang, Pareto-optimal reinsurance policies in the presence of individual risk constraints, Annals of Operations Research, 274(1), pp. 395–423, (2019).

[30] T. Mack and M. Fackler, Exposure-rating in liability reinsurance, Blätter der DGVFM, 26(2), pp. 229–238, 2003.

[31] O. M. Mert and A. S. Selcuk-Kestel, Time dependent stop-loss reinsurance and exposure curves, Journal of Computational and Applied Mathematics, 389, p. 113348, 2021.

[32] Ö. M. Mert and S. Selcuk-Kestel, Optimal premium allocation under stop-loss insurance using exposure curves, Hacettepe Journal of Mathematics and Statistics, pp. 1–20, 2021.

[33] P. E. Protter, Stochastic differential equations, in *Stochastic integration and differential equations*, pp. 249–361, Springer, 2005.

[34] A. D. Putri, S. Nurrohmah, and I. Fithriani, Quota-share and stop-loss reinsurance combination based on value-at-risk (VaR) optimization, in *Journal of Physics: Conference Series*, volume 1725, p. 012097, IOP Publishing, 2021.

[35] C. A. Ramezani and Y. Zeng, Maximum likelihood estimation of asymmetric jump-diffusion processes: Application to security prices, Available at SSRN 606361, 1998.

[36] C. A. Ramezani and Y. Zeng, Maximum likelihood estimation of the double exponential jump-diffusion process, Annals of Finance, 3(4), pp. 487–507, 2007.

[37] W. Reducha, Parameter estimation of the Pareto-Beta jump-diffusion model in times of catastrophe crisis, 2011.

[38] A. E. Renshaw, Chain ladder and interactive modelling.(claims reserving and glim), Journal of the Institute of Actuaries, 116(3), pp. 559–587, 1989.

[39] S. Salcedo-Sanz, L. Carro-Calvo, M. Claramunt, A. Castañer, and M. Mármol, Effectively tackling reinsurance problems by using evolutionary and swarm intelligence algorithms, Risks, 2(2), pp. 132–145, 2014.

[40] R. E. Salzmann, Rating by layer of insurance, in *Proceedings of the Casualty Actuarial Society*, volume 50, 1963.

[41] H. Schmidli, *On Cramer-Lundberg approximations for ruin probabilities under optimal excess of loss reinsurance*, CAF, Centre for Analytical Finance, 2004.

[42] R. Seydel and R. Seydel, *Tools for computational finance*, volume 3, Springer, 2006.

[43] S. E. Shreve et al., *Stochastic calculus for finance II: Continuous-time models*, volume 11, Springer, 2004.

[44] G. K. Smyth and B. Jørgensen, Fitting tweedie's compound Poisson model to insurance claims data: dispersion modelling, ASTIN Bulletin: The Journal of the IAA, 32(1), pp. 143–157, 2002.

[45] K. S. Tan, C. Weng, and Y. Zhang, VaR and CTE criteria for optimal quota-share and stop-loss reinsurance, North American Actuarial Journal, 13(4), pp. 459–482, 2009.

[46] P. Tankov, *Financial modelling with jump processes*, Chapman and Hall/CRC, 2003.

[47] Y.-K. Tse, *Nonlife actuarial models: theory, methods and evaluation*, Cambridge University Press, 2009.

[48] G.-W. Weber, P. Taylan, Z.-K. Görgülü, H. A. Rahman, and A. Bahar, Parameter estimation in stochastic differential equations, in *Dynamics, games and science II*, pp. 703–733, Springer, 2011.

[49] X. Zhou, H. Zhang, and Q. Fan, Optimal limited stop-loss reinsurance under VaR, TVaR, and CTE risk measures, Mathematical Problems in Engineering, 2015.

CURRICULUM VITAE

PERSONAL INFORMATION

Surname, Name: Mert, Özenç Murat
Nationality: Turkish (TC)
Date and Place of Birth: 28.01.1991, Ankara
Marital Status: Single
Phone: 0 312 2102987
Fax: 0 312 2102985

EDUCATION

Degree	Institution	Year of Graduation
M.S.	Institute of Applied Mathematics, METU	2016
B.S.	Department of Mathematics, METU	2014
High School	Çağrıbey Anadolu Lisesi	2009

PROFESSIONAL EXPERIENCE

Year	Place	Enrollment
Nov 2015-Aug 2022	Institute of Applied Mathematics / METU	Research Assistant

AWARDS AND DUTIES

Year	Place	Enrollment
2018	Middle East Technical University	Ph.D. Course Performance Award in Financial Mathematics
2018-2021	SIAM Student Chapter	Secretary of SIAM Student Chapter in Middle East Technical University
2016-2019	Middle East Technical University	The Council of Student Representatives Position: Educational Affairs Chief

PUBLICATIONS

Journal Publications

1) Mert, Ozenc Murat, and A. Sevtap Selcuk-Kestel. "Time dependent stop-loss reinsurance and exposure curves." Journal of Computational and Applied Mathematics, 389 (2021): 113348. [DOI]

2) Çabuk S., Mert Ö.M., Selcuk-Kestel A.S., Kalaycı E. (2021) Forecasting the Hydro Inflow and Optimization of Virtual Power Plant Pricing. In: Dorsman A.B., Atici K.B., Ulucan A., Karan M.B. (eds) Applied Operations Research and Financial Modelling in Energy. Springer, Cham. [DOI]

3) Mert, Ozenc Murat, and A. Sevtap Selcuk-Kestel. "Optimal Premium Allocation under Stop-Loss Insurance using Exposure Curves." Hacettepe Journal of Mathematics & Statistics: 1-20 [DOI]

International Conference Presentations

1) Time Dependent Stop-Loss Reinsurance and Exposure Curves, 24th International Congress on Insurance: Mathematics and Economics (IME), July 5-10, 2021

2) Optimal Stop-Loss Reinsurance: A Dependence Analysis of Aggregate Claims under Certain Distributions, European Actuarial Journal (EAJ) Conference,

September 9-11, 2018

3) Dependence Analysis with Normally Distributed Aggregate Claims in Stop-Loss Insurance, 10th International Statistics Congress (ISC), December 6-8, 2017

National Conference Presentations

1) Applications of The Heston Model on BIST30 Warrants, Operational Research and Industrial Engineering (YAEM) Conference, July 13-15, 2016

Projects

Year	Title
Jul 2019 - Jan 2021	Modeling of Factors Related to Financial Adequacy Criteria in Life and Non-Life Insurance Companies
Jan 2021 - Current	Forecast of Covid-19 Basic Reproduction Number with Country Comparison and the Impact of Pandemic on the US Financial Market